AD-A058 361 WIGGINS (J H) CO REDONDO BEACH CALIF F/G 15/6
MODELING THE DYNAMIC RESPONSE OF SLABS TO OVERPRESSURE.(U)
DEC 77 D A EVENSEN, A J BRONOWICKI DNA001-77-C-0178
UNCLASSIFIED 77-1299 DNA-4535F NL

1 OF 2
AD A058 361

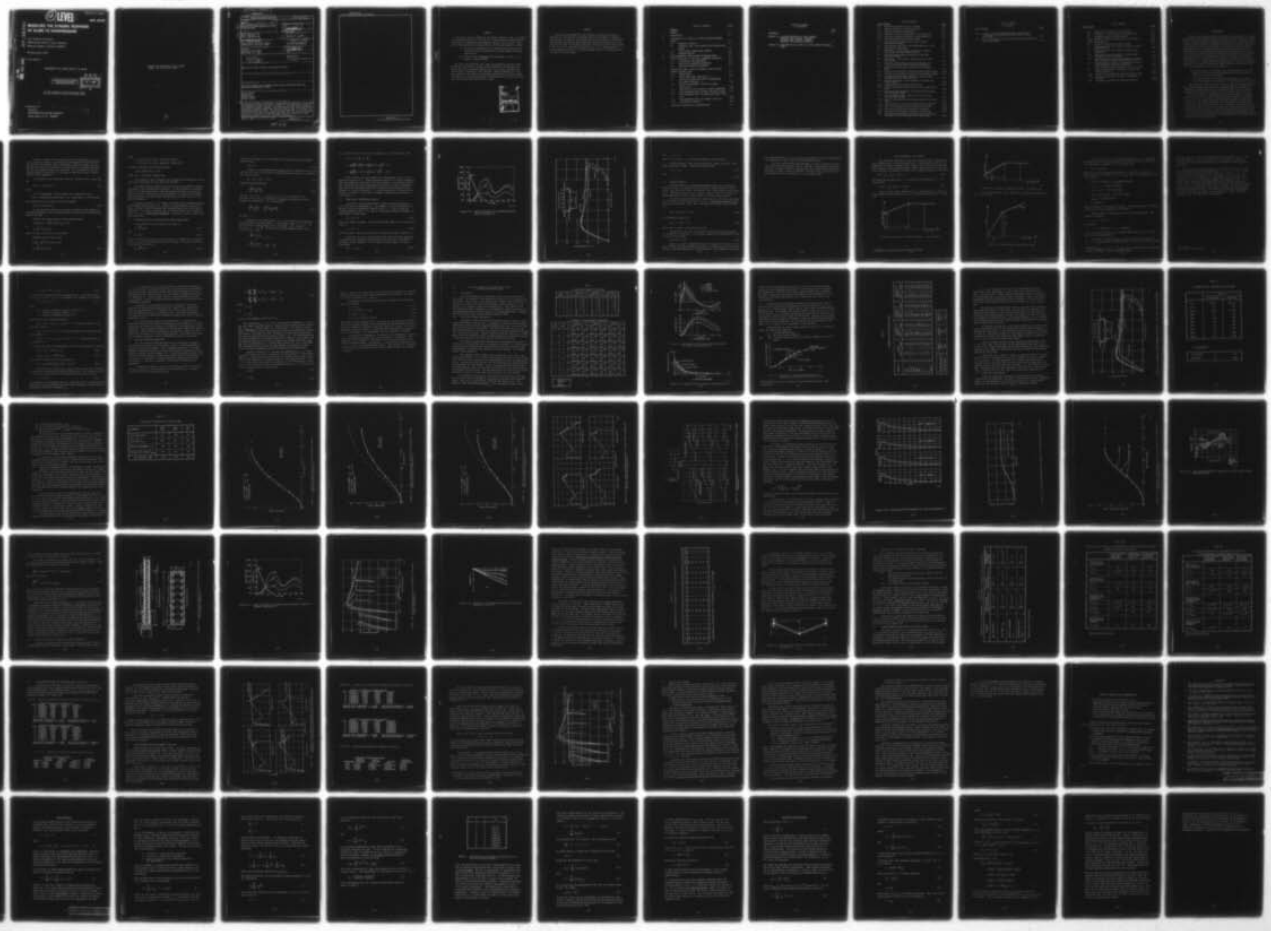


F
361

(12) LEVEL II

DNA 4535F

MODELING THE DYNAMIC RESPONSE OF SLABS TO OVERPRESSURE

J.H. Wiggins Company
1650 South Pacific Coast Highway
Redondo Beach, California 90277

30 December 1977

Final Report

CONTRACT No. DNA 001-77-C-0178

APPROVED FOR PUBLIC RELEASE;
DISTRIBUTION UNLIMITED.

THIS WORK SPONSORED BY THE DEFENSE NUCLEAR AGENCY
UNDER RDT&E RMSS CODE B344077464 Y99QAXSC06221 H2590D.

Prepared for
Director
DEFENSE NUCLEAR AGENCY
Washington, D. C. 20305

Destroy this report when it is no longer needed. Do not return to sender.

(18) DNA, SBIE

UNCLASSIFIED

SECURITY CLASSIFICATION OF THIS PAGE *(When Data Entered)*

(19) **REPORT DOCUMENTATION PAGE**

READ INSTRUCTIONS BEFORE COMPLETING FORM

1. REPORT NUMBER: DNA 4535F
2. GOVT ACCESSION NO.: AD-E300 300
3. RECIPIENT'S CATALOG NUMBER:

(6) 4. TITLE *(and Subtitle)*: MODELING THE DYNAMIC RESPONSE OF SLABS TO OVERPRESSURE.

(9) 5. TYPE OF REPORT & PERIOD COVERED: Final Report.

(14) 6. PERFORMING ORG. REPORT NUMBER: 77-1299

(10) 7. AUTHOR(s): David A. Evensen, Allen J. Bronowicki

(15) 8. CONTRACT OR GRANT NUMBER(s): DNA 001-77-C-0178

9. PERFORMING ORGANIZATION NAME AND ADDRESS:
J. H. Wiggins Company
1650 South Pacific Coast Highway
Redondo Beach, California 90277

(12) 10. PROGRAM ELEMENT, PROJECT, TASK AREA & WORK UNIT NUMBERS: Subtask Y99QAXSC062-21

(11) 11. CONTROLLING OFFICE NAME AND ADDRESS:
Director
Defense Nuclear Agency
Washington, D.C. 20305

12. REPORT DATE: 30 December 1977

13. NUMBER OF PAGES: 138

14. MONITORING AGENCY NAME & ADDRESS *(if different from Controlling Office)*: (12) 135 p.

15. SECURITY CLASS *(of this report)*: UNCLASSIFIED

15a. DECLASSIFICATION DOWNGRADING SCHEDULE:

16. DISTRIBUTION STATEMENT *(of this Report)*

Approved for public release; distribution unlimited.

17. DISTRIBUTION STATEMENT *(of the abstract entered in Block 20, if different from Report)*

18. SUPPLEMENTARY NOTES

This work sponsored by the Defense Nuclear Agency under RDT&E RMSS Code B344077464 Y99QAXSC06221 H2590D.

19. KEY WORDS *(Continue on reverse side if necessary and identify by block number)*

Nuclear Blasts
Overpressure
Dynamic Response
Concrete Slabs

20. ABSTRACT *(Continue on reverse side if necessary and identify by block number)*

A study was performed to determine if single degree-of-freedom non-linear models can adequately represent the dynamic response of reinforced concrete slabs to time-dependent pressure loadings. Test data were used from static and dynamic experiments conducted by Waterways Experiment Station (WES) and the Naval Civil Engineering Laboratory (NCEL). The primary conclusion that 1 d-o-f models can be "fitted" to the data by using model parameters that are physically realistic. Another major conclusion is that non-linear structures (such as R/C slabs) should be tested at a variety of levels of excitation.

DD FORM 1 JAN 73 1473 EDITION OF 1 NOV 65 IS OBSOLETE

UNCLASSIFIED

SECURITY CLASSIFICATION OF THIS PAGE *(When Data Entered)*

407 396

SUMMARY

This report seeks to answer the fundamental question, "Can one simulate the dynamic response of an R/C slab as a single degree-of-freedom system (with realistic parameters and parameter values), using a priori information? This question was simplified into two related questions, namely

(i) Is there an acceptable set of simple model parameters that allow the slab to be modeled as a single degree-of-freedom system? and

(ii) Could one have predicted these parameters a priori, i.e., before a nuclear attack?

The study concludes that yes, there are physically realistic parameters that can be found (using Parameter Estimation Techniques) that allow slabs to be adequately modeled this way and that reproduce that actual dynamic response of slab. Secondly, these parameters can often (but apparently not always) be determined from static test data, elementary theory, or combinations thereof. Recommendations are made concerning the future design and testing of R/C slabs.

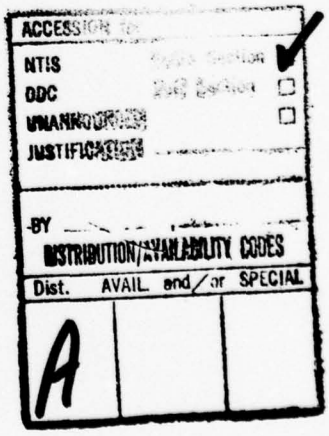

PREFACE

This study was sponsored by the Strategic Structures Division of DNA with Dr. Kent Goering as Technical Monitor; his support, comments, and direction to "keep to the fundamentals of the problem" are gratefully acknowledged. Reports and other data were supplied graciously by Dr. Sam Kiger and Jim Watt of Waterways Experiment Station and also by Bill Keenan of the Naval Civil Engineering Laboratory. Dr. D. A. Evensen was the Program Manager for the J. H. Wiggins Company, and A. J. Bronowicki wrote the computer program PEBLS.

TABLE OF CONTENTS

TABLE OF CONTENTS
(continued)

LIST OF FIGURES

LIST OF FIGURES

(continued)

LIST OF TABLES

1. INTRODUCTION

Estimating the vulnerability of a structure to an attack by a nuclear weapon requires some method of determining the response of the structure to the transient loadings produced by the detonation of the weapon. Single degree-of-freedom systems are commonly used within the defense community as the means of modeling the response of structures to these transient loadings. While it is recognized that estimates of strength and stiffness produced by single-degree-of-freedom system models may be in error, it has been generally argued that the models are adequate since the overalluncertainties of the problem do not justify the use of more complex system models. The objective of this study is to exmamine the question of the adequacy of a single-degree-of-freedom model to predict the transient response of one class of structural member, the slab. The approach used is to seek the answer to two related questions:

1. Is there any set of parameters for a single degree-of-freedom model that will match the experimentally derived transient response of various slab designs?
2. Can these parameters reasonable be estimated on an a priori basis from either static test data or from engineering principles

The analytical procedure used is the technique of Parameter Estimation. This technique basically takes a system model of any degree of complexity and determines that set of model parameters which minimizes the differences between the observed and calculated response values.

The report itself is organized in the following manner. The idealization of the slab as a single degree-of-freedom system is discussed first, (i.e., the assumptions and approximations made), followed by a discussion of the "multi-parameter" one degree-of-freedom model used in the study. The next section deals with estimation of parameters (i.e., fitting the model to the data), followed by results presented for three (widely different R/C slabs. A section of suggested procedures for analyzing slabs as single degree-of-freedom models is then presented, and the report ends with conclusions and recommendations for the future design and testing of such structures.

2. IDEALIZATION OF A SLAB AS A SINGLE DEGREE-OF-FREEDOM SYSTEM

This section follows the discussion by Watt (Reference 3), and similar results are also presented in Biggs (Reference 2) and other texts (Reference 4). In the design of blast-resistant structures, considerable economy can be realized if the design includes not only the elastic but also the plastic resistance of the structure. Plastic behavior is not generally permissible under continuous operating conditions, but is in many cases quite appropriate for design when the structure is subject to a severe dynamic loading only once or twice during its life.

It can be concluded from examination of exact or rigorous dynamic analysis (i.e., Reference 2) that relatively simple structures having simple boundary conditions can be easily analyzed. Otherwise, the analysis, though not impossible, becomes cumbersome. For this reason and for practical design purposes, the idealized spring-mass, single-degree-of-freedom approximate analysis is commonly used. This method provides a means for analyzing the more complex structures rapidly and with a reasonable degree of accuracy (Reference 2).

2.1 EQUATION OF MOTION

The actual deep slab structure and the idealized spring-mass system are shown in Figure 2-1. The first peak value of deflection is of primary interest for this problem, and damping is often neglected (Reference 4), but for completeness it has been retained. From the free-body diagram shown in Figure 2-1, the equation of motion for the equivalent 1 d-o-f system is

$$M_e\ddot{y}(t) + \beta_e\dot{y}(t) + K_e y(t) - F_e(t) = 0 \qquad (2\text{-}1)$$

where M_e = equivalent or effective mass, lb-sec^2/in (Kg)

$\ddot{y}(t)$ = acceleration of slab at time t, in/sec^2 (m/sec^2)

β_e = equivalent or effective damping, lb-sec/in (Newtons-meters/sec)

$\dot{y}(t)$ = velocity of slab at time t, in/sec (m/sec)

K_e = equivalent or effective stiffness, lb/in (Newtons/m)

$y(t)$ = deflection of slab at time t, inches (m)

$F_e(t)$ = equivalent or effective force at t

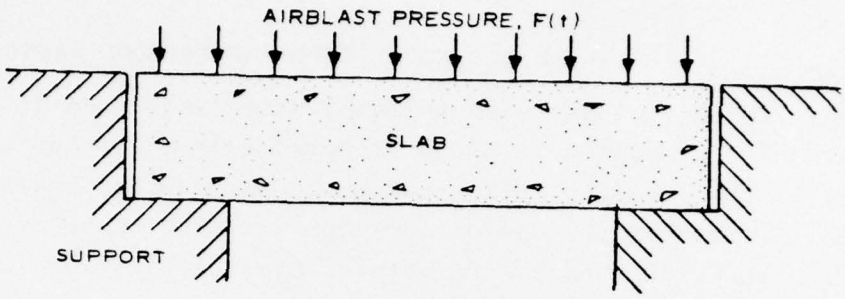

a. DEEP SLAB SPECIMEN ON SUPPORTS

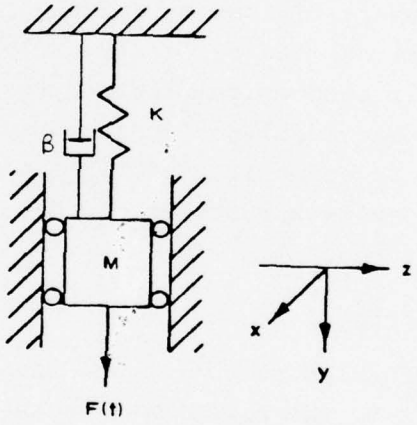

b. IDEALIZED DEEP SLAB SPECIMEN

77-1288

Figure 2-1. Deep Slab Specimen and 1 d-o-f Model

In order to define the equivalent system, the parameters M_e, β_e, K_e, and F_e must be evaluated. The equivalent one-degree-of freedom system is one for which the kinetic energy, dissipation, internal energy, and work done by all external forces are at all times equal to the same quantities for the continuous-mass deep slab structure. It is assumed that the deflected shape of the structure is the same as that due to static loading. (This is a key assumption.)

If any point on the deflecting surface of the deep slab is described by

$$y(x,z,t) = A(t)\phi(x,z) \tag{2-2}$$

where

$A(t)$ = displacement, inches (meters) as a function of time t

$\phi(x,z)$ = assumed deflecting shape (i.e., mode shape) of the deep slab

the velocity $\dot{y}(t)$ of any point on the slab becomes

$$\dot{y}(x,z,t) = \dot{A}(t)\phi(x,z) \tag{2-3}$$

If the equivalent system is to respond similarly to the midspan of the actual structure, then the displacements and velocities of both systems must be the same.

Equating the kinetic energy of both systems yields

$$1/2M_e\dot{A}(t)^2 = 1/2\int^S M[\dot{A}(t)\phi(x,z)]^2\, dS$$

or

$$M_e = \int^S M\phi^2(x,s)\, dS \tag{2-4}$$

where S is the area of the slab (planform).

Equating external work yields

$$F_eA(t) = \int^S F[A(t)\phi(x,z)]\, dS$$

$$F_e = \int^S F\phi(x,z)\, dS \tag{2-5}$$

where

M = mass per unit area, lb-sec^2/in^3 (kg/m^2)

F = force per unit area, pounds/in^2 (Newtons/m^2)

Similarly, equating the dissipation yields

$$\beta_e \dot{A}(t) = \int^S c\dot{A}(t)\phi(x,z)\, dS$$

where c is a "localized" damping term.

The equivalent load of Equation (2-5) applies to the magnitude of the load, while both loads have the same time function.

The resistance or stiffness is the internal force tending to restore the system to its unloaded static position. If the stiffness is defined in terms of the load distribution, then the maximum stiffness is numerically equal to the total load of the same distribution $\phi(x,z)$ which would cause a unit deflection at the point where the deflection is equal to that of the equivalent system.

The shape function $\phi(x,z)$ changes as the deep slab progresses through the different stress ranges, i.e., elastic, elastic-plastic, and plastic. Thus, a complete solution requires that a shape function for each range be considered. Or, to put it another way, the effective mass, M_e, is really $M_e(y)$, i.e., it is displacement-dependent. Similarly, β_e and F_e depend upon the displacement.

2.2 CANONICAL FORM OF THE EQUATION FOR VARIOUS MODE SHAPES

If one defines the total mass (of the slab) by

$$M_T = \int^S \rho h\, dS \qquad (2\text{-}6a)$$

then

$$M_T = \rho h S \qquad (2\text{-}6b)$$

where S is the planform area of the slab and it is assumed that the average density (ρ) and the slab thickness (h) are constant. Similarly, the total force applied is defined by

$$F_T = \int^S p\, dS \qquad (2\text{-}7a)$$

and when the pressure, p(t) is assumed to be uniform (over the planform area) one has

$$F_T = pS \tag{2-7b}$$

Finally, if one combines the preceding results (Equations 2-6b, 2-7b, and 2-4, 2-5, with 2-1) and then divides through by the area, S, he obtains the canonical form

$$\mu M\ddot{y} + \beta_e\dot{y} + k_e(y) = \alpha p(t) \tag{2-8}$$

where the mass coefficient

$$\mu = \left\{\frac{\int_S \rho h\, \phi^2\, dS}{\rho h S}\right\} \tag{2-9a}$$

and the μ is always ≤ 1. Similarly $k_e(y)$ is the restoring force (per unit area) (i.e., it represents the <u>static</u> load-deflection curve, pressure vs. deflection). It is clear that

$$\alpha = \left\{\frac{\int_S F\,\phi\, dS}{pS}\right\} = \left\{\frac{\int_S p(t)\,\phi\, dS}{pS}\right\} \tag{2-9b}$$

and that $\alpha \leq 1$.

Estimates of the coefficients μ and α can be obtained by assuming various forms for the mode shape, ϕ. For example, when $\phi=1$, (i.e., the slab translates through space like a rigid-body), then $\mu=1$ and $\alpha=1$. Similarly, if $\phi = \sin\frac{\pi x}{L}$ (bending like a simply-supported beam in one direction only), then

$$\mu = \frac{\int \sin^2\frac{\pi x}{L}\, dx}{L} = \frac{1}{2} = .5$$

$$\alpha = \frac{\int \sin\frac{\pi x}{L}\, dx}{L} = \left(\frac{2}{\pi}\right) = .6366$$

Or, if the slab acts like a plate (or membrane) in two directions, then

$$\phi(x,z) = \sin \frac{\pi x}{a} \sin \frac{\pi z}{b}$$

$$\mu = \frac{1}{ab}\iint \sin^2\left(\frac{\pi x}{a}\right) \sin^2\left(\frac{\pi z}{b}\right) dxdz = \left(\frac{1}{2}\right)^2 = .25$$

$$\alpha = \frac{1}{ab}\iint \left(\sin \frac{\pi x}{a} \sin \frac{\pi y}{b}\right) dxdz = \left(\frac{2}{\pi}\right)^2 = .4053$$

Thus, a priori, one has bounds on the coefficients α and μ of the canonical Equation (2-8). These "bounding values" will be used subsequently when the parameters of Equation (2-8) are estimated. As stated previously, $k_e(y)$ represents the static load-deflection curve, and $\beta_e \dot{y}$ is the damping term, which has practically negligible influence on the maximum initial response (cf. Biggs, Reference 2). A typical pressure vs. deflection curve is shown in Figure 2-2, and Figure 2-3 shows a representative deflection-time history.

2.3 "REAL-WORLD" EXPERIMENTAL EFFECTS

In practice, the mass coefficient μ (and the force coefficient, α) will vary with the displacement y. For example, a thick slab might be expected to start out deflecting linearly (with $\mu \cong .5$, say), and end up "punching through" (with $\mu \cong 1$, say) as the pressure loading increases. In other words, one might have

$$.5 \leq \mu(y) \leq 1 \qquad (2\text{-}10a)$$

during the dynamic response. Similar restrictions apply to the force coefficient, α,

$$.6 \leq \alpha(y) \leq 1 \qquad (2\text{-}10b)$$

for thick slabs. This type of behavior was observed by Watt, Reference 3.

Conversely, for thin, conventional slabs, Brown and Black (Reference 5) found that they began deflecting linearly (like a plate) and ended up stretching, like a membrane. In this case, one might expect (at least tentatively)

$$.25 \leq \mu \leq .35 \qquad (2\text{-}11a)$$

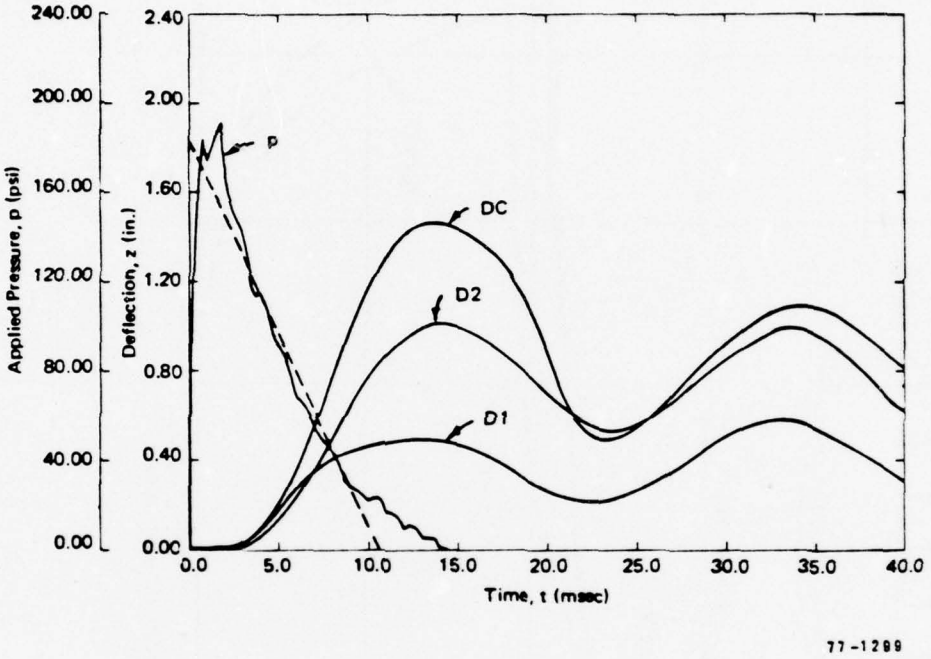

Figure 2-2. Typical Pressure vs. Deflection Curve (Watt, Reference 3)

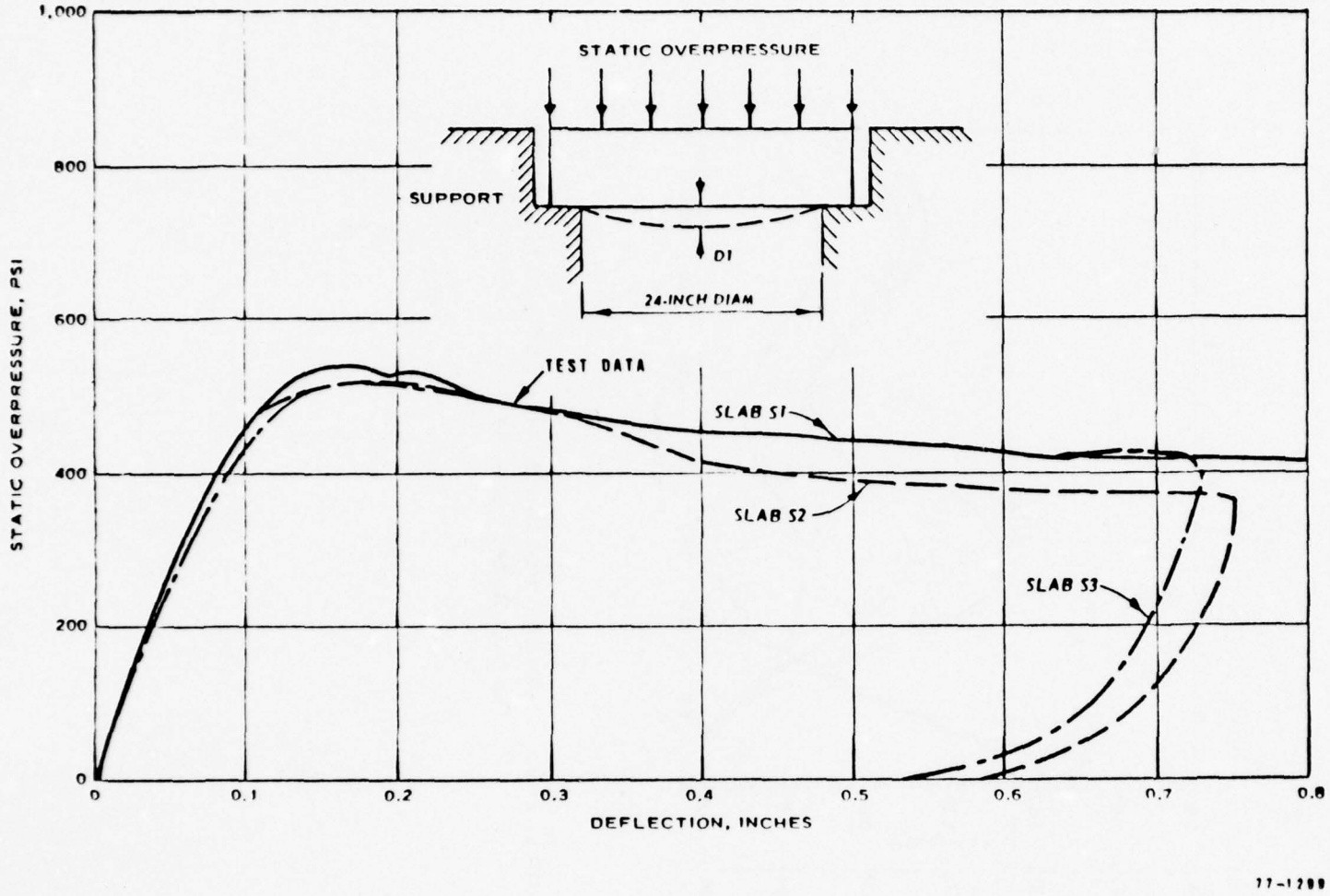

Figure 2-3. Typical Deflection Time-History (Keenan Reference 6)

and $\quad .4 \leq \alpha \leq .5$

where $\mu = \mu(y)$ and $\alpha = \alpha(y)$ both vary somewhat with deflection.

Finally, Keenan's laced slabs (Reference 6) behave much like a wide beam with plastic hinges. Again, one might estimate

$$.25 \leq \mu \leq .33 \tag{2-12a}$$

and

$$.5 \leq \alpha \leq .6 \tag{2-12b}$$

2.4 TEXTBOOK RESULTS

Biggs (Reference 2) presents approximate methods for the design of beams and slabs. In Chapter Five (pp. 199-244), Biggs discusses a "mass factor" K_m (analogous to the μ used herein) and a "load factor" K_L (analogous to α). Tabulated values of K_m (μ) and K_L (α) are given therein for beams and slabs subjected to various dynamic loads, including uniform pressure.

An important observation made by Biggs (and not originally recognized by the authors) is that the factor α (or K_L) is <u>inherently contained in the</u> static-load deflection curve. Thus, the equation of motion can be written as

$$\mu M\ddot{y} + \beta_e \dot{y} + \alpha k(y) = \alpha p(t) \tag{2-13}$$

or, (dividing through by α)

$$M\lambda\ddot{y} + \dot{y} + k(y) = p(t) \tag{2-14}$$

where $\lambda = \frac{\mu}{\alpha}$ is called "the load mass factor".

In equation (2-14) $k(y)$ is the static resistance function (pressure vs. deflection) of the slab. If we neglect damping (as Biggs suggests) then equation (2-14) becomes

$$M\lambda\ddot{y} + k(y) = p(t) \tag{2-15}$$

Finally, if $k(y)$ is approximated by a bi-linear (elasto-plastic) curve, $k(y)$ requires just <u>two</u> parameters to define it, namely P_{lin} (the yield stress) and d_{lin} (the displacement when yielding begins). Thus, equation (2-15) has

just three parameters (λ, P_{lin}, and d_{lin}) as opposed to the more complicated "multi-parameter" model, which will be discussed shortly.

Initially, good results were obtained (in fitting the dynamic response data) using the multi-parameter model. However, as more dynamic data were analyzed, it became clear that the most physically significant results would come from as simple a model as possible. For this reason, equation (2-15) was eventually used in attempting to fit the dynamic data.

3. MULTI-PARAMETER 1 d-o-f MODEL

When this study was begun, it was not known how well a "simple model" (with constant mass μ and force coefficient, α) would perform in trying to approximate the dynamic response data. Hence, the one d-o-f model was made fairly general in the computer program (PEBLS)* which was used in this work. If one rewrites the equation of motion (2-8) (repeated below for convenience)

$$\mu M\ddot{y} + \beta_e\dot{y} + k_e(y) = \alpha P(t) \qquad (2\text{-}8)$$

and notes that the mass term $\mu = \mu(y)$ and the force coefficient $\alpha = \alpha(y)$, then one has

$$M\mu(y)\ddot{y} + \beta_e\dot{y} + k_e(y) = \alpha(y)P(t) \qquad (3\text{-}1)$$

Based upon the limits expected for (α,μ) (see Section 2.) then one might choose a linear variation of (μ,α) with deflection as shown in Figure 3-1.

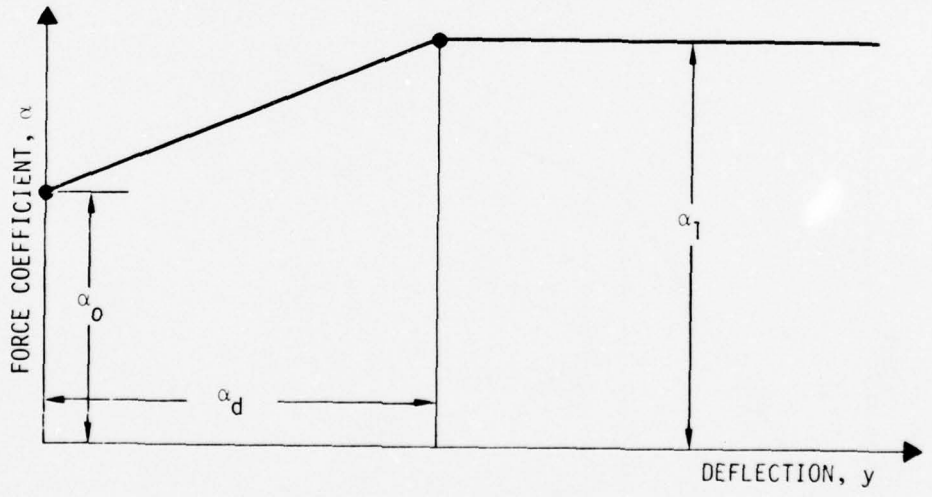

Figure 3-1a. Variation of Force Coefficient α with Deflection

*Parameter Estimation for Blast-Loaded Structures

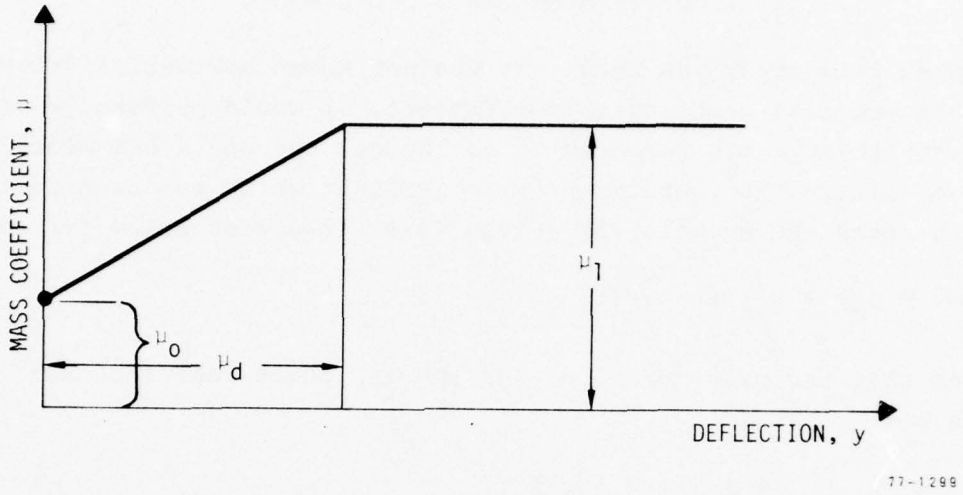

Figure 3-1b. Variation of Mass Coefficient μ with Deflection

For the spring force, $k_e(y)$, PEBLS uses a bi-linear load-deflection curve (Figure 3-2).

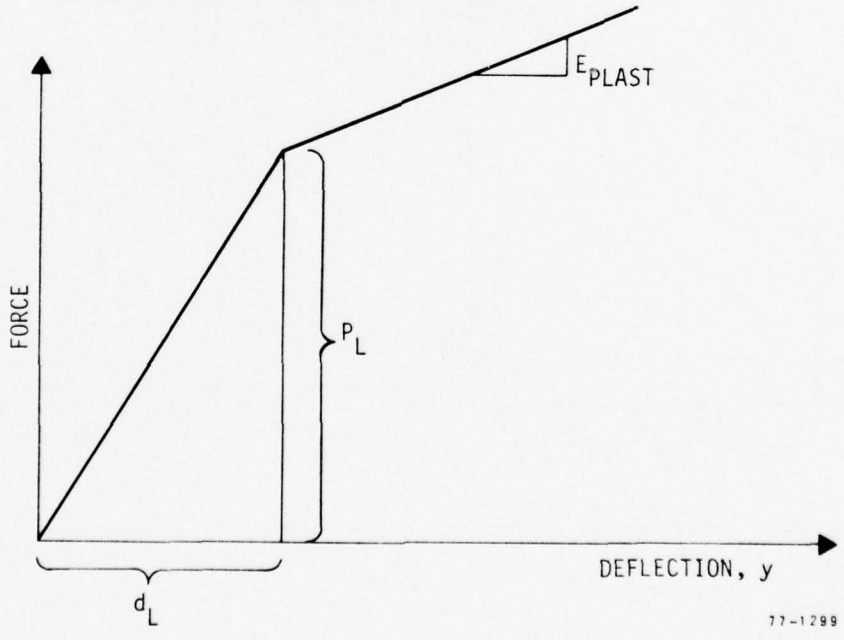

Figure 3-2. Force-deflection Curve Used in PEBLS

If the pressure, p(t), is measured incorrectly, (i.e., the dynamic pressure gage is not reading properly) then one might want to "scale up" (or scale down) the pressure, p. Thus, PEBLS uses

$$p(t) = p_{scale} f(t)$$

where f(t) is the experimental (pressure vs. time) data. Finally, the damping term was kept linear (i.e., just $\beta_e \dot{Y}$) since it was expected to have little effect.

Thus, for generality, the <u>eleven</u> parameters

(μ_o, μ_1, μ_d) ~ mass coefficient

$(\alpha_o, \alpha_1, \alpha_d)$ ~ force coefficient

$(p_{lin}, d_{lin}, E_{plast})$ ~ bi-linear spring

p_{scale} ~ pressure scaling

β ~ damping

were incorporated in the computer program. The resulting model is referred to herein as a "multi-parameter 1 d-o-f model."

Note, of course, that the model can be readily simplified. For example, by setting

$$\mu_d = 0 \quad (\text{or } \alpha_d = 0)$$

one obtains

$$\mu = \mu_1 = \text{constant} \quad (\text{or } \alpha = \alpha_1 \text{ constant})$$

i.e., one can revert back to the "constant mode" model with non-varying mass and force coefficients.

Similarly, by putting $E_{plast} = .001$* (or .01) one can achieve an elastic - perfectly plastic force-deflection curve for the restoring spring.

---

*Do not use $E_{plast} \equiv 0$ or $\beta \equiv 0$ in the computer program, since they appear in the denominator within the FØRTRAN coding.

Putting $p_{scale} = 1.0$ gives no magnification on the pressure, and $\beta = .001$* gives low damping. Thus, at the outset, it was desirable to program a multi-parameter model with the flexibility of progressive simplification just noted.

Having chosen a "multi-parameter" 1 d-o-f model, one is then faced with the problem of selecting its parameters: α_o, α_1, α_d... etc. In most cases, one has theoretical results to guide him, (e.g. $0 \leq \mu \leq 1$), and he may also have some estimate of the mode shape, ϕ, (which allows him to compute μ, α) and in many cases a <u>static</u> load-deflection curve. With these a priori estimates, the analyst has a set of "initial parameters" for his model. Based upon his experience, the analyst also places a quantitative measure of confidence on his initial estimates, and these numerical confidence estimates are used in the search for a final set of parameters. This search for "best estimates" of the parameters is termed "parameter estimation," as discussed in the next section.

*See footnote previous page.

4. FITTING THE MODEL TO THE DATA: PARAMETER ESTIMATION

4.1 INTRODUCTION AND BACKGROUND

The question of selecting the parameters (α_0, α_1, α_d, ..., etc.) of the 1 d-o-f model in such a way that the analytical model "matches" the experimental data is a problem of "parameter estimation." Parameter estimation is related to the more general problem of "system identification" (References 7 and 8). The main idea is to use differences between measured and predicted behavior (e.g., the dynamic response, y, as a function of time, t) to adjust key parameters of a model automatically so as to minimize response differences (i.e., minimize $y_{analytical} - y_{experimental}$). The procedure is quite general and can be applied to either linear or nonlinear mathematical models (cf. Figure 4-1).

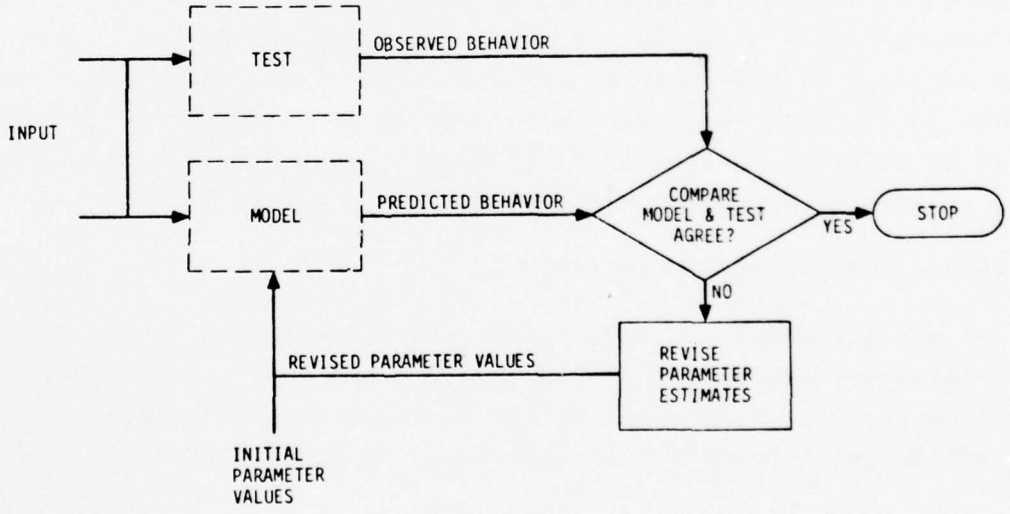

Figure 4-1. Flow Diagram of Model Verification/Parameter Estimation Procedure

In the present study, the model parameters are chosen to minimize the vector norm

$$N = \{\Delta u\}^T\{\Delta u\} \tag{4-1}$$

where the vector $\{\Delta u\}$ is given by

$$\Delta u_1 = (y_{model} - y_{expt}) \text{ at time } t_1$$

$$\Delta u_2 = (y_{model} - y_{expt}) \text{ at time } t_2$$

$$\vdots$$

$$\Delta u_i = (y_{model} - y_{expt}) \text{ at time } t_i, \quad \text{and so forth.}$$

Note that uncertainties must be recognized in both the analysis (model) and the test (experiment). That is, one expects (from a static load-deflection curve, say) to know the yield force (stress) fairly well, but there is still an uncertainty in it (e.g., ±10%). Similarly, in the measured response, y_{expt}, one does not know y exactly, but rather with some uncertainty. Computational methods are available for utilizing this information in a quantitative manner so as to achieve an optimum (minimum variance) fit between analysis and test. In other words, when confidence in the data is greater than confidence in the model (analysis), the model is adjusted so that it tends to match the data. When the converse is true, changes to the model will be relatively small.

4.2 STATISTICAL PARAMETER ESTIMATION

As just discussed, methods for parameter estimation which recognize the respective uncertainties in both analysis and test have an obvious practical advantage. Such a method was employed in this study. The original derivation and application of the method appear in reference 9.

The particular algorithm for statistical parameter estimation described in that paper uses a linear estimator in that it operates on the basis of a linearized relationship between a parameter vector, {r}, and an observation vector, {u}. If r_p and u_p denote prior (initial) estimates of the elements of these vectors based upon analytical models, then the "true" values r and u are assumed to be related through a sensitivity matrix by the equation (linearized Taylor's series expansion)

$$\{(u - u_p)\} = [T]\{(r - r_p)\} + \{\varepsilon\} \tag{4-2}$$

If u represents measured data with random error $\{\varepsilon\}$, and the notation $(u - u_p) \equiv \Delta u$ and $(r - r_p) \equiv \Delta r$ is adopted, then equation (4-2) becomes

$$\{\Delta u\} = [T]\{\Delta r\} + \{\varepsilon\} \tag{4-3}$$

where

$[T]$ = response sensitivity matrix of order $(\bar{n} \times \ell)$

ℓ = length of parameter vector, $\{\Delta r\}$

$\bar{n}$ = length of observation vector, $\{\Delta u\}$

Using the following notation adopted in

$[S_{rr}] = E[\{r - r_p)\}\{(r - r_p\}^T] = (\ell \times \ell)$ covariance matrix of the parameter vector $\{r\}$

$[S_{\varepsilon\varepsilon}] = E[\{\varepsilon\}\{\varepsilon\}^T] = (\bar{n} \times \bar{n})$ covariance matrix of the experimental error vector $\{\varepsilon\}$

$\{S_{rr}{}^*\} = E[\{r^* - r_p)\}\{(r^* - r_p)\}^T] = (\ell \times \ell)$ covariance matrix of the vector $\{r^*\}$

The revised estimate of the parameters $\{r^*\}$ and its covariance are given by

$$\{r^*\} = \{r_p\} + [\bar{G}]\{(u - u_p)\} \tag{4-4}$$

$$[S_{rr}{}^*] = [S_{rr}] - [\bar{G}][T]\{S_{rr}\} \tag{4-5}$$

where the estimator matrix $[\bar{G}]$ is defined as

$$[\bar{G}] = [S_{rr}][T]^T([T][S_{rr}][T]^T = [S_{\varepsilon\varepsilon}])^{-1} \tag{4-6}$$

Equations (4-4) through (4-6) represent the Kalman Filter equations as applied to the estimation problem (Reference 10). The estimator matrix $[G]$ as given by equation (4-6) is derived such that the vector norm

$$N = \{\Delta u\}^T\{\Delta u\} \tag{4-1}$$

is minimized (cf. References 9 and 10). Equation (4-1) is a measure of the mean-square deviation between the experimental (measured) response and the theoretical (calculated) response.

It is important to note at this point that the sensitivity matrix $[T] = [\partial u/\partial r]$ and the estimator matrix [G] are updated as the computational algorithm iterates. The Kalman Filter equations are recursive in nature, and eventually the estimator matrix [G] will reach a steady-state solution (cf. Reference 10). This approach (using a linearized Taylor's series) is conceptually similar to applying Newton's method for solving nonlinear simultaneous equations.

Furthermore, as indicated previously, the method of satistical parameter estimation applies when there are "noisy" data. Experimental error is represented by $\{\varepsilon\}$ in equation (4-3) and is accounted for by the covariance matrix $[S_{\varepsilon\varepsilon}]$ of equation (4-6). The reader interested in further details of Statistical Parameter Estimation may wish to consult References 7 and 8.

Previous structural application (Reference 9) of statistical parameter estimation used natural frequencies and mode shapes (i.e., modal deflections at particular locations) as elements of the observation vector. Reference 11 uses frequency-response data and assumes steady-state harmonic excitation. The estimation procedure can be applied in either the time-domain (cf. Reference 12) or the frequency domain. The present study uses the time-domain approach, since the mathematical model is non-linear.

4.3 BAYESIAN ESTIMATION EQUATIONS

The J.H. Wiggins Company has made use of "Statistical Parameter Estimation" previously (e.g., References 9 and 11), and developments in this area have continued apace. Thus, Isenberg (Reference 13) recently prepared a systematic account of statistical parameter estimation, least-squares, weighted residual methods, etc. From this systematic study, there resulted a set of Bayesian estimation equations, which are presented in this section of the report. (These results have been abstracted from Reference 13). Details of Isenberg's results are included herein as Appendix A).

In Bayesian estimation, one is given a <u>prior</u> estimate of the parameters r_o, along with the associated covariance matrix S_{rr}. One then seeks to minimize the objective function

$$F = \sum_{i=1}^{n} \sum_{j=1}^{n} w_{ij} \left(u_{o_1} - u_i\right) \left(u_{o_j} - u_j\right)$$
$$+ \sum_{i=1}^{n} \sum_{j=1}^{n} \hat{w}_{ij} \left(r_{o_j} - r_i\right) \left(r_{o_j} - r_j\right) \qquad (4\text{-}7)$$

where

$$w = S_{\varepsilon\varepsilon}^{-1}$$

and

$$\hat{w} = S_{rr}^{-1}$$

and S_{rr} is as symmetric matrix as is $S_{\varepsilon\varepsilon}$.

The variables u_{o_i}, u_i, w_{ij}, etc., are defined in Appendix A. To orient the reader, note that $(u_{o_i}-u_i)$ represent the difference between experiment ($u_{observed}$) and the theory (u_i, of the model). The terms w_{ij} represents a "weighting" matrix, where some data points are weighted more heavily than others. The reason for this "weighting" is that <u>all</u> the data points may not have been obtained with equal certainty (i.e., the experimenter may have more confidence in some data points than in others). For example, the experimenter might find it easier to measure the maximum deflection (δ_{max}, say) that the deflection at a (finite) early time (e.g., at t=.1 millisec). The introduction of w_{ij} allows the experimenter to influence the model (which is being estimated) by selectivity weighting his data points.

Similarly, equation (4-7) contains the parameters $(r_{o_i} - r_i)$, where r_{o_1} is the initial (a priori) estimate of the $i^{\underline{th}}$ parameter. The weighting matrix, $\hat{w}_{ij}$ allows the structural analyst to influence the parameters estimated by the algorithm in a fashion similar to the experimentalist. Thus, if the analyst has a great deal of confidence in the $i^{\underline{th}}$ parameter, he can express that confidence through the weighting matrix, $\hat{w}_{ij}$. In actual practice, the matrices w and $\hat{w}$ are given by

$$w = S_{\varepsilon\varepsilon}^{-1} \qquad (4\text{-}8a)$$

and

$$\hat{w} = S_{rr}^{-1} \qquad (4\text{-}8b)$$

where $S_{\varepsilon\varepsilon}$ and S_{rr} are "covariance" matrices defined in Appendix A. The user of PEBLS controls the "route" the program takes (to minimize F in equation 4-7) by his selection of $S_{\varepsilon\varepsilon}$ and S_{rr}.

To summarize the technique of Bayesian estimation, we iteratively solve the sequence

$$T = T\ (r_e) \tag{4-9a}$$

$$S = (\hat{w} + T^T w T)^{-1} = S\ (r_e) \tag{4-9b}$$

$$G = S T^T w = G\ (r_e) \tag{4-9c}$$

$$r = r_o + G\ [u_o - u_e - T\ (r_o - r_e)] \tag{4-9d}$$

and repeat the next sequence with r replacing r_e. We continue to iterate until the difference between r and r_e becomes sufficiently small and the sequence has therefore converged. The final value of S is S^*_{rr}, the revised parameter covariance matrix. It should be noted that when the response is linear with respect to the parameters, only one iteration is required.

As discussed in Appendix A, the matrix T is a "sensitivity" matrix, i.e., the change in response due to a unit change in a parameter. (See equation (42) in Appendix A.) The matrix S is a covariance matrix, and G is the "estimator" matrix. The vector, r, is the set of parameters (e.g., α_0, α_1, α_2, etc.) of the mathematical model. (See Section 3.0) Equations (4-9) are used within PEBLS to obtain the revised estimates of the model parameters.

5.0 RESULTS FOR THREE (WIDELY DIFFERENT) TYPES OF REINFORCED CONCRETE SLABS

5.1 INTRODUCTION

Static and dynamic data from three series of tests were used in this study. The results of the modeling are contained in this section of the report, with Section 5.2 devoted to Watt's (deep) slabs (Reference 3), Section 5.3 to Brown and Black's conventional slabs (Reference 5), and Section 5.4 on Keenan's laced slabs (Reference 6). The sensitivity of the results is given in Section 5.5, and additional results are given for a three-parameter model (of Watt's Slabs), a four-parameter model (of Brown and Black's Slab), and a simple model of Keenan's Slabs.

5.2 WATT'S DEEP SLABS (Reference 3)

Reference 3 reports on static and dynamic tests of deep R/C slabs (span-to-thickness ratio of 4.12). Two types of slabs were tested (namely mach-modeled slabs and environmentally-modeled slabs) but static test data were available only for the latter. The slabs were square in plan, but they were placed over a circular cavity and thus had an unsupported diameter of 24 inches in the center. Dynamic pressure loads were applied by the WES Small Blast Load Generator, which involved detonating an explosive mixture of gases and driving a shock wave against the face of the slab.

The dynamic response was recorded using accelerometers mounted in the center of the slab and also on the support structure. The accelerometer traces were digitized and then integrated in time to give velocities and displacements. Pressure-time histories were also recorded. For further details, see Reference 3.

The computer program, PEBLS, allows velocities to be part of the "observation vector," $\{\Delta u\}$. Since velocities were available in Watt's test data, they were used (along with the displacements) to form the observation vector. Results were obtained only for the Environmentally Designed Slabs, test specimens ED1, ED2 and ED3. Figure 5-1 shows the experimental data which was used as input to the program and Figure 5-2 gives the corresponding pressure-time histories. The experimental data used from Figure 5-1 is tabulated in Table I for the three test specimens, ED1, ED2 and ED3.

In addition to the data on displacement and velocities, note that the user must input an estimate of the <u>error</u> in the experimental observations. (The error in observations relates to the matrix $[S_{\varepsilon\varepsilon}]$ - see Equation (4-8a) discussed previously). Thus, the percent errors in the

TABLE I

A. EXPERIMENTAL RESPONSE FOR THREE SLABS

TIME POINT	TIME M SEC	SLAB ED 1		SLAB ED 2		SLAB ED 3	
		DISPL.	VEL.	DISPL.	VEL.	DISPL.	VEL.
1	.25	.02	180	.01	90	.025	180
2	.5	.08	320	.06	480	.09	350
3	.75	.15	380	.18	435	.18	350
4	1.0	.21	190	.27	310	.26	280
5	1.25	.255	120	.33	235	.32	210
6	1.5	.285	90	.39	210	.37	120
7	2.15	.325	0	.455	0	.41	0

B. CONFIDENCE IN THE EXPERIMENTAL OBSERVATIONS

TIME POINT	TIME M SEC	SLAB ED 1		SLAB ED 2		SLAB ED 3	
		DISPL.	VEL.	DISPL.	VEL.	DISPL.	VEL.
1	.25	.30* / .000036	.25 / 2025.	1.5 / .000225	1.5 / 18225.	.30 / .0000563	.25 / 2025.
2	.50	.20 / .000256	.15 / 2304.	0.5 / .0009	.30 / 20736.	.20 / .000324	.15 / 2756.25
3	.75	.15 / .0005063	.15 / 3249.	.25 / .002025	.25 / 11827.	.15 / .000729	.15 / 2756.25
4	1.0	.10 / .000441	.15 / 812.25	.15 / .001640	.25 / 6006.	.10 / .000676	.15 / 1764.
5	1.25	.10 / .0006503	.20 / 576.0	.15 / .002450	.25 / 3452.	.10 / .001024	.20 / 1764.
6	1.5	.10 / .0008123	.25 / 506.25	.15 / .003422	.30 / 3969.	.10 / .001369	.25 / 900.
7	2.15	.05 / .0002641	= 6 / 506.25	.10 / .002070	= 6 / 3969.	.05 / .000420	= 6 / 900.

* PER CENT ERROR / VARIANCE

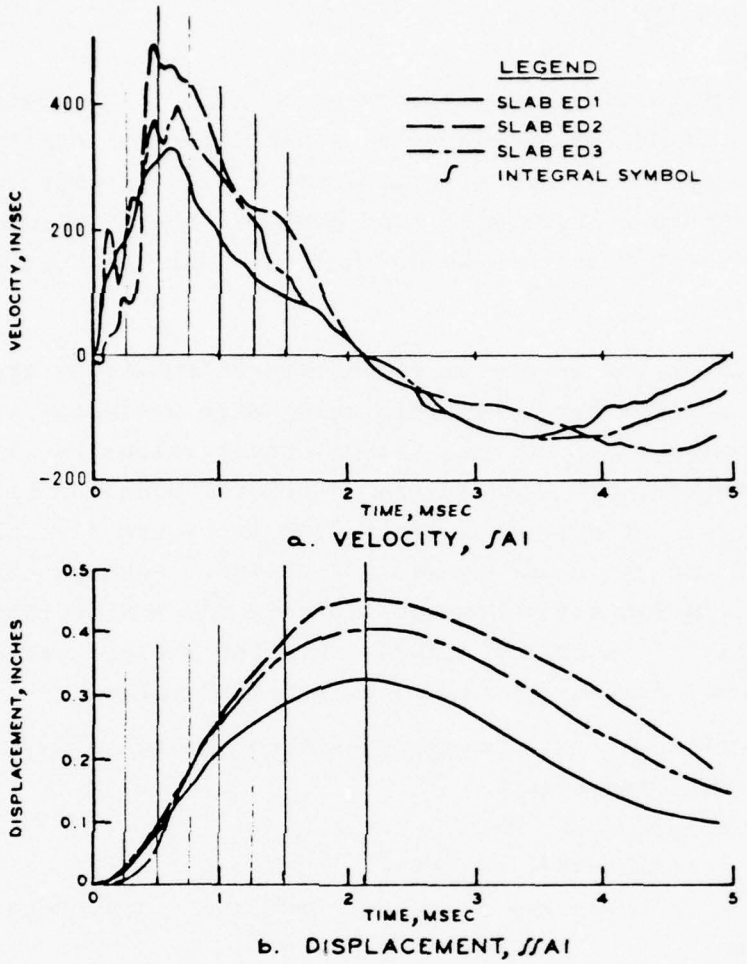

Figure 5-1. Experimental Velocities and Displacements vs. Time (from Reference 3)

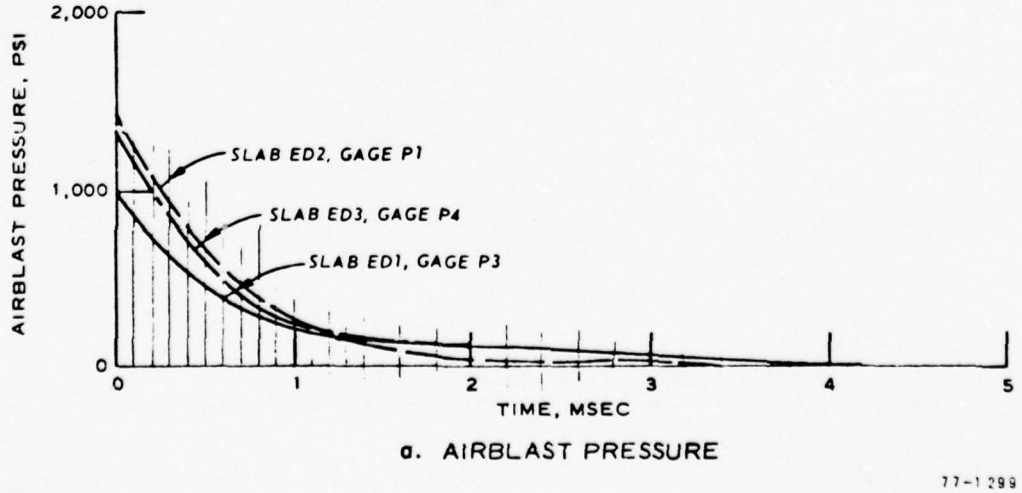

Figure 5-2. Pressure-Time Histories (from Reference 3)

velocities and displacements are also given in Table I (the bottom half) along with the corresponding variances.* A small percent error indicates good confidence in the data, and a large error indicates poor confidence. Thus Table I shows that we have more confidence in the displacements at t_4 through t_7 (the later times) than we do in those near the initial times (t_1 through t_3).

The results of the parameter estimation calculations are shown in Table II, which gives the ten parameters which were estimated (P_{lin}, d_{lin}, E_{plast}, etc.), showing their initial values, their values estimated for each test slab, etc. For example, the initial ("prior") model used a yield stress of 525 LB/IN^2 (P_{lin}), and after the estimation procedure (for slab ED1) the estimated value of the yield stress was 450 LB/IN^2. Perhaps the more important thing to note in Table II, however, is that the RMS deviation decreased from .0428 initially (Slab ED1) to .0048 (when the revised parameters were used), i.e., a factor of ten improvement in the RMS value.

The deflection vs. time is shown plotted in Figure 5-3 for Slab ED1, where the three curves represent

(i) the experimental data,

(ii) the initial model response,

and, (iii) the model response using the "optimum" parameters just estimated.

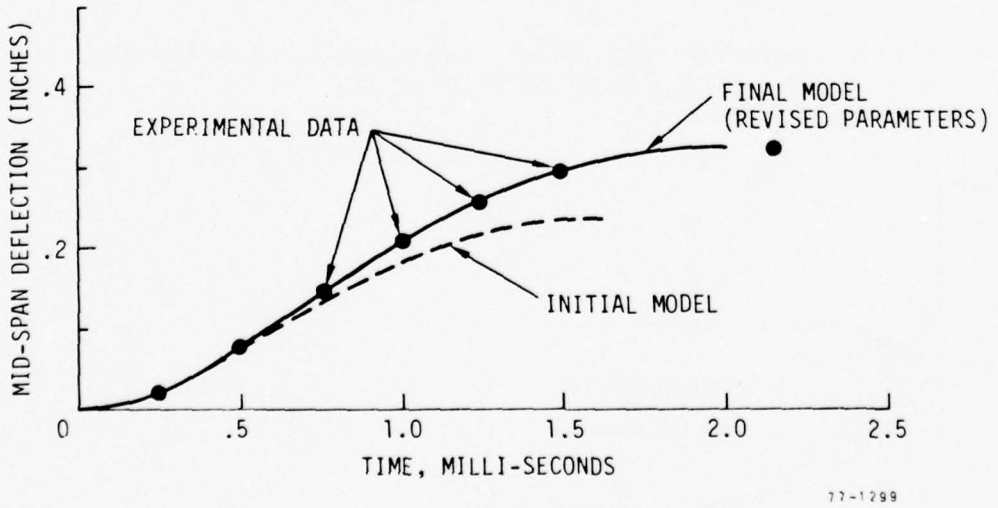

Figure 5-3. Deflection - Time History of Slab ED 1, Showing the Initial and Final Model Results.

*The variance is equal to the square of the standard deviation. See Reference 14.

TABLE II

A. PARAMETER VALUES AND PERCENT ERROR

PARAMETER	INITIAL		ESTIMATES FOR SLAB ED 1		ESTIMATES FOR SLAB ED 2		ESTIMATES FOR SLAB ED 3	
	VALUE	ERROR	VALUE	ERROR	VALUE	ERROR	VALUE	ERROR
PLIN	525.	.50	450.25	.185	448.24	.176	463.2	.169
DLIN	.14	.50	.1465	.438	.1518	.429	.161	.413
EPLAST	-178	2.00	-193.3	1.97	-213.8	1.92	-178.6	1.90
EMUØ	.8	.25	.799	.217	.834	.209	.840	.204
EMU1	1.	.25	1.0005	.238	.966	.234	.936	.229
EMUD	.14	.50	.1414	.4995	.143	.499	.143	.4994
α_o	.8	.25	.807	.214	.760	.204	.761	.195
α_d	.14	.50	.1379	.497	.133	.496	.129	.494
β	.05	4.00	.0356	3.91	.00957	3.86	.0130	3.826
P_{SCALE}	1.	.30	1.0415	.217	.9383	.16	.979	.144

	SLAB ED 1	SLAB ED 2	SLAB ED 3
INITIAL RMS VALUE	.0428	.048	.019
FINAL RMS VALUE	.0048	.0162	.00713

It is also noteworthy that the static load-deflection curve (estimated by this procedure) is a fairly good fit to the static test data. (See Figure 5-4). These results, presented in Table II and Figure 5-3, were based upon a relatively "good" prior model. That is, given the experimental static load-deflection curve of Figure 5-4, one could make a pretty fair guess about the values of the parameters P_{lin}, d_{lin}, E_{plast}, etc.

The question naturally arises, "What if one didn't have the static load-deflection curve?" In this case, he would rely on a combination of experience and analysis to come up with a prior model for the non-linear load-deflection characteristic. But then the question is, "How well would the estimation procedure perform," or more specifically, "Will the estimation procedure still arrive at a good bi-linear approximation to the experimental load-deflection curve?"

To test this problem out, a poor initial model (with a yield stress of only 200 LB/IN^2) was input to the program along with the experimental response data from Table I. The results are shown in Table III and Figures 5-5 and 5-6. Referring to Figure 5-5, note that the response curve for the revised model matches the experimental data almost exactly, although the initial (prior) model gives rather poor results.

Figure 5-6 shows similar results, where the load-deflection curve for the final model is much closer to the experimental data than is the initial model. These preliminary results were encouraging, and it appeared that the 1 d-o-f model (as used herein) was able to match the experimental response for deep slabs.

Refer again for a moment to Table II. Note that Table II contains both the initial estimates of error in the parameters as well as revised error estimates. For some parameters (e.g., EMUD), the initial error estimate was 50%, and after data for three slabs had been supplied to the computer program, the error was barely reduced (i.e., the revised error was 49%). However, note that other parameters (like PLIN, for example) began with an estimated error of 50%, which was subsequently reduced to 17%, i.e., a significant improvement.

Thus, it seemed that everything was working exactly as had been intended, and the parameters (see Table II) were coming out with "reasonable" values. At the suggestion of the Technical Monitor, we simplified the model from ten parameters (Table II) to four parameters, namely:

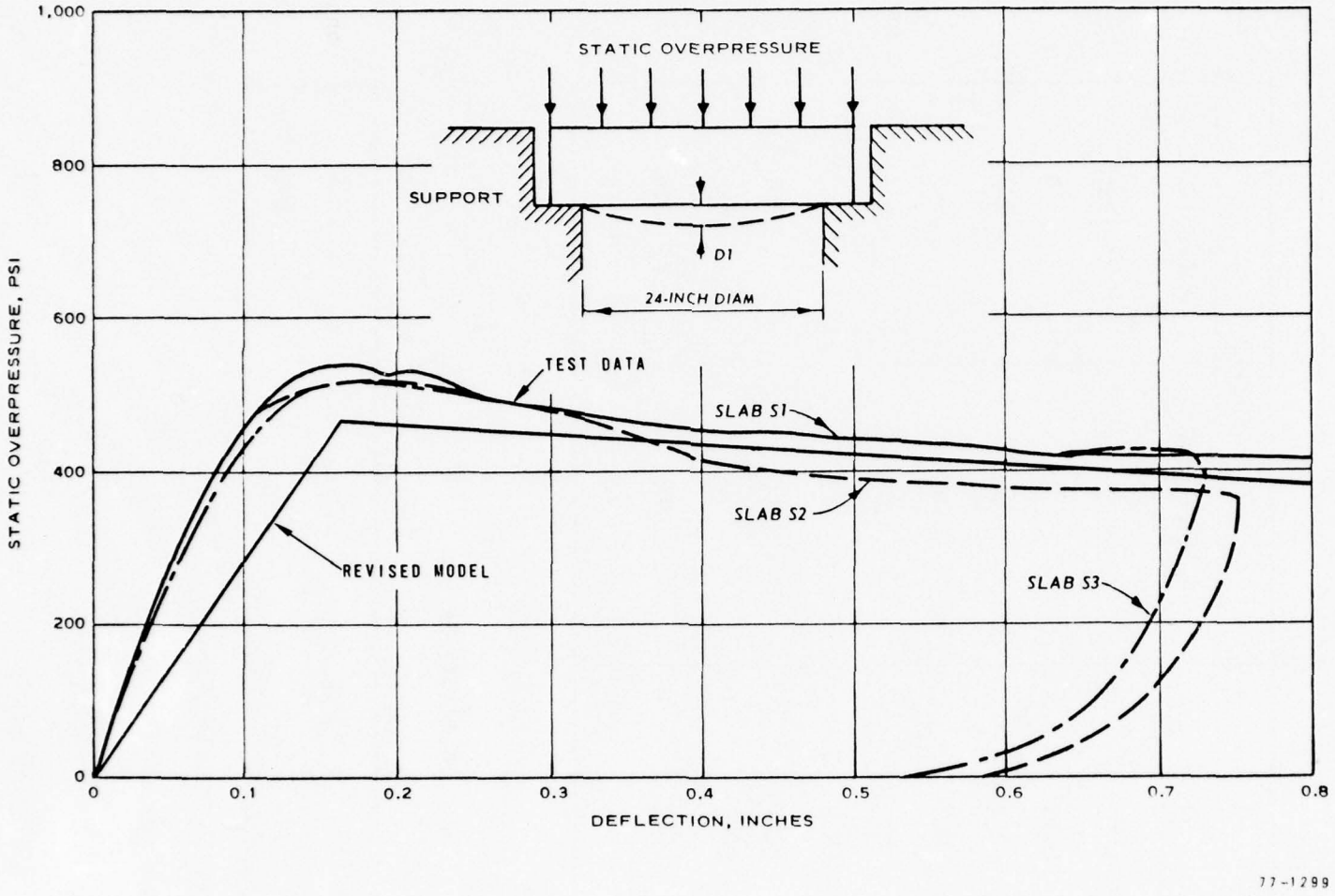

Figure 5-4. Pressure Versus Midspan Deflection: Test Data and Revised Model

TABLE III

A. PARAMETER VALUES, BEGINNING WITH A POOR MODEL

	SLAB ED 1	
	INITIAL VALUE	FINAL VALUE
PLIN	200.00	399.700
DLIN	.07	.105
EPLAST	10.00	11.500
EMUØ	.80	.792
EMU 1	1.00	.965
EMUD	.07	.082
ALPO	.80	.794
ALPD	.07	.030
BETA	.05	.056
PSCALE	1.00	1.016

B. RMS DEVIATION

INITIAL MODEL	.173
FINAL MODEL	.0049

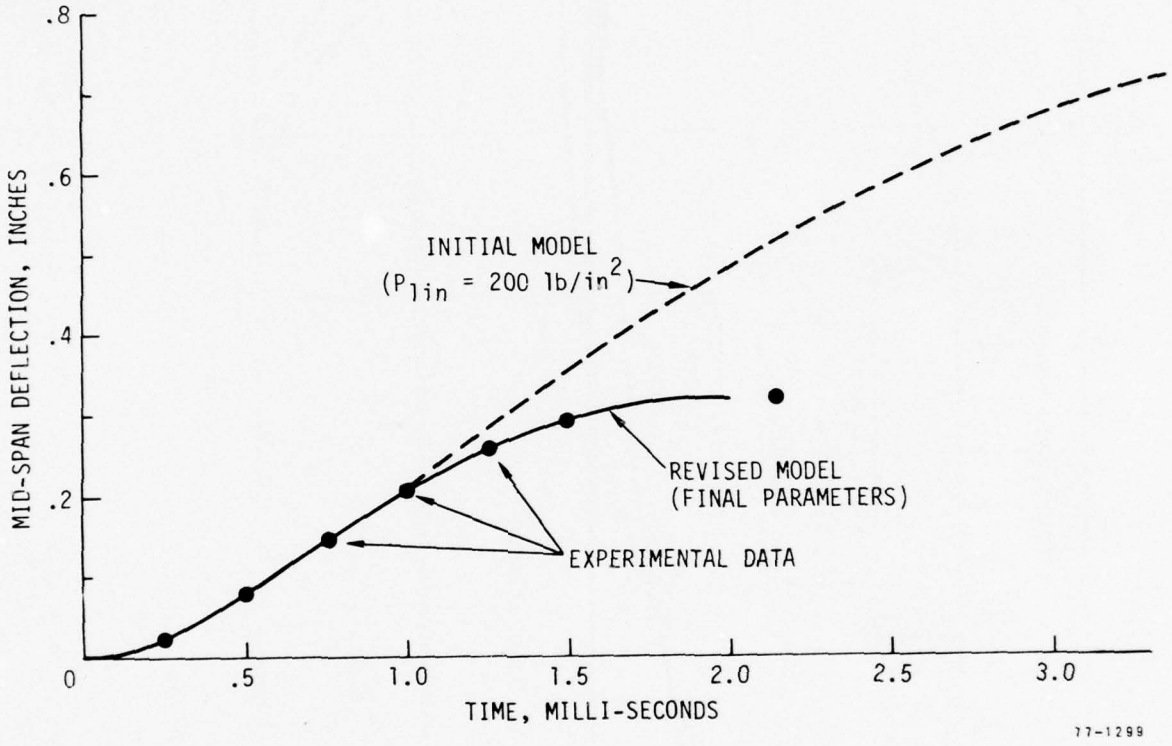

Figure 5-5. Deflection - Time History, Beginning With a Poor Prior Model

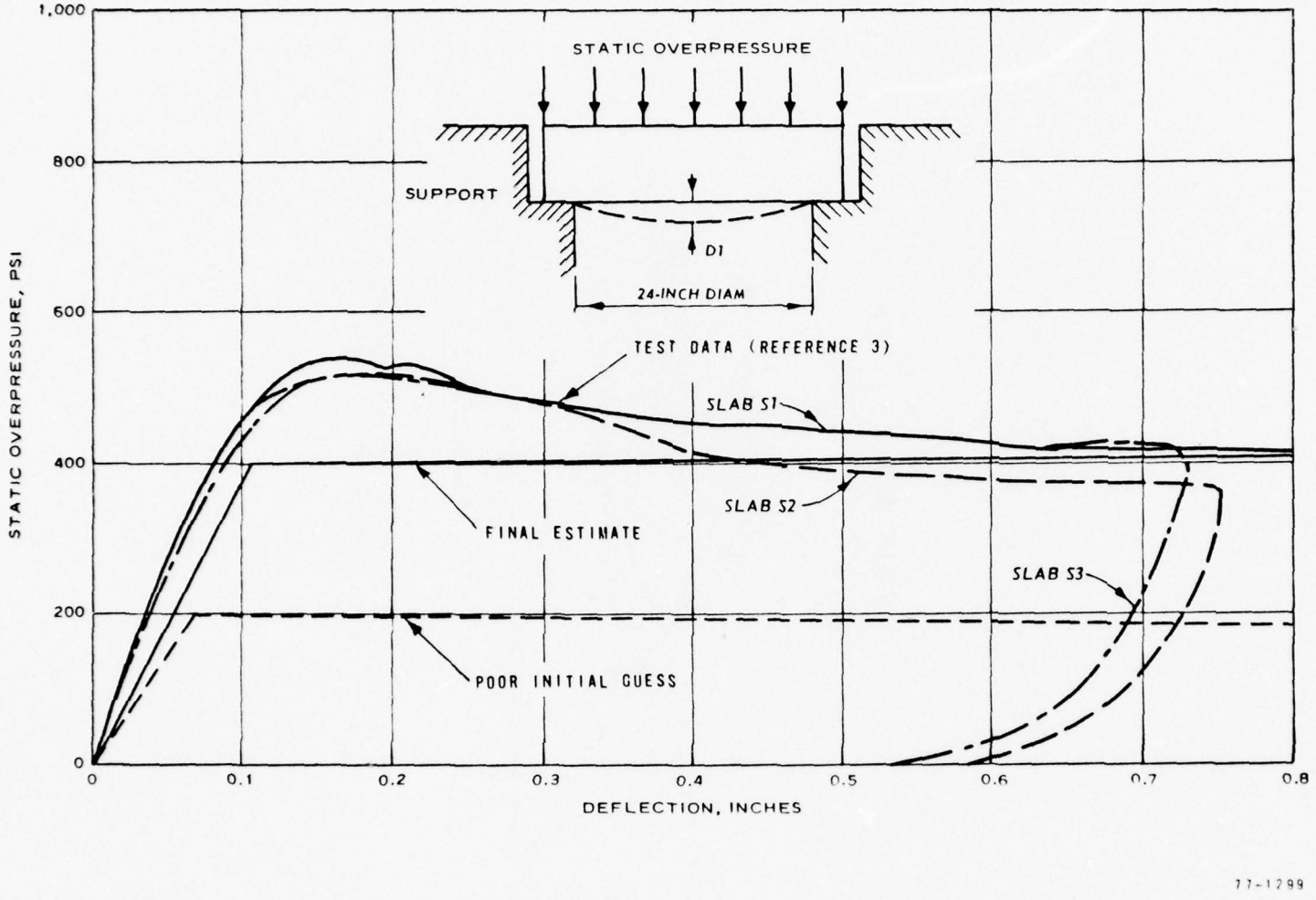

Figure 5-6. Pressure Versus Midspan Deflection Showing Test Data, Poor Initial Guess, and Final Estimate

- A single mass parameter, μ_{avg}
- Two spring-force parameters (P_{lin} and d_{lin})
- And one force parameter, P_{scale} (the α value was set equal to unity).

The results of this "four-parameter model" are shown in Table IV, and Figures 5-7 through 5-9, respectively, for slabs ED1, ED2, and ED3. Note that by adjusting these four parameters (μ, p_{lin}, d_{lin} and p_{scale}). The parameter estimation program was still able to closely fit the displacement time-histories. The parameters still seemed to have reasonable values, but it was somewhat disturbing that the force-deflection parameters (p_{lin}, d_{lin}) did not match the static load-deflection data as well as had been expected. These discrepancies were thought to be due to slight variations in the individual slabs, however.

At this point in the study, everything looked rosy, and it was (somewhat naively) assumed that similar results would be obtained for the other types of slabs as well. However, that was not the case, as is discussed in the sections which follow.

5.3 RESULTS FOR BROWN AND BLACK'S CONVENTIONAL R/C SLABS (Reference 5)

Reference 5 provides both static and dynamic test data on conventional R/C slabs, where the slabs were square in plan and had a span of 29 inches and a thickness of .89 inches. The static test data are shown in Figure 5-10. Note that these static tests were continued to destruction of the slab, i.e., until the slab could carry no more load, at a deflection of approximately 4 inches. At this point in the test, the concrete was highly fractured, and the reinforcing steel was stretched to its ultimate capacity. (For additional details and photograph of the damaged slabs, see Reference 5).

Brown and Black's tests are noteworthy for the fact that they determined the ultimate pressure capacity of their slabs (From 20 to 25 psi, see Figure 5-10) and the corresponding maximum deflection (i.e.,about 4 inches). This information was not obtained for Watt's deep slabls, discussed previously (cf. Figure 5-6). Thus, from their static tests, Brown and Black knew that a deflection of about 4 inches corresponded to the ultimate capacity of their slabs. Yet, in the dynamic tests (see Figure 5-11), the slabs were all driven to amplitudes well in excess of 5 inches.

Not surprisingly, each of the dynamically tested slabs was severely damaged. (See Reference 5 for photos of the tested slabs). These tests

Table IV

Estimated Parameters for Watt's Slabs

PARAMETER	SLAB ED 1	SLAB ED 2	SLAB ED 3
MASS COEFFICIENT μ	.93	1.00	.95
YIELD FORCE P_{lin}	400	360	443
ELASTIC DISPLACEMENT d_{lin}	.137	.173	.168
PRESSURE SCALE FACTOR P_{scale}	.96	.82	.90
RMS DEVIATION ΔRMS	.005	.015	.003

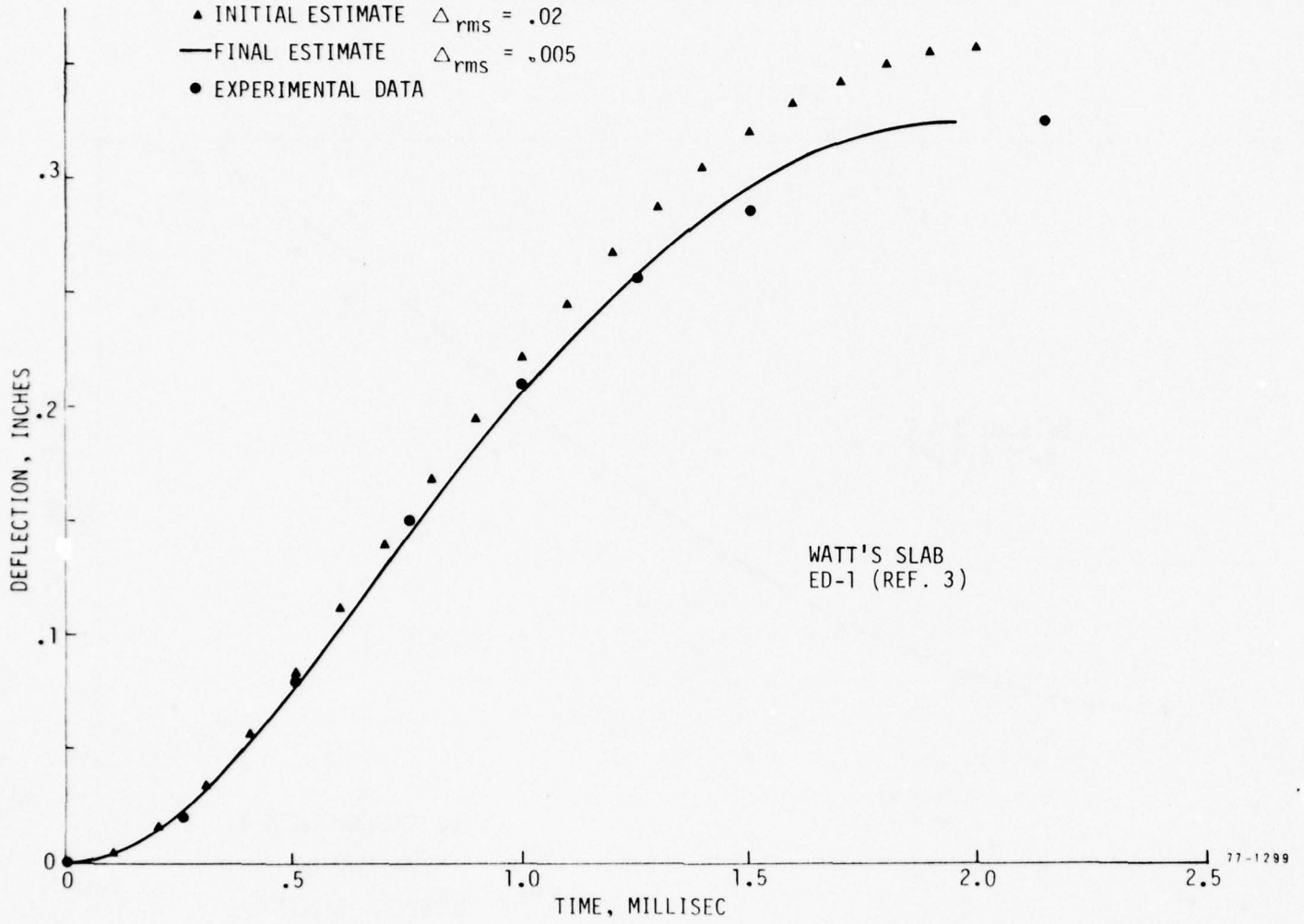

Figure 5-7. Deflection Time-History Fitted by Four-Parameter Model. (Watt's Slab ED-1, Reference 3)

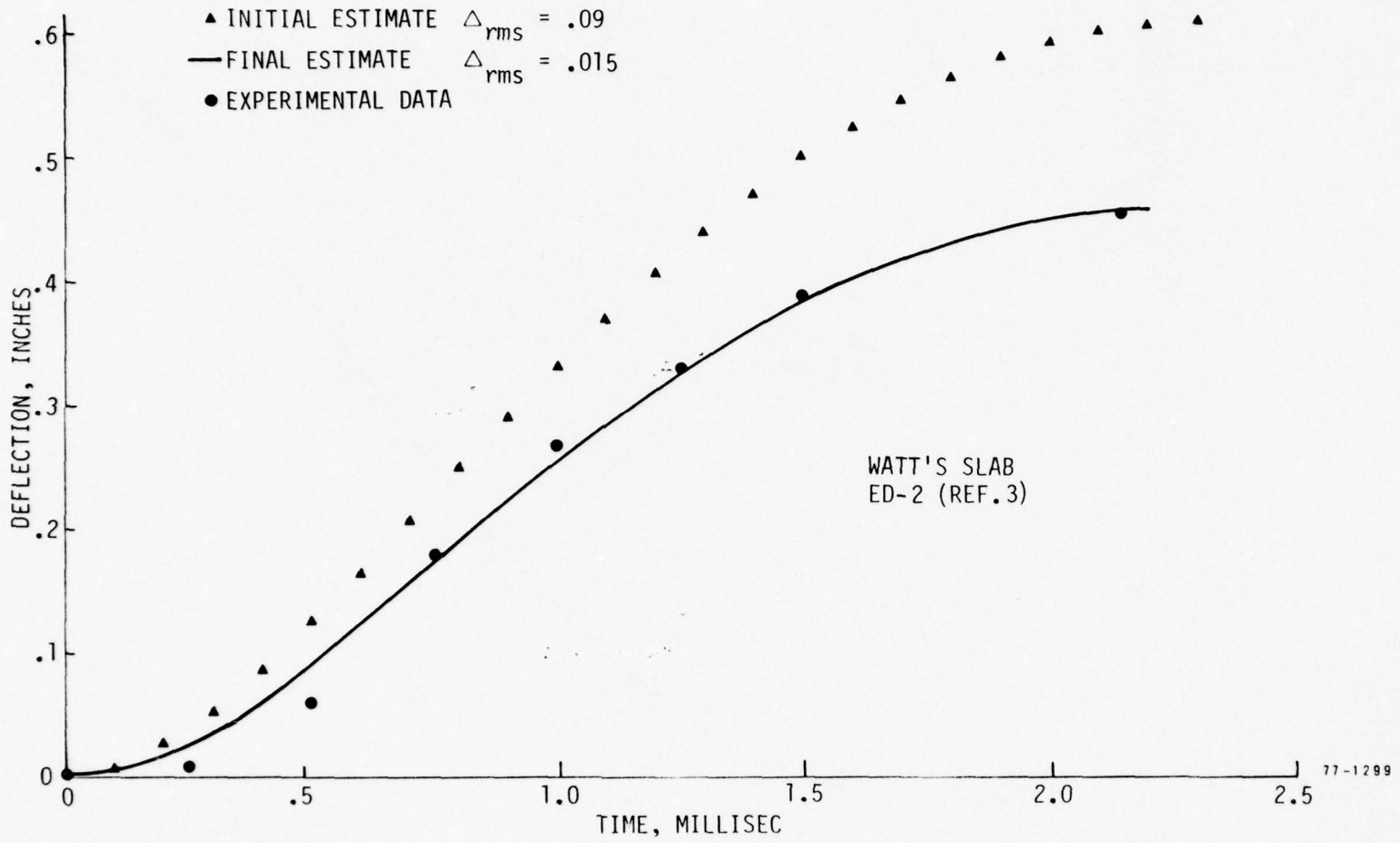

Figure 5-8. Deflection Time-History Fitted by Four-Parameter Model. (Watt's Slab ED-2, Reference 3)

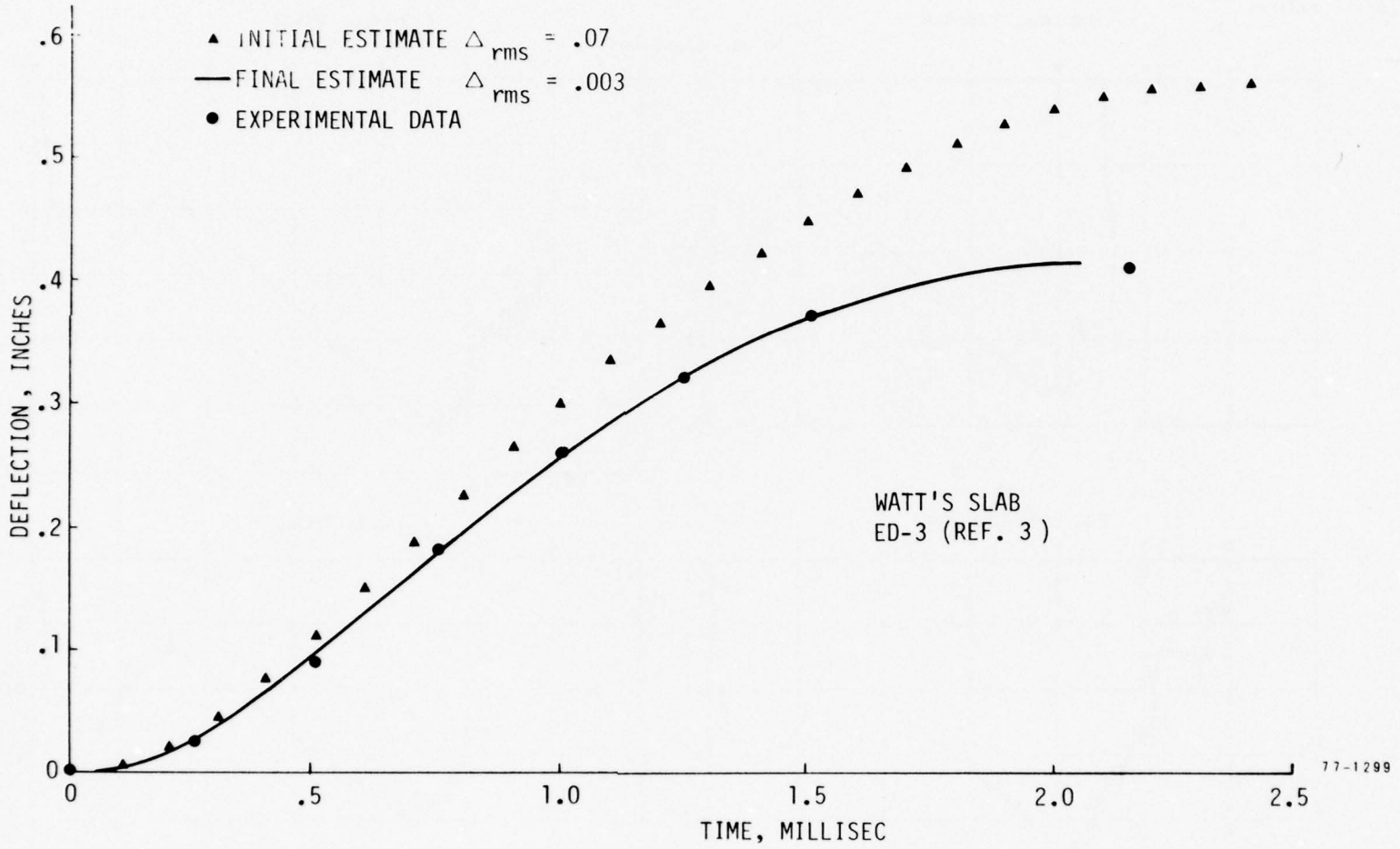

Figure 5-9. Deflection Time-History Fitted by Four-Parameter Model. (Watt's Slab ED-3, Reference 3)

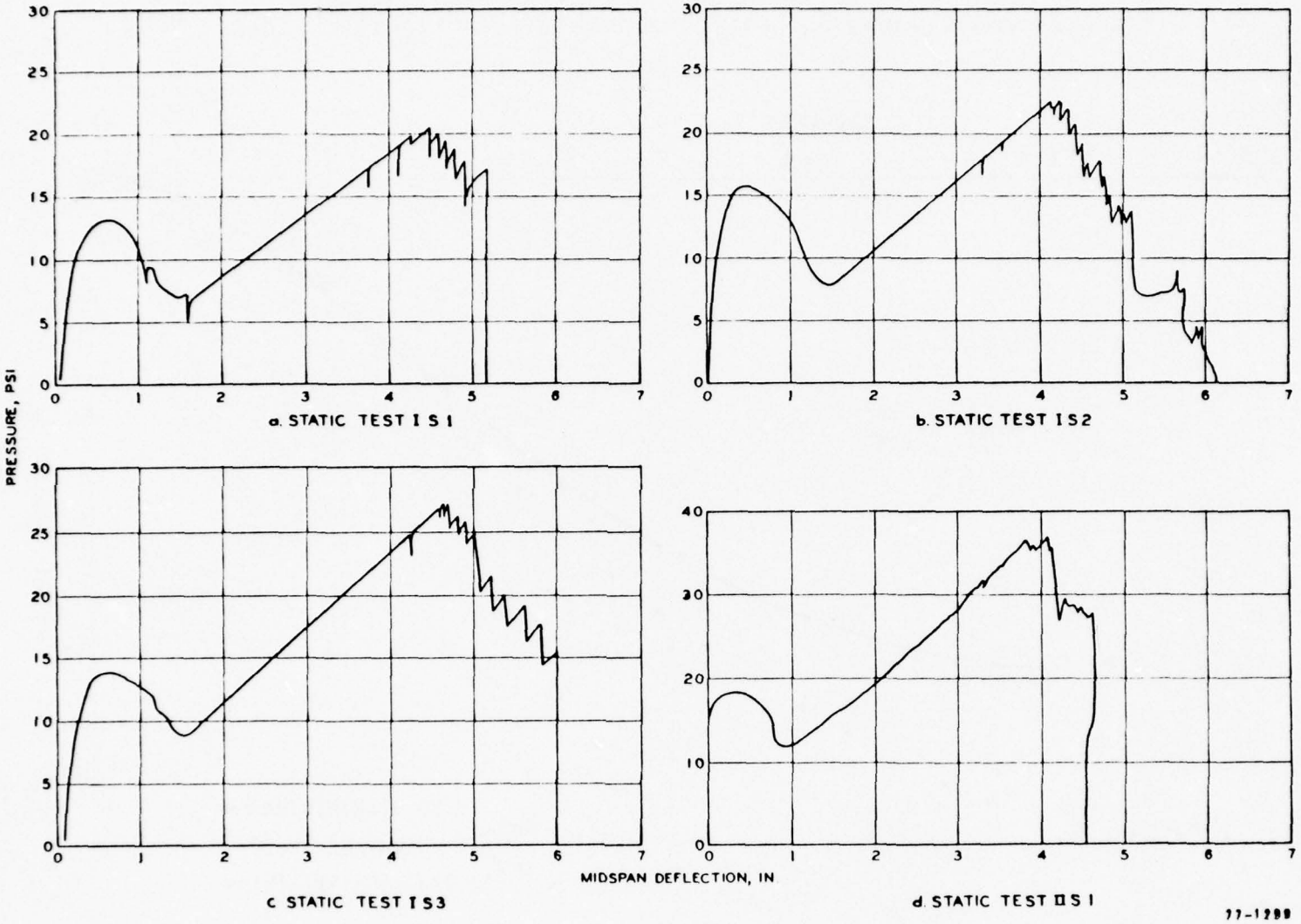

Figure 5-10. Pressure Versus Midspan Deflection, Static Tests of Slabs IS1, IS2, IS3, and IIS1 (Reference 5)

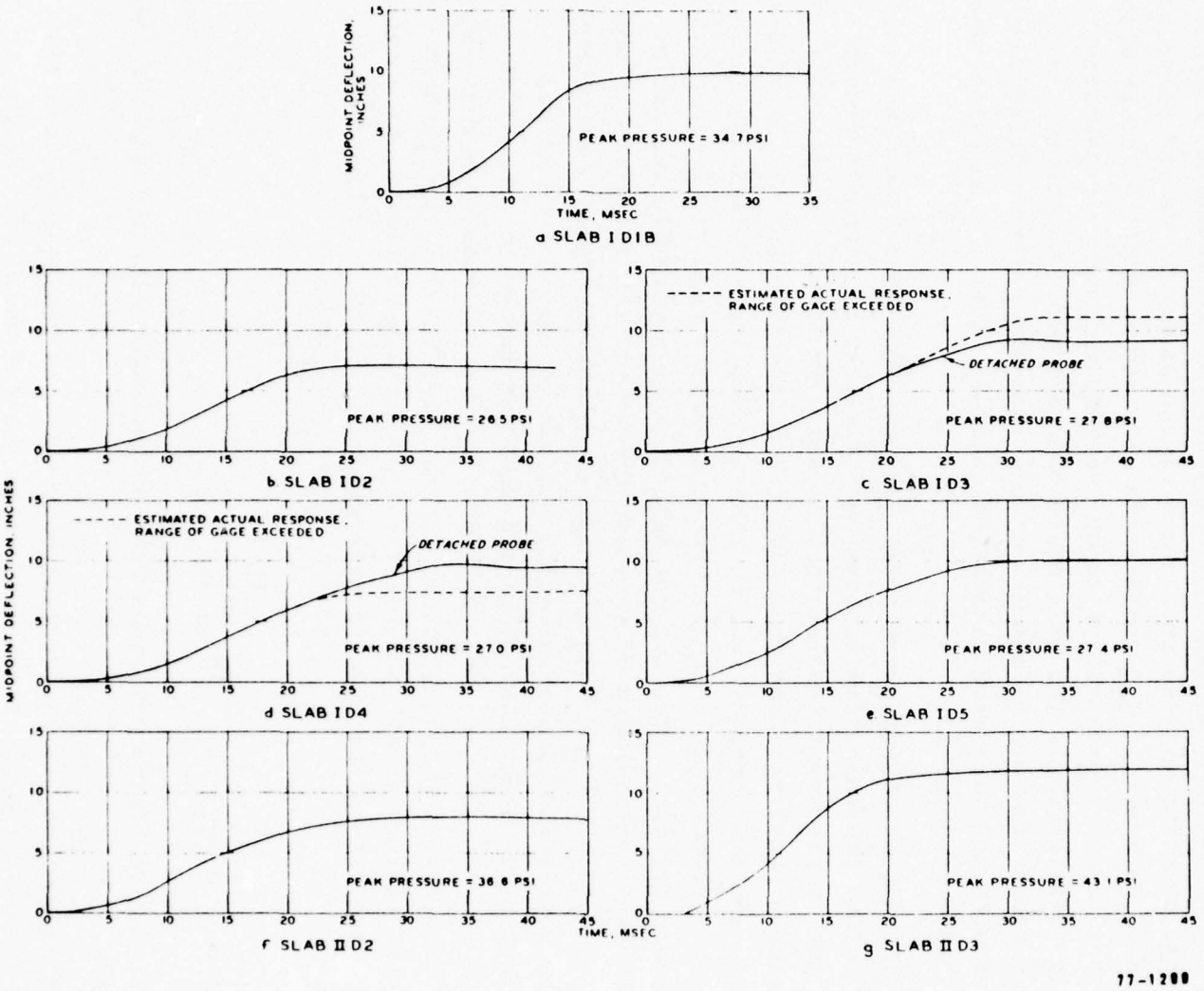

Figure 5-11. Dynamic Deflection-Time Histories for Brown and Black's Slabs (Reference 5)

(by Brown and Black) were therefore fundamentally different than Watt's tests, where the ultimate capacity of the slabs was not measured, and the dynamic tests were run at less than the ultimate strength. On the other hand, the authors of Reference 5 did measure the ultimate strength of their slabs, and then they tested (dynamically) to well-beyond the static capability. These basic differences in the test philosophy and test results were not immediately recognized by the writer. It was only after difficulties were experienced with the parameter estimation procedure that a closer look was made into the test details.

Initially, a 10-parameter model was used to fit the test data for slab ID-2. (The pressure-time history for this test is given in Figure 5-12, and the displacement time-history is shown in Figure 5-13.) This multi-parameter model resulted in a good fit to the time-history data (see Figure 5-14) and the force-deflection results also looked promising (cf. Figure 5-15). However, in contrast with the earlier results (Section 5.2) the parameters for α, μ, etc, did not appear to be physically realistic. To get a better understanding of what was happening, the 10-parameter model was simplified (e.g., μ was held constant, α was held constant, etc.) but E_{plast} (the post-yield slope) was still allowed to vary (since it was expected that a bi-linear characteristic would be needed to approximate the force-deflection curve). Several parameter estimation runs were then made (they are tabulated in Table V) each with the same result: the program arrived at a "nearly-linear" force-deflection curve when fitting the dynamic test data. The fit to the dynamic data was fairly good in each case, as denoted by

$$\Delta_{rms} = \left\{ \frac{1}{N} \sum_{i=1}^{N} \left(y_{th_i} - y_{ex_i} \right)^2 \right\}^{1/2}$$

which is a measure of the deviation between the model (theory) and the test (experiment).

At this point, it was decided to try to use a linear force-deflection curve and see what the parameter estimation program would do. Again, it achieved a fairly good fit to the dynamic test data, with Δ_{rms} less than .01. (See the last line of Table V.) These results were disturbing, at least initially, since they were unexpected. What had been expected was that some form of strain-hardening (e.g., like Figure 5-15) would be required to satisfactorily fit the dynamic data. It was thought that the strain-

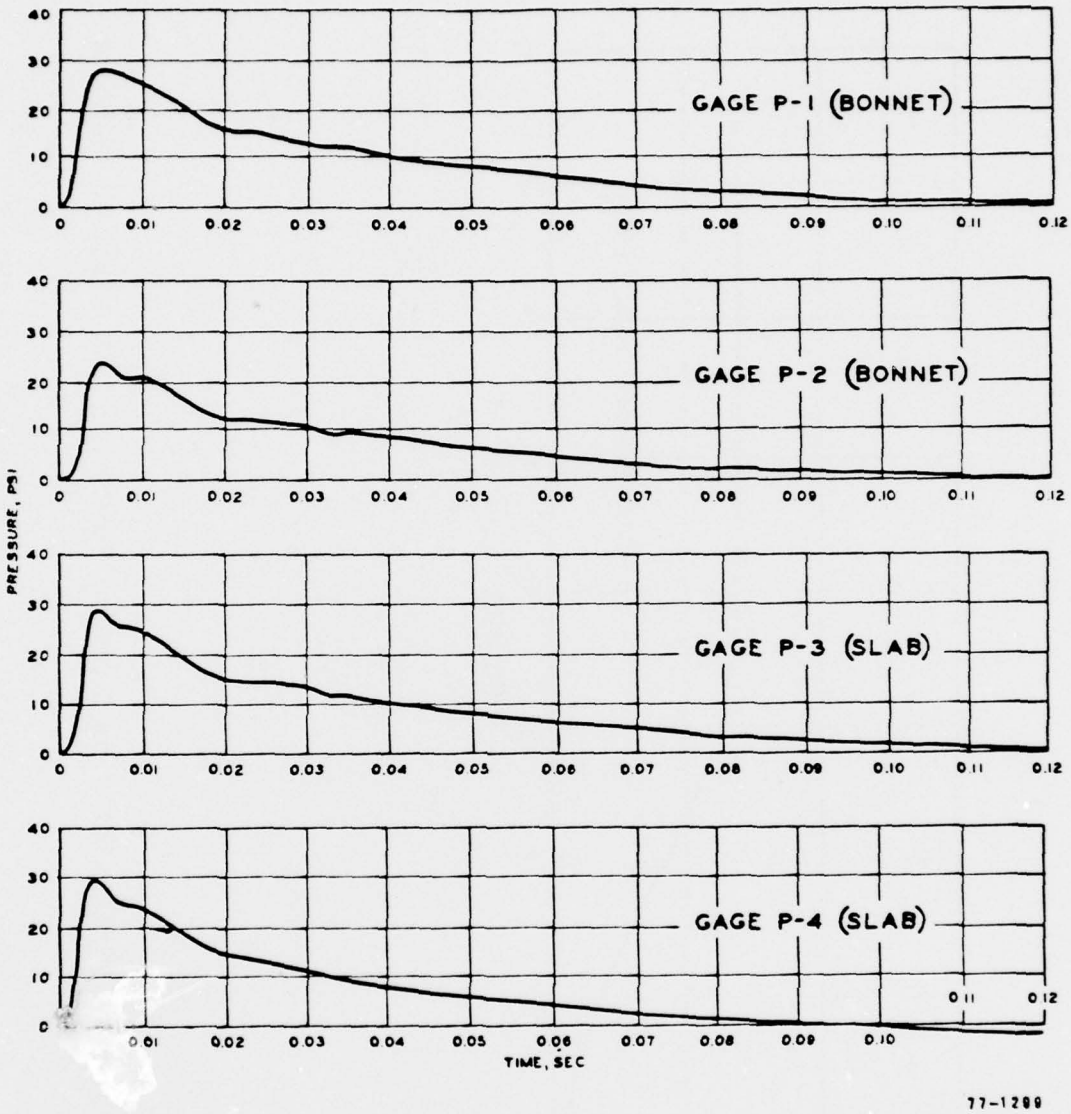

Figure 5-12. Overpressure-Time Records for Slab D2 (Reference 5)

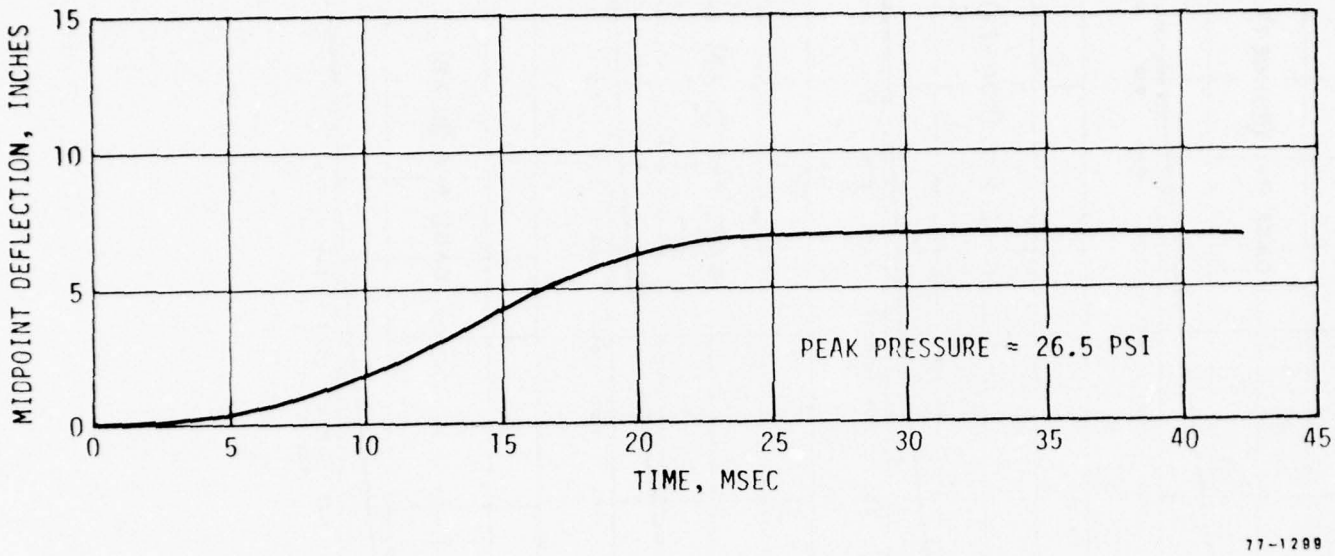

Figure 5-13. Dynamic Deflection-Time History for Brown and Black's Slab ID2

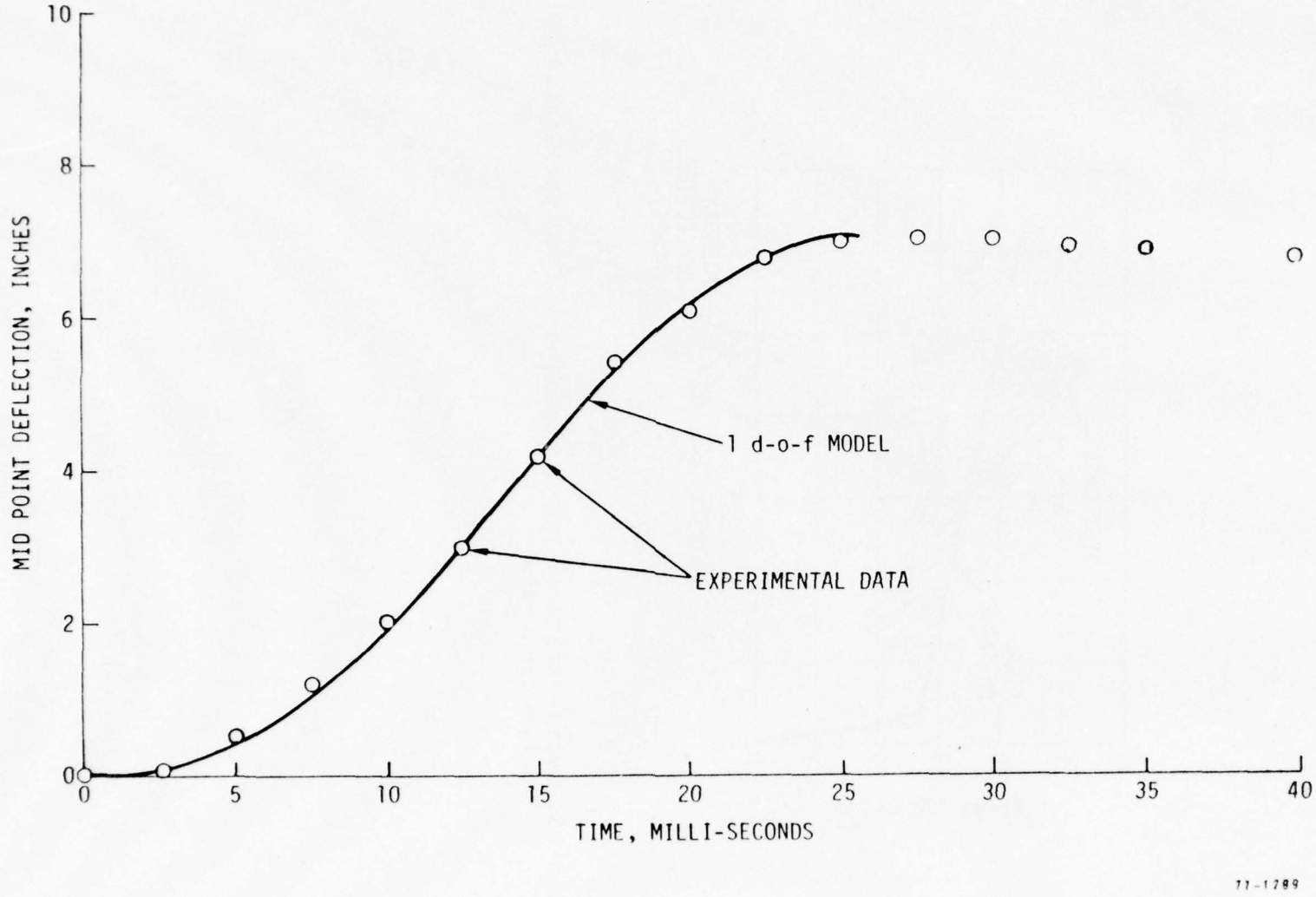

Figure 5-14. Deflection- Time Histories for Conventional Slab (Reference 5) and Multi-Parameter Model

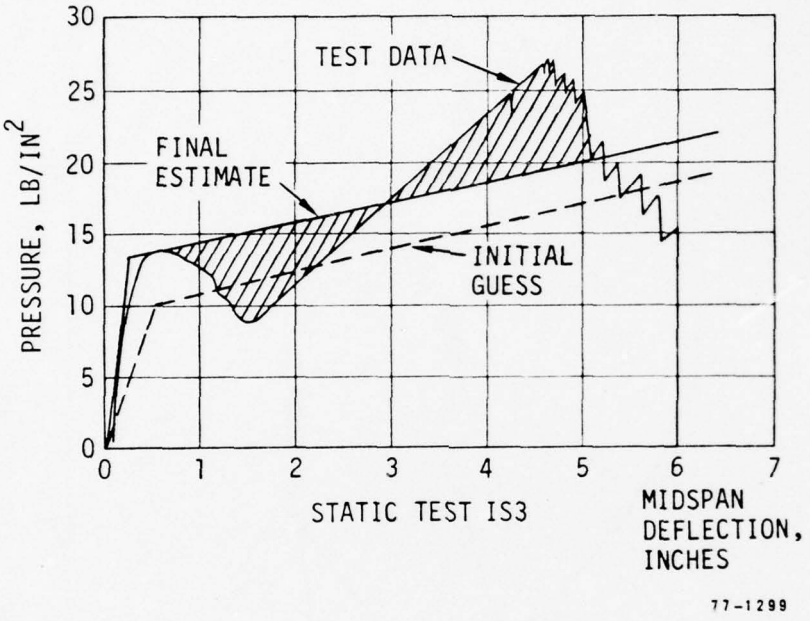

Figure 5-15. Multi-Parameter Model, Showing Fit to the Static Force-Deflection Data

Table V

Parameters Which "Fit" Brown and Black's Dynamic Data (Slab ID-2)†

α_0	α_d	α_1	μ_0	μ_d	μ_1	P_{lin}	d_{lin}	k*	E_{plast}	P_{scale}
.61	2.7	1	1	0	1	2.4	.57	4.2	2.7	1.0
.49	2.7	1	.59	.53	1	2.3	.59	3.9	2.8	1.0
.40	1.8	1	---	---	1.21	2.2	.54	4.0	3.7	1.8
.41	3.5	1	1	0	1	2.8	.53	5.3	3.7	1.8
.31	2.3	1	.69	.54	1	2.6	.55	4.8	3.5	1.8
.34	2.9	1	.60	.55	1	2.7	.54	4.9	3.5	1.7
.34	2.9	1	.60	.55	1	32.4	9.0	3.6	.01	1.6

†The parameters listed herein gave a "fit" measured by Δ_{rms} of .10 or better.

*$k = p_{lin}/d_{lin}$ is the elastic slope

hardening would be required because the static load-deflection data was strongly non-linear (c.f. Figure 5-10). However, the parameter estimation equations kept fitting the dynamic data and using a nearly-linear model to do so.

Finally, after some hand calculations using the method of equivalent linearization (Reference 15) it was recognized that the dynamic data (or at least the maximum deflection, δ_{max}) can <u>always</u> be fitted by an "equivalent linear model". For any loading function, p(t), the response of the 1 d-o-f system is well-approximated by

$$y(t) = (1 - \cos \omega_{eq} t)\ \delta_{max} \tag{5-1}$$

where ω_{eq} is the frequency of the equivalent linear oscillator,

$$\omega_{eq}^2 = \frac{k_{eq}}{m} \tag{5-2}$$

and k_{eq} is the "equivalent linear stiffness".

If one begins with the non-linear differential equation

$$m\ddot{y} + f_{nl}(y) = p(t) \tag{5-3}$$

and the approximate solution

$$y(t) = \delta_{max}\ (1-\cos\ \omega_{eq} t) \tag{5-4}$$

(where $f_{nl}(y)$ is <u>any</u> non-linear force-deflection curve) then multiplying both sides of the equation (5-3) by

$$\dot{y} = \omega_{eq} \delta_{max} \sin \omega_{eq}\ t \tag{5-4}$$

and integrating the result gives

$$\frac{m\dot{y}^2}{2} + \int f_{nl}(y)\ \frac{dy}{dt}\ dt = \int p(t)\ \omega_{eq} \delta_{max} \sin \omega_{eq}\ t\ dt \tag{5-5}$$

The limits on the integration are from y=0 to $y=\delta_{max}$, or in terms of the time, t, from t=0 to $t = \frac{\pi}{\omega_{eq}}$. At both these times, the velocity, $\dot{y}$, is zero, and the kinetic energy term vanishes. Equation (5-5) then reduces to

$$\int_0^{\delta_{max}} f_{nl}(y)dy = \int_0^{\pi/\omega_{eq}} p(t)\omega_{eq}\delta_{max} \sin \omega_{eq} t\ dt \tag{5-6}$$

which says that the strain energy (stored in the nonlinear spring) is equal to the "work done" by the applied force p(t).

As a first approximation, one might try $p(t) = p_o$ = a constant, if the loading function does not change much during the initial response. Then, the right-hand-side of equation (5-6) gives

$$\int p_o \omega_{eq} \delta_{max} \sin \omega_{eq} t \, dt = 2 p_o \omega_{eq} \delta_{max} \tag{5-7}$$

and one finally has

$$\int_0^{\delta_{max}} f_{nl}(y) dy = 2 p_o \omega_{eq} \delta_{max} \tag{5-8}$$

which can be solved for the equivalent linear frequency (ω_{eq}) and thence the equivalent linear stiffness (k_{eq}). Note that ω_{eq} is given in terms of the area (strain energy) under the force-deflection curve, and the maximum displacement, δ_{max}. Also note that no restriction has been placed on the force-deflection characteristic, $f_{nl}(y)$.

Based upon the foregoing discussion, it is the author's opinion that the parameter estimation algorithm performed an "equivalent linearization" (or something similar) to achieve a good fit to the dynamic test data of Reference 5 with a nearly-linear force-deflection curve. If this hypothesis is correct, it is only natural to inquire as to why something similar did not occur previously, e.g., in the case of Watt's slabs (Section 5.2). A possible explanation for this difference in behavior is that Watt's slabs were tested in a "moderately nonlinear" range (with the maximum deflection δ_{max} equal to just 2 or 3 elastic deflections, d_{lin}) whereas Brown and Black's slabs were loaded to their ultimate capacity. For the latter, the maximum deflections were on the order of 15 to 20 times the elastic deflections. As stated previously, there was a fundamental difference in the testing philosophies used in References 3 and 5. This point will be discussed in more detail in Section 5.9.

5.4 RESULTS FOR KEENAN'S "LACED" R/C SLABS (REFERENCE 6)

Reference 6 presents results for static and dynamic tests of uniformly-loaded one-way reinforced, "laced" slabs. The slabs had a span of

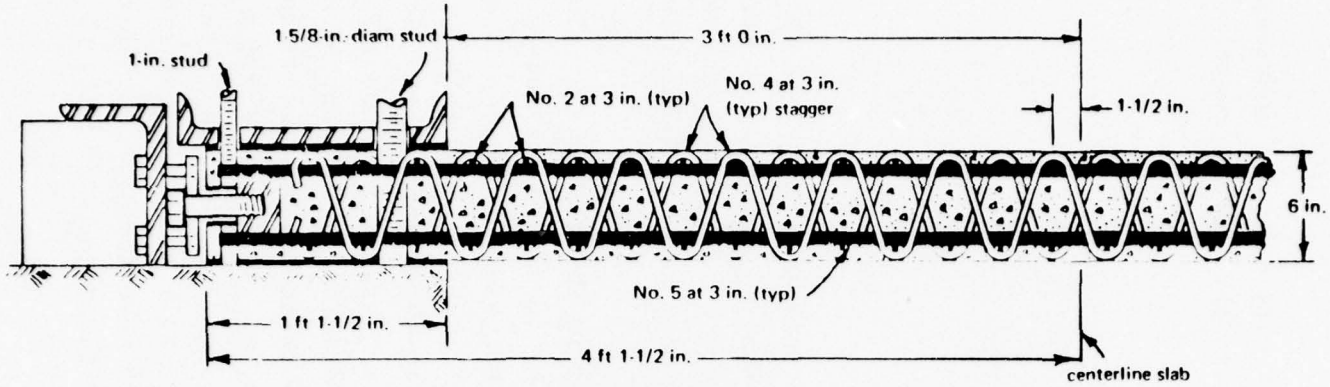

(a) Typical longitudinal section.

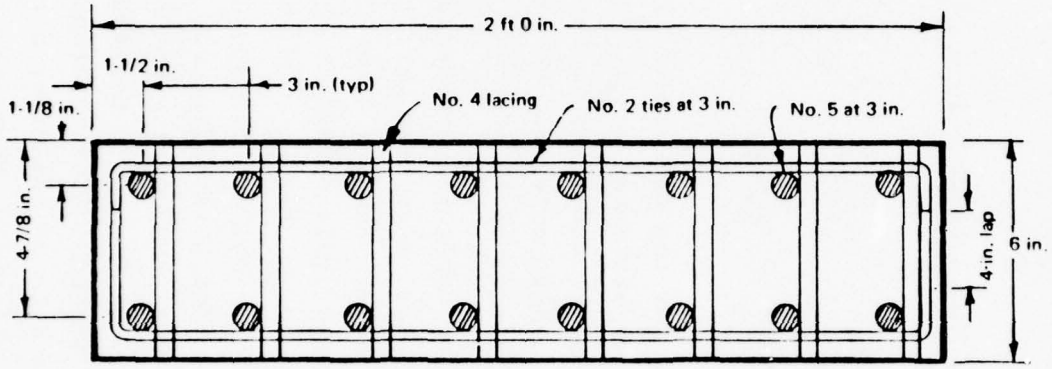

(b) Typical transverse section.

77-1299

Figure 5-16. Typical Longitudinal and Transverse Section of Laced Slab (Keenan, Reference 6)

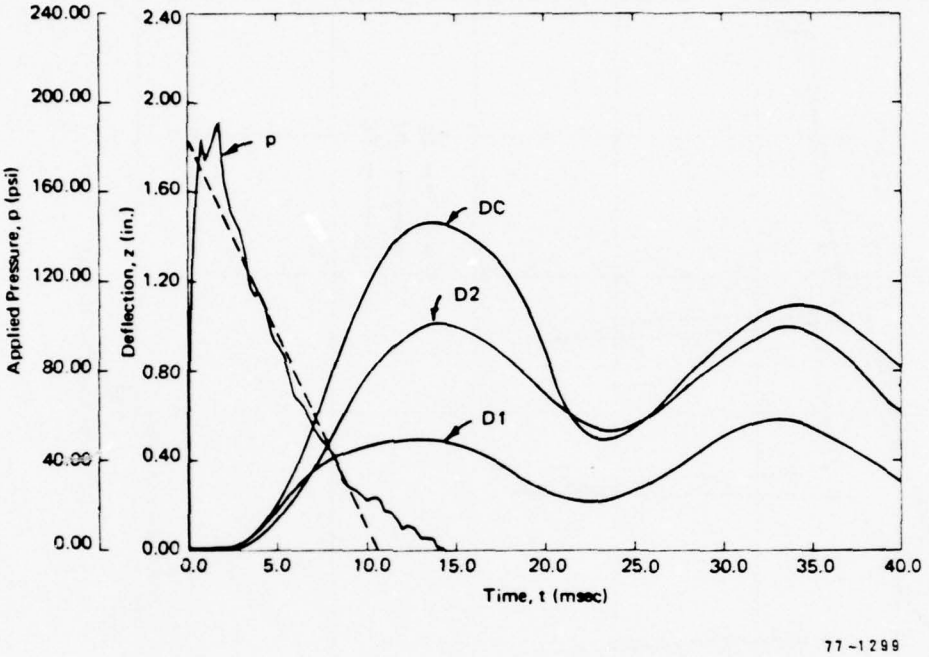

Figure 5-17. Time Variation of Pressure and Deflection, Slab D3-1 (Keenan, Reference 6)

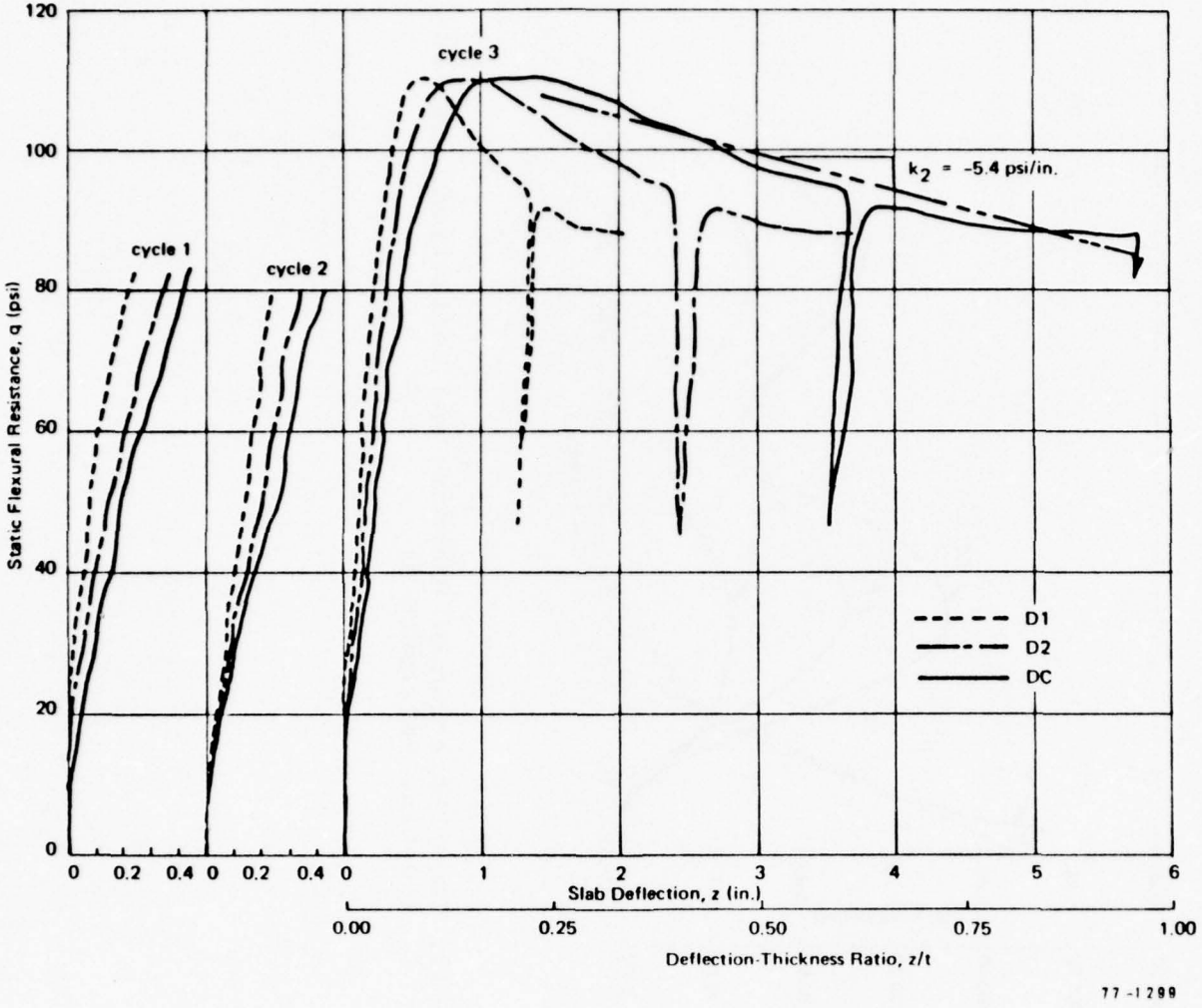

Figure 5-18. Static Load Deflection Relationship of the Slab (Keenan, Reference 6)

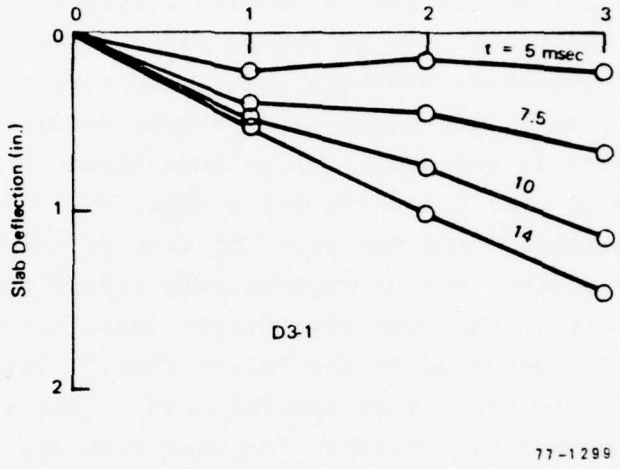

Figure 5-19. Variation of Deflection Across the Semi-Span (Keenan's Slab D3-1)

6 feet (72 inches) and a thickness of 6 inches, giving a span-to-depth ratio of 12. These slabs are unusual because of their "lacing" reinforcement, which is shown in Figure 5-16. Keenan's tests are also unusual by virtue of the fact that the tests were conducted at several different pressure levels. Recall that Watt's tests (Reference 3) and Brown and Black's (Reference 5) were each conducted at basically a single (dynamic) pressure level. Keenan recognized that a nonlinear system (such as an R/C slab) should be tested throughout its nonlinear range. Thus, his tests began at a low level of (dynamic) pressure, p(t), and became progressively more severe. However, a testing program of this type requires either several identical specimens (which is expensive) or several tests on the same specimen (which results in cyclic loading and progressive failure). Both alternatives are undesirable, from the point of view of the test engineer. Keenan chose the latter course, and he successively tested the slabs to higher and higher pressures. The most significant data, from the point of view of the present study, occurred on the "first shot." Thus, the attention is focused herein on Keenan's test specimen D3-1. The pressure vs. time history and displacement time history for this slab are shown in Figure 5-17. A typical static pressure vs. deflection curve for such slabs is shown in Figure 5-18.

Referring to Figure 5-17, note that there are three displacement traces, namely D1, D2, and DC. These traces refer to three separate displacement-measuring gages, mounted at points along the span of the slab, with gage, DC in the center. By using three displacement gages (instead of just one, in the center) Keenan observed that the displacements varied in space, as well as with time. For example, Figure 5-19 shows the readings of the three displacement gages (connected by straight lines) at identical times. It is clear from Figure 5-19 that more than one mode is participating in the response, and in particular, it appear that the first mode (like $\sin \frac{\pi x}{L}$) is interacting with the third mode (like $\sin \frac{3\pi x}{L}$).

Several attempts were made to "fit" the central response (gage DC) of Keenan's slab D3-1 to the one degree-of-freedom model. The results which were successful are given in Table VI in terms of the model of parameters. Of particular note was the fact that the "force coefficient", α, was always estimated as befinning at a very low value (e.g., .02, etc.) initially. Attempts to fit the response curve with a constant α (like an α_{avg} such as was successful with Watt's slabs) were totally unsuccessful in this case.

Table VI

Parameters Which "Fit" Keenan's Dynamic Data (Slab D3-1)*

α_0	α_d	α_1	μ_0	μ_d	μ_1	P_{lin}	d_{lin}	E_{plast}	P_{scale}
.028	.22	1	.61	.97	1	75	.14	-.88	1.6
.018	.22	1	.76	1.0	1	85	.16	-.85	2.0
.033	.14	1	.86	.99	1	71	1.3	.01	1.0
.031	.14	1	.85	.98	1	68	1.2	.01	1.0
.022	.25	1	.53	.96	1	74	.18	.01	1.6
.014	.25	1	.61	.98	1	82	.18	.01	1.9

* The parameters listed herein gave a "fit" measured by Δ_{rms} of .10 or better.

By beginning with $\alpha_o \simeq .02$ and then going up to $\alpha_1 = 1$, the force coefficient deemphasized the initial pressure peak, since the force applied to the 1 d-o-f model is given by the product of α and p(t). Without this significant "re-shaping" of the pressure pulse, it was not possible to achieve a very good fit to the dynamic response data for Keenan's laced slabs.

Keenan's tests used prima-cord explosives placed in vented firing tubes to produce the dynamic over-pressure on the slabs. Possibly, because of non-uniformity of pressure loading or perhaps because of gas leakage (around the edges of the slab) Keenan's initial pressure reading may have been too high. Or, another possibility is that the interaction of the fundamental mode with the higher modes occurred in such a fashion that the "effective force" on the fundamental mode was initially reduced.

In that regard, it is worth noting that tha slab failure occurred (both statically and dynamically) with a hinging action at the supported ends and in the center (see Figure 5-20). Yet from the linear theory of vibrations, one expects the slab to respond initially (i.e., at small amplitudes) in terms of the vibration modes of a clamped-clamped beam. Thus, the slab response must make a (fairly significant) transition from several vibration modes at small amplitudes to a hinged mode at large amplitudes. This modal transition might be the "cause" of the reduced force coefficient (α) which the estimation algorithm seems to require in fitting the response data for Keenan's slab D3-1.

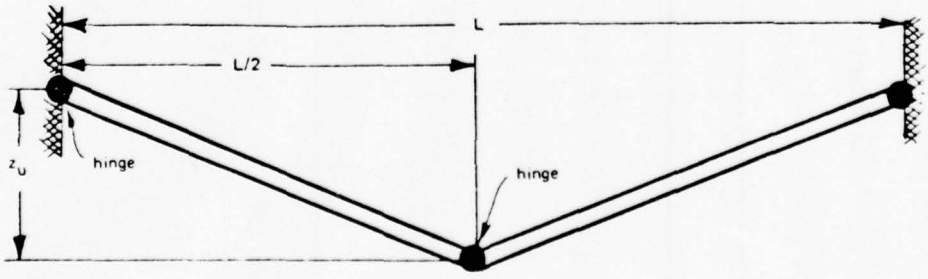

Figure 5-20. Deflection Mode Typical of Keenan's Laced Slabs (Reference 6)

5.5 SENSITIVITY OF THE RESULTS TO MODEL PARAMETERS

In the parameter estimation algorithm, the "sensitivity matrix", [T], is calculated and used in arriving at the revised parameters. The individual elements of [T] constitute the "change in response per unit change in a given parameter," and these sensitivities are tabulated in the computer printout. To give the reader a feeling for which parameters have the most significance, Tables VII through IX have been prepared. These tables give the sensitivities at three locations in the dynamic response time-history, namely

(i) the sensitivities during the initial response, when the deflection is near zero,

(ii) the sensitivities at the mid-response, when the velocity is a maximum, and

(iii) the sensitivities at the maximum response.

Admittedly, Tables VII through IX are somewhat misleading, in that the absolute sensitivities(which are used and output by the computer program) have been tabulated. Thus, Table VII gives $\Delta y_1/\Delta\mu$ as $-2.4\text{x}10^{-2}$, which means the displacement y_1 *changes* $|2.4\text{x}10^{-2}|$ for a unit change in the mass coefficient μ. Note, however, that y_1 itself may have been only $1\text{x}10^{-2}$ initially so $\Delta y_1/\Delta\mu$ could mean a relative change in y_1 of 240%. It would be desirable (if possible) to present the relative sensitivities, like $(\Delta y_1/y_1)$ (divided by) $(\Delta\mu/\mu)$. To do so at this point in time would require many hours of searching through old computer runs and was not thought to be worthwhile. Subsequent changes to PEBLS (to print out relative as well as absolute sensitivities) are definitely indicated at a future date.

This is not to imply that Tables VII through IX are not useful; note, for example in Table IX that the sensitivity $\Delta y_i/\Delta\alpha_o$ was 75.5 at the maximum response point. Clearly y_i is very sensitive to α_o, as indicated by the high value, namely 75.5.

5.6 THREE-PARAMETER MODEL RESULTS FOR WATT'S SLABS

As stated in Section 2.4, it eventually became evident that a three-parameter model (involving λ, the load-mass factor, P_{lin} and d_{lin}) was the simplest elasto-plastic model one can consider (cf. Biggs, Reference 2). Accordingly, an attempt was made to "fit" Watt's dynamic test data using this three-parameter model. The results are summarized in Table X, which shows that a pretty fair fit (e.g., an RMS error of .01) can be obtained

Table VII

Sensitivity of the Response to Various Model Parameters (Watt's Slab ED-1)*

PARAMETER	INITIAL RESPONSE (NEAR-ZERO DEFLECTION)	MID-RESPONSE (NEAR MAXIMUM VELOCITY)	MAXIMUM RESPONSE (AT MAXIMUM DEFLECTION)
MASS COEFFICIENT, μ	$\frac{\Delta y_1}{\Delta \mu} = -2.4 \times 10^{-2}$	$\frac{\Delta y_4}{\Delta \mu} = -.17$	$\frac{\Delta y_7}{\Delta \mu} = -.20$
YIELD FORCE, P_{lin}	$\frac{\Delta y_1}{\Delta P_\ell} = -7.8 \times 10^{-7}$	$\frac{\Delta y_4}{\Delta P_\ell} = -1.4 \times 10^{-4}$	$\frac{\Delta y_7}{\Delta P_\ell} = 9.6 \times 10^{-4}$
ELASTIC DISPLACEMENT, d_{lin}	$\frac{\Delta y_1}{\Delta d_\ell} = 2.2 \times 10^{-3}$	$\frac{\Delta y_4}{\Delta d_\ell} = .31$	$\frac{\Delta y_7}{\Delta d_\ell} = .91$
PRESSURE MULTIPLIER, P_{scale}	$\frac{\Delta y_1}{\Delta P_s} = 2.4 \times 10^{-2}$	$\frac{\Delta y_4}{\Delta P_s} = .22$	$\frac{\Delta y_7}{\Delta P_s} = .60$

*See also Table IV, column one.

Table VIII

Typical Sensitivities of the Response to Various Model Parameters
(Brown and Black's Slab ID-2)*

	INITIAL RESPONSE (NEAR-ZERO DISPLACEMENT)	MID-RESPONSE (NEAR MAXIMUM VELOCITY)	MAXIMUM RESPONSE (AT MAXIMUM DISPLACEMENT)
SENSITIVITY TO FORCE PARAMETERS:			
$\Delta y_i/\Delta\alpha_o$	.16	6.5	3.8
$\Delta y_i/\Delta\alpha_d$	-1.5×10^{-4}	-.43	-.41
SENSITIVITY TO MASS PARAMETERS:			
$\Delta y_i/\Delta\mu_o$	1×10^{-3}	-1.0	-.53
$\Delta y_i/\Delta\mu_d$	.16	.34	.19
SENSITIVITY TO BI-LINEAR SPRING PARAMETERS:			
$\Delta y_i/\Delta P_{lin}$	-2×10^{-4}	-.13	-.30
$\Delta y_i/\Delta d_{lin}$	1.0×10^{-3}	.53	1.08
$\Delta y_i/\Delta E_{plast}$	0	-.06	-1.05
SENSITIVITY TO PRESSURE-SCALING PARAMETER: $\Delta y_i/\Delta P_{scale}$	.22	2.5	5.04

*See also Table VI, row two.

Table IX

Typical Sensitivities of the Response to Various Model Parameters (Keenan's Slab D3-1)*

	INITIAL RESPONSE (NEAR-ZERO DISPLACEMENT)	MID-RESPONSE (NEAR MAXIMUM VELOCITY)	MAXIMUM RESPONSE (AT MAXIMUM DISPLACEMENT)
SENSITIVITY TO FORCE PARAMETERS:			
$\Delta y_i/\Delta\alpha_o$	.49	27.3	75.5
$\Delta y_i/\Delta\alpha_d$	-.01	-5.3	-16.0
SENSITIVITY TO MASS PARAMETERS:			
$\Delta y_i/\Delta\mu_o$	-.013	-1.46	-4.36
$\Delta y_i/\Delta\mu_d$	3.9×10^{-6}	.018	.062
SENSITIVITY TO BI-LINEAR SPRING PARAMETERS:			
$\Delta y_i/\Delta P_{lin}$	-8.4×10^{-6}	-7.5×10^{-3}	-4.5×10^{-2}
$\Delta y_i/\Delta d_{lin}$	4.3×10^{-3}	2.67	7.82
$\Delta y_i/\Delta E_{plast}$	0	-2.2×10^{-4}	-1.5×10^{-2}
SENSITIVITY TO PRESSURE-SCALING PARAMETER $\Delta y_i/\Delta P_{scale}$	5.6×10^{-3}	.95	3.74

*See also Table V, row six.

with the simple model. Note, also, the "yield force" P_{lin} was typically estimated at about 450 Lb/in^2, in pretty fair agreement with the static test data, (cf. Figure 5-4 and 5-21). As shown in Figure 5-21, the estimated elasto-plastic load-deflection curves are quite close to the results from static tests. Thus, one can get a fairly good estimate of the analytical load-deflection curve from static test data.

Note that Table X also gives estimated load-mass factor of close to unity. A load-mass factor of exactly unity is predicted if the slab "punches through" with no spanwise bending. Watt's tests (Reference 3) showed that many of his slabs did "punch through", which accounts for the load-mass factors estimated and shown in Table X. It is felt that the parameters given in Table X are "physically realistic" for Watt's slabs, and this confirms the earlier result that simple models will work pretty well for Watt's data.

Table X. Three-Parameter Model Estimates for Watt's Slabs

PARAMETER	SLAB ED1	SLAB ED2	SLAB ED3
LOAD-MASS FACTOR,	.98	1.19	1.05
YIELD FORCE, P_{lin}	422	439	480
ELASTIC DISPLACEMENT, d_{lin}	.137	.137	.135
GOODNESS OF FIT, i.e., Δrms	.006	.016	.005

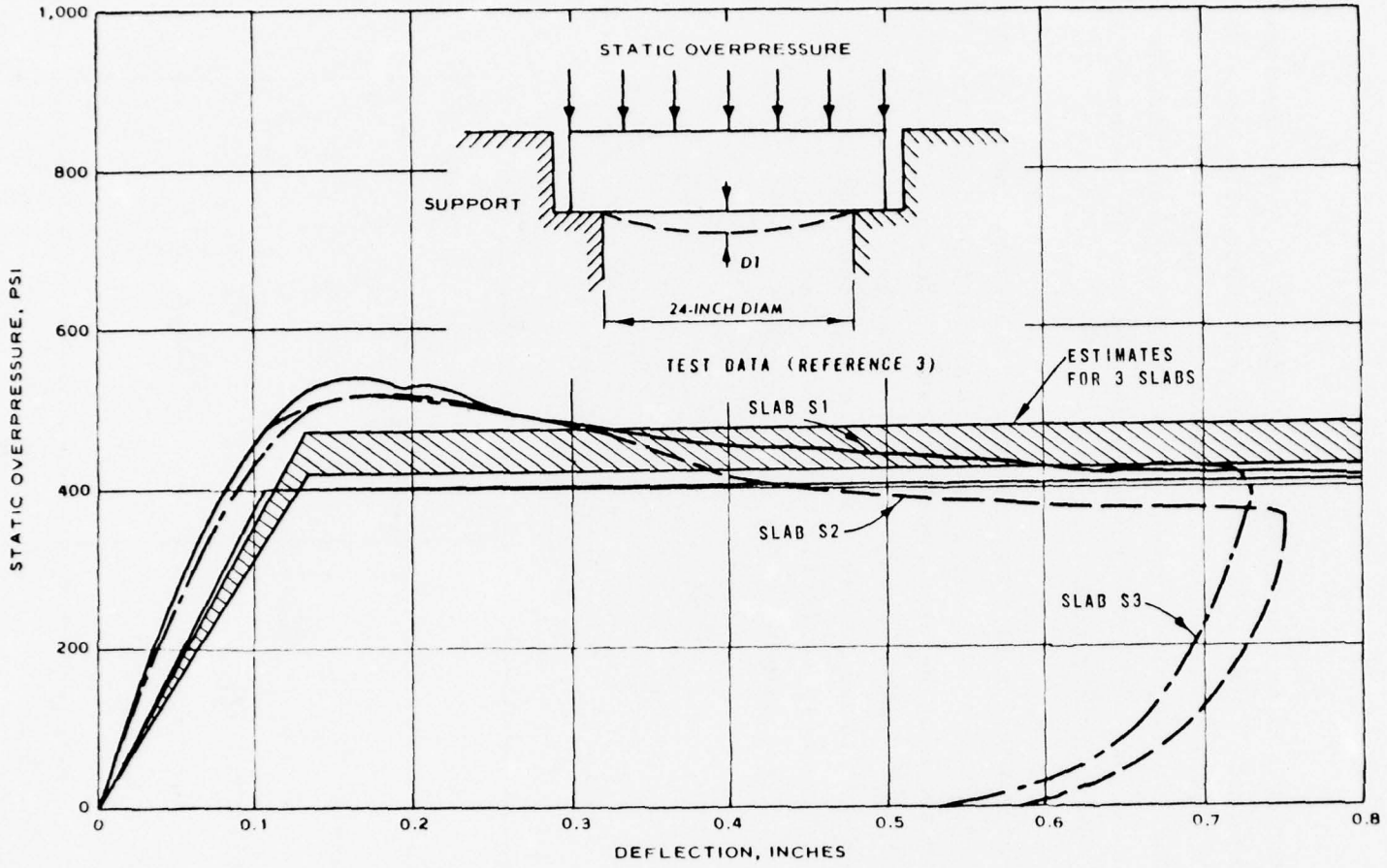

Figure 5-21. Pressure Versus Midspan Deflection Showing Test Data and Range of Final Estimates Found Using PEBLS

5.7 FOUR-PARAMETER MODEL FOR BROWN AND BLACK'S SLAB ID-2

In keeping with the theme of using the "simplest possible model", a four-parameter model was attempted with Brown and Black's test data. The four parameters were λ (the load-mass factor) P_{lin}, d_{lin} and E_{plast}, the latter being added primarily because of the stronger non-linear force-deflection results (cf. Figure 5-10).

Table XI. Results of Estimation Procedure for Brown and Black's Slab ID-2

COMPUTED AND OBSERVED DISPLACEMENT RESPONSE

POINT	TEST TIME	U-ANALYTIC	U-OBSERVED	Y=U-UTEST
1	0.25000E-02	0.94341E-01	0.80000E-01	0.14341E-01
2	0.50000E-02	0.54926	0.50000	0.49256E-01
3	0.75000E-02	1.5285	1.2000	0.32851
4	0.10000E-01	2.9738	2.0000	0.97379
5	0.12500E-01	4.6882	3.0000	1.6882
6	0.15000E-01	6.4588	4.2000	2.2588
7	0.17500E-01	8.0667	5.4000	2.6667
8	0.20000E-01	9.2944	6.1000	3.1944
9	0.22500E-01	9.9598	6.8000	3.1598
10	0.30000E-01	9.6021	7.0400	2.5621

OBJECTIVE DUE TO OBSERVATIONS = 179.769 RMS ERROR IN OBSERVATIONS = 2.07064
OBJECTIVE DUE TO PARAMETERS = 0.000000 TOTAL OBJECTIVE FUNCTION = 179.769

COMPUTED AND OBSERVED DISPLACEMENT RESPONSE

POINT	TEST TIME	U-ANALYTIC	U-OBSERVED	Y=U-UTEST
1	0.25000E-02	0.80862E-01	0.80000E-01	0.86156E-03
2	0.50000E-02	0.47053	0.50000	-0.29471E-01
3	0.75000E-02	1.1535	1.2000	-0.46527E-01
4	0.10000E-01	2.0801	2.0000	0.80120E-01
5	0.12500E-01	3.1507	3.0000	0.15069
6	0.15000E-01	4.2646	4.2000	0.64625E-01
7	0.17500E-01	5.3191	5.4000	-0.80906E-01
8	0.20000E-01	6.2040	6.1000	0.10399
9	0.22500E-01	6.8204	6.8000	0.20403E-01
10	0.30000E-01	6.8452	7.0400	-0.19475

OBJECTIVE DUE TO OBSERVATIONS = 1.06444 RMS ERROR IN OBSERVATIONS = 0.959385E-01
OBJECTIVE DUE TO PARAMETERS = 1.53308 TOTAL OBJECTIVE FUNCTION = 2.59753

Table XII. Parameters Estimated for Brown and Black's Slab

PARAMETER CONFIDENCE LEVELS

PARAMETER	INITIAL ESTIMATE	LATEST ESTIMATE	VARIANCE	PERCENT CONFIDENCE
PLIN	14.000	19.266	2.8877	12.138
DLIN	0.25000	0.33194	0.11518E-01	42.928
EPLS	1.4000	0.37343	0.33278	41.205
EMU1	0.70000	0.82844	0.36831E-01	27.416

The results from the computer run are shown in Table XI which gives the initial response (top half) and the final response (bottom half of Table XI). Note that the RMS error in observation went from a value of 2.07 (initially) to a value of only .0959 (final estimate).

The final estimated parameter values are given in Table XII, which shows P_{lin}, d_{lin}, E_{plast} and λ (labeled EMU1) each having a significant improvement in confidence level (e.g., from 75% to 12%, etc.). Note also that the values estimated appear to be "physically reasonable" and acceptable from an intuitive standpoint. (For example, see the text by Biggs, Reference 2, for typical load-mass factors, and Figure 5-22 for the static load-deflection curve). Biggs test, p. 214, gives theoretical load-mass factors in the range

$$.51 \leq \lambda \leq .67$$

for square two-way slabs ($^a/b = 1$). Table XII gives a load-mass factor of .82, which is in fair agreement with the theory. Note that Biggs' values are calculated assuming "yield-line theory" for the failure of the slab.

Figure 5-22 shows the estimated bi-linear pressure vs. deflection fair amount of scatter is indicated by the test data, suggesting that the slabs were of non-uniform quality. Again one sees that simplified theory and the static load-deflection data provide fairly good estimates of the final model parameters.

5.8 FOUR PARAMETER MODEL FOR KEENAN'S SLAB D3-1

Keenan's data (on his Slab D3-1) proved to be fairly difficult to "fit" with the simple four-parameter model. Several computer runs were made using the data shown in Figure 5-17). Discussed previously in Section 5.4). Accepting the data as accurate, the computer program PEBLS originally estimated a load-mass factor of about three (3) for Slab D3-1. This result was unexpected (and we felt it was incorrect) so a closer look was taken at the data (Figure 5-17).

Referring to Figure 5-17, note that the displacement trace DC shows a deflection of nearly-zero out to a time of .002 sec (2 milli-seconds). Note also that the pressure, p(t) is the highest during this early time period. Thus the possibility occurred that perhaps Keenan's displacement trace was in error, since when the pressure is greatest, (and the acceleration is a maximum) one would expect that displacement would occur (and not be near-zero).

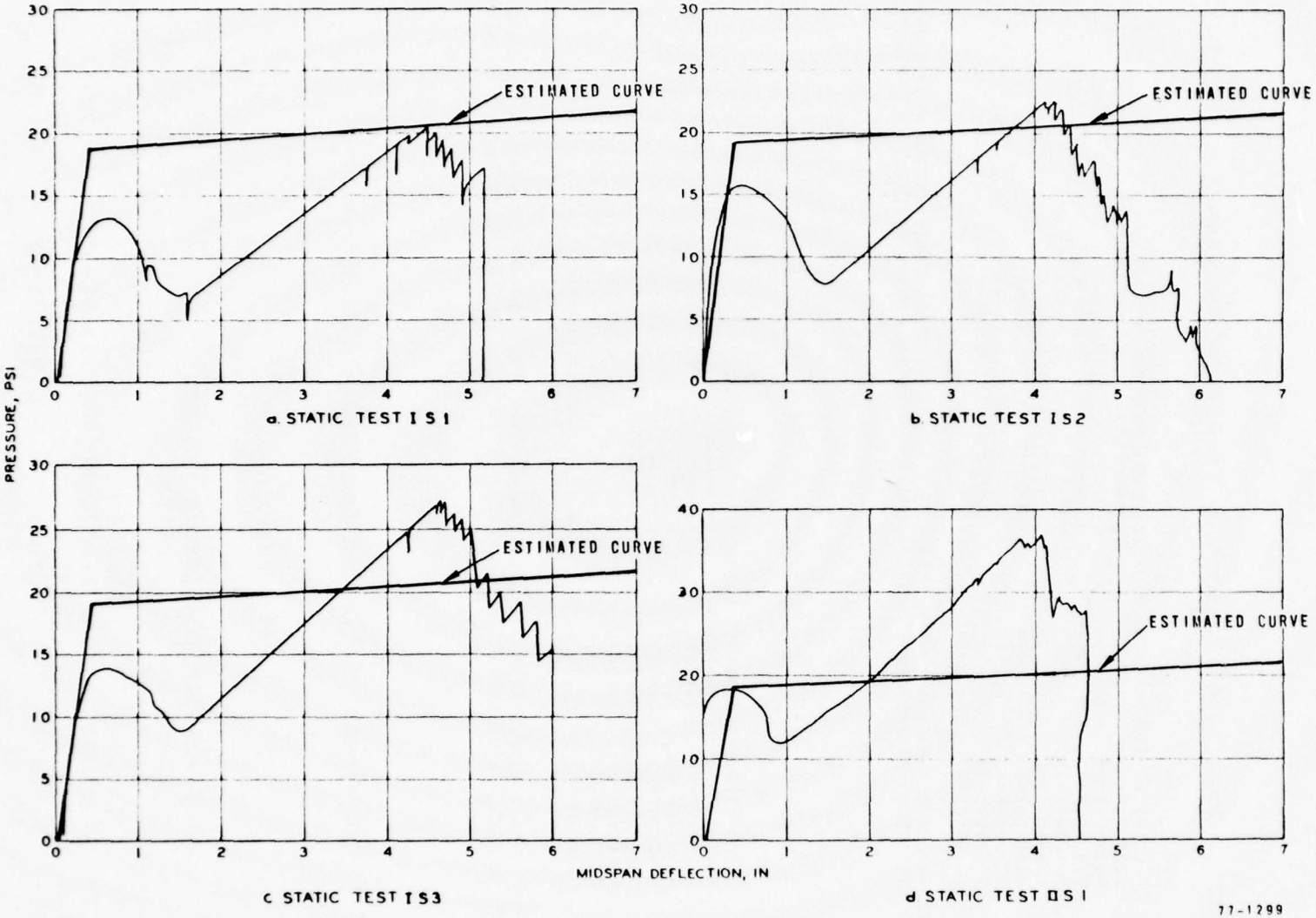

Figure 5-22. Pressure Versus Midspan Deflection, Static Tests of Reference 5 and Estimated Characteristic Found Using PEBLS

Table XIII. Results of Estimation Procedure for Keenan's Slab D3-1

COMPUTED AND OBSERVED DISPLACEMENT RESPONSE

POINT	TEST TIME	U-ANALYTIC	U-OBSERVED	Y=U-UTEST
1	0.20000E-02	0.32253	0.20000	0.12253
2	0.30000E-02	0.60658	0.35000	0.25658
3	0.40000E-02	0.89463	0.53000	0.36463
4	0.50000E-02	1.1630	0.75500	0.40801
5	0.60000E-02	1.3919	0.96000	0.43189
6	0.70000E-02	1.5662	1.1600	0.40623
7	0.80000E-02	1.6745	1.2900	0.38446
8	0.10600E-01	1.5771	1.4600	0.11710

OBJECTIVE DUE TO OBSERVATIONS = 83.9786 RMS ERROR IN OBSERVATIONS = 0.334168
OBJECTIVE DUE TO PARAMETERS = 0.000000 TOTAL OBJECTIVE FUNCTION = 83.9786

COMPUTED AND OBSERVED DISPLACEMENT RESPONSE

POINT	TEST TIME	U-ANALYTIC	U-OBSERVED	Y=U-UTEST
1	0.20000E-02	0.19966	0.20000	-0.34455E-03
2	0.30000E-02	0.37947	0.35000	0.29471E-01
3	0.40000E-02	0.57767	0.53000	0.47666E-01
4	0.50000E-02	0.77838	0.75500	0.23378E-01
5	0.60000E-02	0.96830	0.96000	0.83005E-02
6	0.70000E-02	1.1374	1.1600	-0.22642E-01
7	0.80000E-02	1.2778	1.2900	-0.12229E-01
8	0.10600E-01	1.4548	1.4600	-0.52067E-02

OBJECTIVE DUE TO OBSERVATIONS = 0.459336 RMS ERROR IN OBSERVATIONS = 0.235729E-01
OBJECTIVE DUE TO PARAMETERS = 1.98882 TOTAL OBJECTIVE FUNCTION = 2.44815

Table XIV. Parameters Estimated for Keenan's Slab D3-1

PARAMETER CONFIDENCE LEVELS

PARAMETER	INITIAL ESTIMATE	LATEST ESTIMATE	VARIANCE	PERCENT CONFIDENCE
PLIN	110.00	86.471	112.11	9.6256
DLIN	0.34000	0.88527E-01	0.23315E-01	44.909
EPLS	1.0000	0.75941	24.797	497.97
EMU1	0.80000	1.1863	0.98243E-01	39.180

For this reason, the displacement data was "shifted" to the left in time a distance of .002 sec. Thus, the time t = 0 was taken as the time that the pressure-trace began, and the time on the displacement trace was shifted to a new time, (t' = t - .002). When this adjustment to Keenan's data was made, a fairly satisfactory "fit" was obtained using the four-parameter model. *

Using the static load-deflection curve (Figure 5-18), one can estimate P_{lin}, d_{lin}, and E_{plast} fairly well for Slab D3-1. Then, using these values with a representative load-mass factor, the results shown in Table XIII are obtained (top half). Note that the RMS error value is .33, indicating a poor initial model. After a number of interations, PEBLS had reduced the RMS deviation to .023, as shown in the lower half of Table XIII. The final values of the parameters P_{lin}, d_{lin}, E_{plast}, and μ_1 (where the latter now represents the load-mass factor, λ) are given in Table XIV. Again, it is felt that these parameter values are "physically reasonable" and roughly in agreement with intuition.

Biggs' text, P.209, gives load-mass factors in the range

$$.66 \leq \lambda \leq .78$$

for simply-supported one-way slabs. These values are in contrast with the factor 1.18 estimated by PEBLS and given in Table XIV. Also note that the estimated pressure-vs-deflection curve does not fit the static data very well (Figure 5-23).

In retrospect it is thought that the initial values (P_{lin} = 110, d_{lin} = .34) were "poor estimates" and that they contributed to the relatively poor performance of the estimation program in this instance. For example, referring to Figure 5-23, one sees that a better "initial estimate" might have been (P_{lin} = 110, d_{lin} = 1.0) for example. It is speculated that a better initial estimate would have produced more realistic results for the load-mass factor and for the pressure vs-deflection curve.

---

* The reader will recall that the "multi-parameter" model (Section 5.4) selected α_o such that the initial pressures were (in effect) "cut off" (i.e., the pressure pulse was reshaped in time).

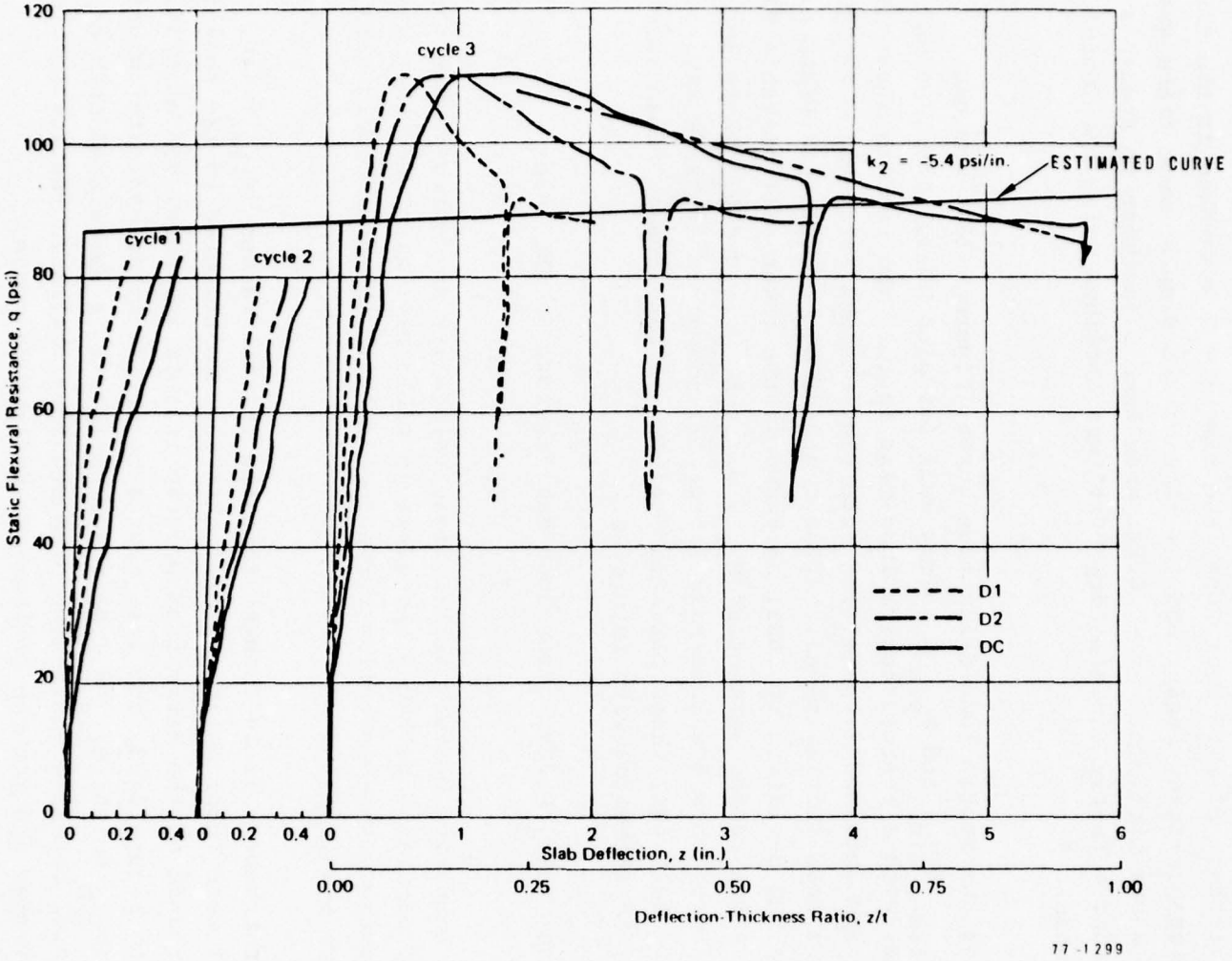

Figure 5-23. Static Load Deflection Data (Reference 6) and Estimated Characteristic Found Using PEBLS

5.9 DISCUSSION OF RESULTS

These results (especially those in Section 5.6, 5.7, and 5.8) led to the conclusion that realistic parameters can be found that allow single degree-of-freedom models to accurately reproduce dynamic response data for actual slabs. It also appears that (in many cases) these model parameters are close to those which would be predicted a priori.

A major result of this effort is the recommendation that

- "Tests on any non-linear structure (or element such as reinforced concrete slab) should be conducted at several levels of force excitation".

When put in the above terms, such a recommendation seems almost trivial. Any student of non-linear vibrations or non-linear circuit theory knows that the dynamic response (i.e., output) depends in a non-linear fashion upon the excitation (i.e., upon the input). This non-linear dependence is the very basis for labeling the problem as "non-linear" in the first place. Nevertheless, such a non-linear dependence between the dynamic response and the applied over-pressure p(t) was not examined in two of the three main references used herein as sources of dynamic test data. This situation can perhaps best be illustrated by an analogy with earthquake engineering, as follows.

Suppose one has a single-story steel-framed structure, where the behavior of the steel columns is thought to be represented by a bi-linear (elasto-plastic) spring. The structural engineer wishes to identify the non-linear characteristic (i.e., force-deflection curve) of his structure, so he can calculate if the structure will fail during a major earthquake. If the structure is excited only at small amplitudes (e.g., by, say, magnitude 3 or 4 earthquakes) it will never (or very seldom) be driven into the non-linear range, and there will be no way humanly possible for the engineer to identify (with any reasonable degree of certainty) the non-linear characteristics of his structure.

A similar, but less-obvious condition exists when the structure experiences only one non-linear event, say a magnitude of 6.5 earthquake. Now the engineer finds that his structure has been driven into the non-linear range, and he can calculate (i.e., identify) the yield stress, say, of his bi-linear elasto-plastic force-deflection curve. However, he still cannot predict (with very much certainty) whether or not his structure will collapse if it is hit by a major earthquake (e.g., magnitude 7.8, say). He needs test data at several levels of excitation for his non-linear structure.

To return to the problem at hand, namely the response of R/C slabs, Watt's tests (reference 3) are analogous to the magnitude 6.5 earthquake just considered. The slabs were driven into the non-linear range (with a maximum dynamic deflection of about .4 inches) but the static load-deflection curve showed the slab still yielding at a deflection of .8 inches. Without further testing, one has little or no way of knowing whether these deep slabs will withstand a dynamic overpressure of 2000 psi or 20,000 psi before failing catastrophically. They have not been tested to a magnitude 7.8 (major earthquake event).

Conversely, all of Brown and Black's tests (reference 5) drove the test slabs to major failure. They measured a static failure deflection of about 4 inches, yet each of their test slabs was driven to dynamic deflection on the order of 7 inches or more. They tested to only major earthquakes (using our analogy) and experienced no moderate or low-level loading. Clearly, if the structure is always driven to collapse, one obtains little information about its behavior throughout its dynamic range.

This state of affairs leads to the following major recommendation:

- "Future dynamic testing (of slabs, box-like bunkers, or other non-linear structures) should be conducted at three fairly distinct levels of excitation. For want of a more precise definition, the three levels recommended are:
  (i) moderately non-linear (e.g., 2 or 3 elastic deflections)
  (ii) strongly non-linear (e.g., 7 or 8 elastic deflections)
  (iii) to complete failure (e.g., total collapse)

Such a test sequence may (possibly) triple the cost of a typical test program. However, an incomplete or inconclusive test program may prove misleading and might actually end up costing more in the long run. Keenan (reference 6) recognized the need to test at various dynamic pressure levels, which he accomplished with the adverse side-effect of having to retest partially damaged slabs. Presumably, Keenan was under a budget constraint which limited the number of virgin test specimens at his disposal.

A difficulty with Keenan's work (reference 6) was that his static tests were not taken to complete failure of his test slab. His dynamic tests covered the ranges of linear, moderately non-linear, and strongly non-linear tests, but the failure load (i.e., total collapse) of the slabs was not determined. This situation led to the following recommendation:

- "Static tests of non-linear structural elements (or complete

structures) should be continued to the point of total collapse if at all possible."

The preceeding remarks and recommendations are among the major conclusions which kept recurring to the writers of this report. They have been emphasized herein with the hope that they can be utilized in planning and conducting future tests. It is recognized, however, that in any test program compromises must be made, and test planners may choose not to accept all of our recommendations.

The estimation program was successful in fitting Watt's deep slab data with both a "multi-parameter" model and a simplified four-parameter model where the values of the parameters obtained were "physically reasonable" (i.e., they agreed with intuition). For Brown and Black's conventional slab data, it was again possible to fit the dynamic response results, but the result was a "near-linear" model which was much less satisfying intuitively. Similarly, it was possible to fit Keenan's laced slab data (with the multi-parameter model) but the estimation scheme greatly de-emphasized the initial pressures (of the pressure-time history).

Successful attempts were also made to fit the various test data with simple three and four-parameter models. These results were significant, in that the models thus estimated were physically realistic, (and still quite simple) yet they gave a good "fit" to the dynamic data (i.e., low RMS error values). Thus, the authors were led ultimately to the major conclusion that, "Simple models can be made to work", as discussed in detail in Section 5.0.

Regarding recommendations for future work in this area of dynamic modeling, it may be said that greater emphasis should be placed on finding parameters which agree with "physical intuition" or elementary theory, rather than on making a general model which can encompass all the test data. When the study was begun, it was not known whether a simple (3 parameter, say) model would suffice or not. Watt's report showed that the slab went through three distinct phases of deformation, and orginally it was decided to model deformation-dependent properties for the mass, stiffness, and applied force. The result was that (by using all the parameters) one could "fit" the response data rather easily. But, the problem (which did not become evident until later) was that the parameter values obtained were not readily acceptable from a physical standpoint. The mathematics of system identification was originally over-emphasized with respect to the physics of the slab-deformation problem.

It is also recommended that some "sensitivity studies" be conducted, namely to see how much that maximum displacement (Y max) veries with changes in the parameters (λ, p_{lin}, d_{lin}, etc.) For example, just how significant is the fact that the load-mass factor was estimated at .82 (vs. a theoretical value ranging from .51 to .67) for Brown and Black's slabs. Would a value of λ = .7 have changed the results much? The answer to these questions are left to a future study.

6. CONCLUDING REMARKS AND RECOMMENDATIONS

The primary conclusion of this report is that

. Realistic parameters can be found (using Parameter Estimation) that allow single degree-of-freedom models to accurately reproduce dynamic response data for actual slabs.

A related secondaty conclusion is that

Often (but not always) these model parameters can be estimated fairly accurately. The estimates can be provided by static test (if available), and by yield-line theory if test data is missing.

These conclusions are substantiated in the body of the report. Major recommendations of this report are that

- "Tests on any non-linear structure (or element such as reinforced concrete slab) should be conducted at several levels of force excitation".
- "Future dynamic testing (of slabs, box-like bunkers, or other non-linear structures) should be conducted at three fairly distinct levels of excitation. For want of a more precise definition, the three test levels recommended are:

(i) moderately non-linear, (e.g., 2 or 3 elastic deflections)
(ii) strongly non-linear, (e.g., 7 or 8 elastic deflections)
(iii) to complete failure (e.g., total collapse)

- "Static tests of non-linear structural elements (or complete structures) should be continued to the point of total collapse if at all possible."

The rationale behind these recommendations is included in the main text.

7. REFERENCES

1. R.E. Crawford, C.J. Higgins, and E.M. Bultmann, The Air Force Manual for Design and Analysis of Hardened Structures, AFWL-TR-74-102, Air Force Weapons Laboratory, October, 1974.

2. J.M. Biggs, Introduction to Structural Dynamics, McGraw-Hill Book Company, New York, 1964.

3. J.M. Watt, Jr., Response of Deep Two-Way Reinforced and Unreinforced Concrete Slabs to Static and Dynamic Loading, Technical Report N-69-2, Waterways Experiment Station, June, 1974.

4. C.H. Norris, et al, Structural Design for Dynamic Loads, McGraw-Hill Book Company, New York, 1959.

5. W.M. Brown and M.S. Black, "Dynamic Strength Study of Small Fixed-Edge, Longitudinally Restrained Two-Way Reinforced Concrete Slabs," Technical Report N-73-8, Waterways Experiment Station, December 1973.

6. W.A. Keenan, "Strength and Behavior of Laced Reinforced Concrete Slabs Under Static and Dynamic Loads," Tech. Report R-620, Naval Civil Engineering Laboratory, April, 1969.

7. System Identification of Vibrating Structures, Mathematical Models of Test Data, W.D. Pilkey and R. Cohen, eds, American Society of Mechanical Engineers, New York, 1972.

8. G.C. Hart, and J.T.P. Yao, "System Identification in Structural Dynamics," ASCE/EMD Specialty Conference, Dynamic Response of Structures: Instrumentation, Testing Methods, and System Identification, UCLA, March 30-31, 1976, pp. 61-85.

9. J.D. Collins, G.C. Hart, T.K. Hasselman, and B. Kennedy, "Statistical Identification of Structures, AIAA Journal, Vol. 12, No. 2, February, 1974, pp. 185-190.

10. H.W. Sorenson, and A.R. Stubberud, "Linear Estimation Theory," in AGARDOGRAPH-129, Ed. by C.T. Leondes, Theory and Application of Kalman Filters, Published 1970.

11. J.D. Chrostowski, D.A. Evensen and T.K. Hasselman, "Model Verification of Mixed Dynamic Systems," ASME Paper 77-DET-85 (to appear in the ASME Journal of Mechanical Design)

12. N. Distefano and B. Pena-Pardo, "System Identification of Frames under Seismic Loads", ASCE National Structural Engineering Convention, New Orleans, LA, April 14-17, 1975, Meeting Preprint 2446

13. J. Isenberg, "A Unified Approach for Bayesian Estimation", J.H. Wiggins Company Report 78-1319/A to Civil Engineering Research Laboratory, under contract to the Air Force Weapons Laboratory.

14. J.R. Benjamin and C.A. Cornell, Probability, Statistics and Decision Making for Civil Engineers, McGraw-Hill, New York, 1970.

15. W.D. Iwan, "Application of Nonlinear Analysis Techniques", in ASME/AMD-Vol. 8 Applied Mechanics in Earthquake Engineering, Amer. Soc. of Mec. Engrs., New York, 1974.

16. J.A. Blume, J. S. Dalal, and K.K. Honda, "Statistical Study on the Strength of Structural Materials and Elements", URS/John A. Blume & Associates, Engineers, Report JAB-99-118, 130 Jessie Street, San Francisco, California, under contract AT(26-1)-99 for ERDA.

17. D.A. Evensen and J.D. Collins, "Test Planning with Uncertainty", Defense Nuclear Agency Report DNA 4099F, 1 February 1977.

18. D.A. Evensen, "Probabilistic Test Planning", Defense Nuclear Agency Report DNA 4271F, 18 July 1977.

APPENDIX A

A UNIFIED TREATMENT OF

LEAST SQUARES

WEIGHTED LEAST SQUARES

NONLINEAR WEIGHTED LEAST SQUARES

MINIMUM VARIANCE

AND

BAYESIAN ESTIMATION

Jerrold Isenberg
J.H. Wiggins Company
1650 South Pacific Coast Highway
Redondo Beach, California 90277

Abstracted from J.H. Wiggins Report No. 78-1319/A
"A Unified Approach for Bayesian Estimation"

Least Squares

In the least squares approach first developed by Gauss two centuries ago, we define the residual U_i as the difference between the observed value of the response (or dependent variable) and the calculated value of the response:

$$U_i \equiv u_{o_i} - u_i \tag{1}$$

where

$$u_i = u(x_{1i}, x_{2i} \ldots x_{mi}, r_1, r_2, r_3 \ldots r_p) \tag{2}$$

In Eq. 2, the vector x_i represents the independent variables used to generate the calculated response and for a ground shock calculation are represented by location and time. Of crucial importance to the least squares method is that the equation chosen for u_i is the best representation of the experiment being simulated.

By the Gauss or least squared method, we seek to minimize the sum of the squares residuals given by

$$F = \sum_{i=1}^{n} U_i^2 = \sum_{i=1}^{n} (u_{o_i} - u_i)^2 \tag{3}$$

where n is the total number of experimental measurements. Thus, Eq. (3) is the objective function first evolved by Gauss. Note that this objective function does not account for possible errors in the independent variable. Experience has shown that errors in the dependent variable are usually two orders of magnitude higher than those in the independent variable

thus allowing the latter's errors to be neglected. Nonetheless, for those special cases where the two types of errors are of equal magnitude, Eq. (3) can be suitably modified (see Ref. 1).

If the measurements x_i and u_{o_i} are repeated n times and the average values computed these average values should approach the true values as n approaches infinity. This will occur if systematic errors do not affect the measurements. Such errors consistently cause the measured response to be either larger or smaller than the true values. The errors can arise from three sources:

1. A mistake in the measuring technique
2. A fault in a measuring instrument
3. Failure to account for a factor affecting the experiment.

Thus for example, if temperature affects the response of an accelerometer, such a devise located in close proximity to the heat of a blast might contain a systematic error in its measurement.

The simplest case of least squares is that of the polynomial. For a straight line this becomes

$$F = \sum_{i=1}^{n} (u_{o_i} - r_1 - r_2 x_i)^2 \qquad (4)$$

where for the sake of simplicity we are considering the case of a single independent variable, x_i. We see than that the objective function, F, is a function of r_1 and r_2. Of the

many values that these parameters can assume, we seek the set that minimizes F. At this minimum, we require that

$$\frac{\partial F}{\partial r_1} = 0 \tag{5}$$

$$\frac{\partial F}{\partial r_2} = 0 \tag{6}$$

which yields two equations. (It should be noted that no maximum exists for F since for any maximum one might postulate, an even greater maximum can be found.) Applying the criteria of Eqs. (5) and (6) to Eq. (4) yields the two linear equations

$$r_1 n + r_2 \sum_{i=1}^{n} x_i = \sum_{i=1}^{n} u_{o_i} \tag{7}$$

$$r_1 \sum_{i=1}^{n} x_i + r_2 \sum_{i=1}^{n} x_i^2 = \sum_{i=1}^{n} x_i u_{o_i} \tag{8}$$

which can be readily solved for r_1 and r_2.

The above derivation can be extended to any polynomial of order p-1 defined by

$$u_i = \sum_{k=1}^{p} r_k x_i^{k-1} \tag{9}$$

If we cast the resulting set of equations (7) and (8) in matrix form obtaining

$$Cr = V \tag{10}$$

it can readily be shown that the elements of C and V are given by:

$$C_{jk} = \sum_{i=1}^{n} x_i^{j+k-2} \tag{11}$$

and

$$V_j = \sum_{i=1}^{n} x_i^{j-1} u_{o_i} \tag{12}$$

An interesting phenomenon arises when the degree of the polynomial becomes too high. If we normalize our independent variable so that it ranges from 0 to 1 (which is always possible) and employ a sample of uniformly distributed data, then the elements of C are given by

$$C_{jk} \approx n\int_o^1 x^{j+k-2}dx = \frac{n}{j+k-1} \tag{13}$$

The terms represented by $\frac{1}{j+k-1}$ are elements of the so-called Hilbert matrix. The determinant of this matrix is given by (ref. 2)

$$D_p = \frac{[1!2!3!\ldots(p-1)!]^3}{p!(p+1)!\ldots(2p-1)!} \tag{14}$$

which approaches zero very rapidly as the matrix grows as shown in Table 1.

p	D_p
1	
2	$8.3X10^{-2}$
3	$4.6X10^{-4}$
4	$1.7X10^{-7}$
5	$3.7X10^{-12}$
6	$5.4X10^{-18}$
7	$4.8X10^{-25}$
8	$2.7X10^{-33}$
9	$9.7X10^{-43}$

Table 1. Determinants of Hilbert-like Matrices as a Function of Matrix Size

When the determinant of the matrix associated with a linear set of equations approaches zero, the system is said to be ill-conditioned. The set of parameters, r, generated from such a system are adversely affected by round-off, i.e. it has a large error associated with it. In the extreme, the determinant will be so close to zero so as to render the matrix to be computationally singular. Experience has shown that this occurs when the number of parameters is about 6 (fifth-order polynomial). The method most often used to circumvent this problem is the implementation of orthogonal polynomials. However, since the desired effect is somewhat artificial, it is preferable to employ a lower order polynomial (fourth-order or lower).

The least squares method is not confined to polynomials. The method can easily be extended to other functions by allowing u_i to assume a form that is <u>linear</u> with respect to the parameters:

$$u_i = r_1 g_1(x_i) + r_2 g_2(x_i) + \ldots + r_p g_p(x_i)$$

$$= \sum_{k=1}^{p} r_k g_k(x_i) \qquad (15)$$

By inserting Eq. (15) into Eq. (13) and requiring that

$$\frac{\partial F}{\partial r_k} = 0 \quad k = 1, 2 \ldots p \qquad (16)$$

we again obtain a linear set of equations of the form

$$Cr = V \qquad (10)$$

where now the elements of C and V are:

$$C_{jk} = \sum_{i=1}^{n} g_j(x_i) g_k(x_i) \qquad (17)$$

and

$$V_k = \sum_{i=1}^{n} g_k(x_i) u_{o_i} \quad . \qquad (18)$$

It is seen that the polynomial of Eq. (9) is a special case of Eq. (15) where

$$g_k(x_i) = x_i^{k-1} \qquad (19)$$

Since most functions are expandable into polynomials, the earlier comments regarding the Hilbert-like matrix generated by the use of high-order polynomials can be extended to most functions defined by Eq. (15).

A cursory examination of C_{jk} in Eq. (17) will reveal that C is a symmetric matrix. This property which also applies to the matrix generated through the polynomial (see Eq (11)) permits a substantial savings in computational time since only the upper or lower triangle of C need be computed (along with its diagonal elements).

For ease of notation, define the matrix T by

$$T_{ij} \equiv g_j(x_i) \tag{20}$$

where T is $n \times p$. Then in matrix form, the parameter estimate, r, in Eq. (10) is given by

$$r = (T^T T)^{-1} T^T u_o \cdot \tag{21}$$

Therefore, the matrix given by

$$G = (T^T T)^{-1} T^T \tag{22}$$

is that vehicle which yields the estimate, r, as a linear transformation of the experimental response (vector of observations).

It is obvious that the least squares technique cannot be employed when the number of parameters exceeds the number of measurements, i.e. $p > n$. When this occurs, the system of Eq. (10) is said to be underdetermined. When p is equal to n each of the residuals in Eq. (3) will be zero resulting in a minimum value of zero for F. For this case the system is said to possess zero degrees of freedom which is the difference between p and n.

Weighted Least Squares

The formulation of Eq. (3)

$$F = \sum_{i=1}^{n} U_i^2 \tag{3}$$

has two implicit assumptions: firstly, that all the experimental points are measured with the same degree of precision, and secondly, that all the residuals have the same dimensions. Therefore, if some points were measured with high precision, Eq. (3) would treat these points with equal weight as the other observations. As an example of the second assumption, if some of the responses were in units of seconds and the rest in units of meters/second (as might happen in a velocity waveform response to a ground shock) the formulation of Eq. (3) would be untenable.

The above two problems are solved by adding statistical weighting to the least squares formulation. Each squared residual, U_i^2, is multiplied by a weight, w_{ii}, which is equal to the inverse of the square of the uncertainty or standard deviation or:

$$w_{ii} = \frac{1}{\sigma_i^2} = \frac{1}{S_{\varepsilon\varepsilon_{ii}}} \tag{23}$$

where $S_{\varepsilon\varepsilon_{ii}}$ is the variance of the i^{th} observation. The resulting weighted least squares formulation is given by

$$F = \sum_{i=1}^{n} w_{ii} U_i^2 \rightarrow \min \tag{24}$$

Minimizing this scalar with respect to each parameter again yields a linear system of equations:

$$Cr = V \tag{10}$$

where

$$C_{jk} = \sum_{i=1}^{n} w_{ii} g_j(x_i) g_k(x_i) \tag{25}$$

and

$$V_k = \sum_{i=1}^{n} w_{ii} g_k(x_i) u_{o_i} \tag{26}$$

It should be noted the C matrix defined through Eq. (25) is again symmetric.

In matrix form, the parameter estimate, r, in Eq. (10) is now given by

$$r = (T^T w T)^{-1} T^T w u_o \tag{27}$$

where the matrix, T, is again given by:

$$T_{ij} = g_j(x_i) \tag{20}$$

and

$$w = S_{\varepsilon\varepsilon}^{-1} \tag{23}$$

where both w and $S_{\varepsilon\varepsilon}$ are diagonal matrices. Thus, the linear transformation from u_o to r is achieved by

$$r = G u_o \tag{28}$$

where

$$G \equiv (T^T w T)^{-1} T^T w \tag{29}$$

Now the covariance of the estimate is given by

$$S^*_{rr} \equiv E(Z^*_{rr} Z^{*T}_{rr}). \tag{30}$$

Z^*_{rr} is the random error in r, and E denotes expectation. By the transformation of Eq. (28):

$$S^*_{rr} = E[GZ_{\varepsilon\varepsilon}(GZ_{\varepsilon\varepsilon})^T] = GE(Z_{\varepsilon\varepsilon} Z^T_{\varepsilon\varepsilon}) G^T \tag{31}$$

where $E(Z_{\varepsilon\varepsilon} Z^T_{\varepsilon\varepsilon})$ is the expectation of the observation error, $u - u_o$, and related to $S_{\varepsilon\varepsilon}$ by

$$S_{\varepsilon\varepsilon} = E(Z_{\varepsilon\varepsilon} Z^T_{\varepsilon\varepsilon}) \tag{32}$$

where $Z_{\varepsilon\varepsilon}$ is the random error in u_o.

Returning to Eq. (31)

$$S^*_{rr} = GE(Z_{\varepsilon\varepsilon} Z^T_{\varepsilon\varepsilon}) G^T = G\, S_{\varepsilon\varepsilon} G^T$$

$$= (T^T w T)^{-1} T^T w w^{-1} [(T^T w T)^{-1} T^T w]^T$$

$$= (T^T w T)^{-1} T^T [(T^T w T)^{-1} T^T w]^T$$

$$= (T^T w T)^{-1} [(T^T w T)^{-1} (T^T w T)]^T$$

$$= (T^T w T)^{-1} = (T^T S^{-1}_{\varepsilon\varepsilon} T)^{-1} = C^{-1}. \tag{33}$$

At this point we should now pose the question, "How do we know that the estimate of the experimental error of the response is correct?" This estimate is based on the judgement of the

experimentalist and when the measurements are conducted by a team it is unusual for a group to agree on an error estimate.

To answer the above question, we resort to Eq. (32)

$$S_{\varepsilon\varepsilon} = E\left(Z_{\varepsilon\varepsilon} Z_{\varepsilon\varepsilon}^T\right) \tag{32}$$

Having chosen a mathematical model for our experiment, we believe this model to be correct. Thus, if there were no experimental errors, and the correct model was postulated, our experimental points would coincide with those of the model, i.e., all the residuals would be zero. Therefore, the residual $Z_{\varepsilon\varepsilon}$ appearing in Eq. (32) can be attributed to experimental and mathematical error and can then be used as a check on the input covariance. If Eq. (32) does not yield a covariance matrix similar to the input covariance matrix, then $S_{\varepsilon\varepsilon}$ should be adjusted and the least squares process repeated. When Eq. (32) is finally satisfied, the error estimates will be substantially correct. Unless the above steps are carried out, Eq. (33), which specifies the revised parameter covariance will be incorrect.

When the above errors are experimental, we have implicitly assumed that the mathematical model is correct. When the model is incorrect, we have failed to account for factors affecting the experiment and possibly introduced a systematic error. Under this condition, the residual $Z_{\varepsilon\varepsilon}$ in Eq. (32) will not be completely generated by experimental error. However, it is reasonable to assume that if several models are postulated and the above steps executed, such that Eq. (32) is obeyed, then the model with the best fit would be closest to the true mathematical model.

The technique of adjusting the covariance matrix, $S_{\varepsilon\varepsilon}$, should not be interpreted as casting doubt on the credibility of the experimentalist who first estimates the experimental errors. If the experimentalist is regarded to be competent, then a substantial disparity between the original and adjusted covariances would most likely indicate that the mathematical model is incorrect and a reappraisal is suggested.

AD-A058 361 WIGGINS (J H) CO REDONDO BEACH CALIF F/G 15/6
MODELING THE DYNAMIC RESPONSE OF SLABS TO OVERPRESSURE.(U)
DEC 77 D A EVENSEN, A J BRONOWICKI DNA001-77-C-0178
UNCLASSIFIED 77-1299 DNA-4535F NL
2 OF 2
AD A058 361

END
DATE FILMED
10-78
DDC

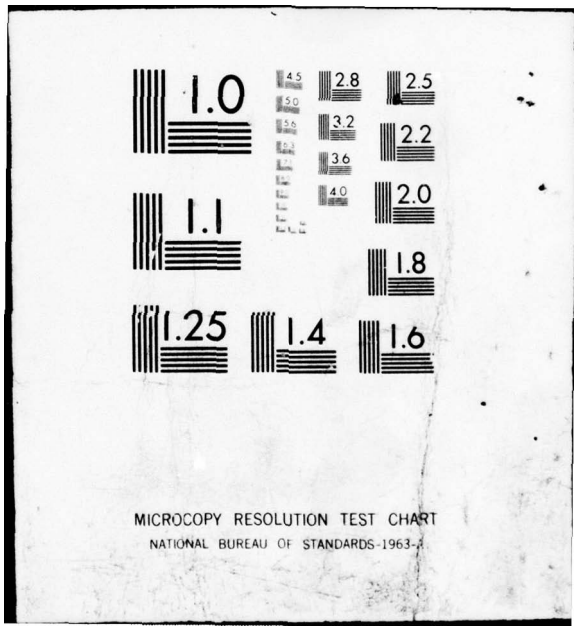
1.0
1.1
1.25
1.4
1.6
1.8
2.0
2.2
2.5
2.8
3.2
3.6
4.0
4.5
5.0
5.6
MICROCOPY RESOLUTION TEST CHART
NATIONAL BUREAU OF STANDARDS-1963-A

Nonlinear Weighted Least Squares

The case of nonlinear least squares occurs when the function u_i appearing in the objective function

$$F = \sum_{i=1}^{n} w_{ii} U_i^2 = \sum_{i=1}^{n} w_{ii} (u_{o_i} - u_i)^2 \qquad (34)$$

is a nonlinear combination of the parameter vector r:

$$u_i = u(x_i, r_1, r_2 \ldots r_p) \qquad (35)$$

Note that for the sake of clarity, we have assumed only one independent variable in Eq. (34). Nonetheless, the ensuing derivation can readily be extended to multiple independent variables by substituting a vector for x_i.

The reader can readily determine that minimizing Eq. (34) using Eq. (35) leads to a set of nonlinear equations. Rather than treat each case individually, it is preferable to start with Eq. (35) and develop a general technique.

Minimizing the objective function of Eq. (34) with respect to each parameter, r_k, yields

$$\sum_{i=1}^{n} w_{ii} (u_{o_i} - u_i) \frac{\partial u_i}{\partial r_k} = 0 \qquad k = 1, 2, 3 \ldots p \qquad (36)$$

In order to obtain a linearized formulation, we expand u into a truncated Taylor series evaluated at an estimated value of r denoted by the index, e:

$$u_i \approx u_{e_i} + \left(r_1 - r_{e_1}\right)\left(\frac{\partial u_i}{\partial r_1}\right)_{r=r_e} + \left(r_2 - r_{e_2}\right)\left(\frac{\partial u_i}{\partial r_2}\right)_{r=r_e}$$

$$+ \ldots + \left(r_p - r_{e_p}\right)\left(\frac{\partial u_i}{\partial r_p}\right)_{r=r_e} \tag{37}$$

We now define a sensitivity matrix T by

$$T_{ij} \equiv \left(\frac{\partial u_i}{\partial r_j}\right)_{r=r_e} \tag{38}$$

and a perturbation vector R by

$$R_j \equiv r_j - r_{e_j} \tag{39}$$

where T is n × p and R is of length p. Eq. (37) then becomes

$$u_i \approx u_{e_i} + R_1 T_{i1} + R_2 T_{i2} + \ldots + R_p T_{ip} \tag{40}$$

It should be noted that for the linear case where

$$u_i = \sum_{j=1}^{p} r_j g_j(x_i) \tag{15}$$

then

$$\frac{\partial u_i}{\partial r_k} = g_k(x_i) \tag{41}$$

Therefore the T matrix defined by Eq. (38) is the same as the T matrix specified by Eq. (20).

Returning to the nonlinear problem, we take the derivative of u_i in Eq. (40) with respect to r_k:

$$\frac{\partial u_i}{\partial r_k} = T_{ik} \tag{42}$$

Inserting Eqs. (40) and (42) into Eq. (36) yields

$$\sum_i w_{ii}\left(u_{o_i} - u_{e_i} - R_1 T_{i1} - R_2 T_{i2} - \ldots - R_p T_{ip}\right) T_{ik}$$

$$= 0 \qquad k = 1, 2, 3 \ldots p \tag{43}$$

The expression of Eq. (43) gives the linear set of equations of the form

$$CR = V \tag{44}$$

where the elements of C and V are

$$C_{jk} = \sum_{i=1}^{n} w_i T_{ij} T_{ik} \tag{45}$$

and

$$V_k = \sum_{i=1}^{n} w_i T_{ik}\left(u_{o_i} - u_{e_i}\right) \tag{46}$$

Note that C is symmetric.

When the system of Eq. (44) is solved for R, the new estimate of r is given by

$$r = r_e + R \tag{47}$$

This value of r is only approximate, but if the sequence is converging, it is a better estimate than the previous set in r_e. Therefore, if we replace the values in r_e by those from r and repeat the sequence, we will get an even better set for r. In the limit as r approaches r_e, the higher order terms in Eq. (37) go to zero faster than R, and the formulation becomes exact.

The choice of the initial guess for r_e in the above sequence can be of paramount importance. Experiments for nonlinear cases have shown that some cases have converged when the initial and final values differed by a factor of 10^7, while in other cases, the sequence diverged when the initial values differed from the true values by only 20%. In general, however, the better the initial guess, the greater the chances for convergence. When divergence does occur, other methods can be employed. Often a seemingly diverging problem can be brought to convergence by implementing a search algorithm (see Ref. 3).

Eqs. (44) - (47) are quite general, and can be applied to the linear case. For this purpose, we set r_e equal to zero. The reader can readily determine that the linear case is then retrieved, and is solved in a single iteration.

In matrix form, the parameter estimate r in Eq. (47) is

$$r = r_e + R = r_e + C^{-1}V$$

$$= r_e + (T^T w T)^{-1} T^T w(u_o - u_e)$$

or

$$r = r_e + G(u_o - u_e) \qquad (48)$$

where G has been derived previously as

$$G = (T^T w T)^{-1} T^T w \tag{29}$$

The covariances of the estimate and the observation are respectively

$$S^*_{rr} = E(Z^*_{rr} Z^{*T}_{rr}) \tag{30}$$

and

$$S_{\varepsilon\varepsilon} = E(Z_{\varepsilon\varepsilon} Z^T_{\varepsilon\varepsilon}) \tag{32}$$

As has been derived earlier $Z_{\varepsilon\varepsilon}$ is related to Z^*_{rr} by

$$Z^*_{rr} = G Z_{\varepsilon\varepsilon} \tag{49}$$

Here, however, we must assume that the true value of r and the calculated value of r are sufficiently close so that the G matrix is the same for both. With this assumption, we continue, and applying Eq. (33) obtain the revised covariance matrix.

$$S^*_{rr} = (T^T S^{-1}_{\varepsilon\varepsilon} T)^{-1} \tag{33}$$

As has been noted for the linear case, this derivation is based on the assumption that Eq. (32) for the observation covariance matrix is valid. If the expectation of $Z_{\varepsilon\varepsilon} Z^T_{\varepsilon\varepsilon}$ is not equal to $S_{\varepsilon\varepsilon}$, then $S_{\varepsilon\varepsilon}$ should be adjusted and the sequence of iterations repeated until we obtain a close approximation for $S_{\varepsilon\varepsilon}$ in $E(Z_{\varepsilon\varepsilon} Z^T_{\varepsilon\varepsilon})$.

The problem of ill-conditioning associated with the C matrix in linear least squares is also found to occur with the C matrix of Eq. (45) in the nonlinear mode. This is because most functions can be approximated by a power series. This author has found the problem to be more severe in the nonlinear case having noted severe ill-conditioning commonly manifested when 5 parameters were used.

Minimum Variance

Up to now we have assumed that the errors in the measurements are statistically independent so that the covariance matrix $S_{\varepsilon\varepsilon}$ is diagonal. In many experiments a cross-correlation exists such that other elements of $S_{\varepsilon\varepsilon}$ are non-zero. One important property of this matrix is the fact that it must be symmetric since the matrix is defined by $E(Z_{\varepsilon\varepsilon} Z^T_{\varepsilon\varepsilon})$.

For the most general case which is nonlinear the objective function is

$$F = \sum_{i=1}^{n} \sum_{j=1}^{n} w_{ij} \left(u_{o_i} - u_i\right) \left(u_{o_j} - u_j\right) \tag{50}$$

or in matrix form

$$F = (u_o - u)^T w (u_o - u) \rightarrow \min \tag{51}$$

where w is a weight matrix defined by

$$w \equiv S^{-1}_{\varepsilon\varepsilon} \tag{52}$$

and since $S_{\varepsilon\varepsilon}$ is symmetric

$$w = w^T. \tag{53}$$

Minimizing the objective function of Eq. (50) with respect to each parameter, r_k, yields:

$$\sum_{i=1}^{n} \sum_{j=1}^{n} w_{ij} \left[\left(u_{o_i} - u_i\right) \frac{\partial u_j}{\partial r_k} + \left(u_{o_j} - u_j\right) \frac{\partial u_i}{\partial r_k} \right] = 0 \tag{54}$$

or

$$\sum_{i=1}^{n} \sum_{j=1}^{n} w_{ij} \left(u_{o_j} - u_j \right) \frac{\partial u_i}{\partial r_k} = 0 \qquad (55)$$

due to the symmetry of w. By the truncated Taylor series of Eq. (37) and substitution from Eqs. (38) and (39), Eq. (55) takes the form

$$\sum_i \sum_j w_{ij} \left(u_{o_j} - u_{e_j} - R_1 T_{j1} - R_2 T_{j2} - \ldots - R_p T_{jp} \right) T_{ik} = 0 \qquad (56)$$

or

$$R_1 \sum_i \sum_j w_{ij} T_{j1} T_{ik} + R_2 \sum_i \sum_j w_{ij} T_{j2} T_{ik} + \ldots + R_p \sum_i \sum_j w_{ij} T_{jp} T_{ik}$$

$$= \sum_i \sum_j w_{ij} T_{ik} \left(u_{o_j} - u_{e_j} \right) \qquad k = 1, 2, 3 \ldots p \qquad (57)$$

The expression of Eq. (57) yields the linear set of equations of the form

$$CR = V \qquad (58)$$

where the elements of C and V are defined by

$$C_{k\ell} \equiv \sum_i \sum_j w_{ij} T_{ik} T_{j\ell} \qquad (59)$$

and

$$V_k = \sum_i \sum_j w_{ij} T_{ik} \left(u_{o_j} - u_{e_j} \right) \qquad (60)$$

In matrix form the parameter estimate, r, imbedded in Eq. (58) is given by:

$$r = r_e + (T^T w T)^{-1} T^T w (u_o - u_e) \tag{61}$$

As in the case of nonlinear least squares the solution is obtained by iteration. The matrix used for the linear transformation is seen to be

$$G = (T^T w T)^{-1} T^T w = C^{-1} T^T w. \tag{62}$$

It is interesting to note the difference between least squares and minimum variance as embodied in the transformation matrices of Eqs. (29) and (62). The weight matrix w appearing in Eq. (29) is diagonal while its counterpart in Eq. (62) is not. However, as seen in Eq. (59), since the inverse of C is symmetric, C is also symmetric which is also true for the least squares case. Similarly the dangers implicit in the ill-conditioning of the C matrix resulting from the use of too many parameters can also be carried over to minimum variance.

The covariance matrix associated with the parameter estimate is specified by Eq. (33)

$$S^*_{rr} = (T^T S^{-1}_{\varepsilon\varepsilon} T)^{-1} = C^{-1}. \tag{33}$$

It should be noted, however, that $S_{\varepsilon\varepsilon}$ as defined in this section will now be full and not diagonal.

Bayesian Estimation

As seen earlier, the technique of minimum variance constitutes the most general tool for parameter estimation. Theoretically, the problem is well-posed and barring any ill-conditioning in the C matrix and divergence for the nonlinear case, has a well-defined solution. However, for a substantial number of observations, the weight matrix, being of size L × L, the storage capacity of the computer may be exceeded. The problem can be resolved by dividing the experimental data into batches and processing them sequentially. However, to accomplish this we must transfer from batch to batch the knowledge we have gained concerning the parameter estimate. Mathematically, this technique is known as "Bayesian Estimation" after the mathematician who first expressed the concept in terms of probability.

In Bayesian estimation we are given a <u>prior</u> estimate of the parameters, r_o, along with the associated covariance matrix S_{rr}. We then seek to minimize the objective function

$$F = \sum_{i=1}^{n}\sum_{j=1}^{n} w_{ij}\left(u_{o_i} - u_i\right)\left(u_{o_j} - u_j\right) + \sum_{i=1}^{p}\sum_{j=1}^{p} \hat{w}_{ij}\left(r_{o_i} - r_i\right)\left(r_{o_j} - r_j\right) \tag{63}$$

where $$w = S_{\varepsilon\varepsilon}^{-1} \tag{64}$$

and $$\hat{w} = S_{rr}^{-1} \tag{65}$$

and S_{rr} is a symmetric matrix as is $S_{\varepsilon\varepsilon}$. In comparing this objective function with that of Eq. (50), we find that the second double

series term on the right-hand side of Eq. (63) accounts for our knowledge of the Bayesian prior. Then logically the new parameter estimate we will obtain via Eq. (63) will be a compromise between our knowledge concerning the experimental data (the first double series term in Eq. (63)) and the Bayesian prior. This means that were we to solve for the new parameter estimate using Eq. (50), the solution would be the same as that for the extreme case for Eq. (63) when $S_{rr} \to \infty$.

Minimizing Eq. (72) with respect to each parameter r_k gives

$$\frac{\partial F}{\partial r_k} = -\sum_i \sum_j w_{ij} \left[\left(u_{o_i} - u_i \right) \frac{\partial u_j}{\partial r_k} + \left(u_{o_j} - u_j \right) \frac{\partial u_i}{\partial r_k} \right]$$

$$+ \sum_j \hat{w}_{kj} \left(r_{o_j} - r_j \right) \frac{\partial \left(r_{o_k} - r_k \right)}{\partial r_k}$$

$$+ \sum_i \hat{w}_{ik} \left(r_{o_i} - r_i \right) \frac{\partial \left(r_{o_k} - r_k \right)}{\partial r_k} = 0 \qquad (66)$$

Since the function u is nonlinear, we expand it again into a truncated Taylor series evaluated at an estimated value, r_e:

$$u_\ell \approx u_{e_\ell} + R_1 T_{\ell 1} + R_2 T_{\ell 2} + \ldots + R_P T_{\ell P} \qquad (67)$$

and note that

$$\frac{\partial u_\ell}{\partial r_k} = T_{\ell k} \qquad (68)$$

and

$$\frac{\partial\left(r_{o_k} - r_k\right)}{\partial r_k} = -1 . \tag{69}$$

Substituting Eqs. (75), (76) and (77) into Eq. (74) gives

$$\sum_i \sum_j w_{ij}\left(u_{o_j} - u_{e_j} - R_1 T_{j1} - R_2 T_{j2} - \ldots - R_p T_{jp}\right) T_{ik}$$

$$+ \sum_i \sum_j w_{ij}\left(u_{o_i} - u_{e_i} - R_1 T_{i1} - R_2 T_{i2} - \ldots - R_p T_{ip}\right) T_{jk}$$

$$+ \sum_j \hat{w}_{kj}\left(r_{o_j} - r_j\right) + \sum_i \hat{w}_{ik}\left(r_{o_i} - r_i\right) = 0 \tag{70}$$

Since $S_{\varepsilon\varepsilon}$ and S_{rr} are symmetric, w and $\hat{w}$ are also symmetric. Therefore the two double series terms of Eq. (70) are identical as are the two single series terms. Eq. (70) then simplifies to

$$\sum_i \sum_j w_{ij}\left(u_{o_j} - u_{e_j} - R_1 T_{j1} - R_2 T_{j2} - \ldots - R_p T_{jp}\right) T_{ik}$$

$$+ \sum_j \hat{w}_{kj}\left(r_{o_j} - r_j\right) = 0 \tag{71}$$

We then note that

$$r_{o_j} - r_j = r_{o_i} - r_{e_j} - R_j \tag{72}$$

which upon insertion into Eq. (71) and some manipulation gives

$$R_1\left(\hat{w}_{k1} + \sum_i \sum_j w_{ij} T_{ik} T_{j1}\right)$$

$$+ R_2\left(\hat{w}_{k2} + \sum_i \sum_j w_{ij} T_{ik} T_{j2}\right)$$

$$+ \ldots + R_p\left(\hat{w}_{kp} + \sum_i \sum_j w_{ij} T_{ik} T_{jp}\right)$$

$$= \sum_{j=1}^{p} \hat{w}_{kj}\left(r_{o_j} - r_{e_j}\right) + \sum_{j=1}^{n}\left(u_{o_j} - u_{e_j}\right) \sum_{i=1}^{n} w_{ij}\, T_{ik}$$

$$k = 1, 2, \ldots p \qquad (73)$$

The expression of Eq. (73) gives the linear set of equations of the form

$$CR = V \qquad (74)$$

where the elements of C and V are defined by

$$C_{k\ell} = \hat{w}_{k\ell} + \sum_{i=1}^{n} \sum_{j=1}^{n} w_{ij} T_{ik} T_{j\ell} \qquad (75)$$

and

$$V_k = \sum_{j=1}^{p} \hat{w}_{kj}\left(r_{o_j} - r_{e_j}\right) + \sum_{j=1}^{n}\left(u_{o_j} - u_{e_j}\right) \sum_{i=1}^{n} w_{ij}\, T_{ik} \qquad (76)$$

As seen from Eq. (75), the C matrix is symmetric which again eases much of the computation.

In matrix form the parameter estimate is obtained by iteratively solving the relation

$$r = r_e + \left(\hat{w} + T^T w T\right)^{-1}\left[\hat{w}\left(r_o - r_e\right) + T^T w\left(u_o - u_e\right)\right] \qquad (77)$$

The iteration starts with r replacing r_e, calculating T as a function of the independent variables and r_e, and then generating r by Eq. (77). When r converges to r_e, the iterations are terminated.

An alternate expression for r will now be determined. If the term

$$T^T w T \left(r_o - r_e \right) \tag{78}$$

is added and subtracted to the terms appearing in the square brackets on the right-hand side of Eq. (77), we obtain

$$\begin{aligned}
r &= r_e + \left(\hat{w} + T^T w T \right)^{-1} \Big[\hat{w} \left(r_o - r_e \right) \\
&\quad + T^T w T \left(r_o - r_e \right) - T^T w T \left(r_o - r_e \right) \\
&\quad + T^T w \left(u_o - u_e \right) \Big] \\
&= r_e + \left(\hat{w} + T^T w T \right)^{-1} \left(\hat{w} + T^T w T \right) \left(r_o - r_e \right) \\
&\quad + \left(\hat{w} + T^T w T \right)^{-1} \Big[-T^T w T \left(r_o - r_e \right) + T^T w \left(u_o - u_e \right) \Big] \\
&= r_e + \left(r_o - r_e \right) \\
&\quad + \left(\hat{w} + T^T w T \right)^{-1} \Big[T^T w \left(u_o - u_e \right) - T^T w T \left(r_o - r_e \right) \Big] \\
&= r_o + \left(\hat{w} + T^T w T \right)^{-1} T^T w \Big[u_o - u_e - T \left(r_o - r_e \right) \Big] \\
&= r_o + G \Big[u_o - u_e - T \left(r_o - r_e \right) \Big]
\end{aligned} \tag{79}$$

where

$$G \equiv \left(\hat{w} + T^T w T\right)^{-1} T^T w . \tag{80}$$

The revised covariance matrix of the parameter is found by noting that the error of the new estimate is related to the error in the observation, $Z_{\varepsilon\varepsilon}$, and the prior parameter error Z_{rr} by Eq. (77)

$$Z^*_{rr} = \left(\hat{w} + T^T w T\right)^{-1} \hat{w}\, Z_{rr} + \left(\hat{w} + T^T w T\right)^{-1} T^T w\, Z_{\varepsilon\varepsilon} \tag{81}$$

The revised covariance matrix is then

$$\begin{aligned} S^*_{rr} &= E\left(Z^*_{rr} Z^{*T}_{rr}\right) \\ &= \left(\hat{w} + T^T w T\right)^{-1} \hat{w} E\left(Z_{rr} Z^T_{rr}\right)\left[\left(\hat{w} + T^T w T\right)^{-1} \hat{w}\right]^T \\ &\quad + \left(\hat{w} + T^T w T\right)^{-1} T^T w E\left(Z_{\varepsilon\varepsilon} Z^T_{\varepsilon\varepsilon}\right)\left[\left(\hat{w} + T^T w T\right)^{-1} T^T w\right]^T \end{aligned} \tag{82}$$

where the cross-correlation between Z_{rr} and $Z_{\varepsilon\varepsilon}$ is assumed to be zero. Noting that

$$E\left(Z_{rr} Z^T_{rr}\right) = \hat{w}^{-1} \tag{83}$$

and

$$E\left(Z_{\varepsilon\varepsilon} Z^T_{\varepsilon\varepsilon}\right) = w^{-1} \tag{84}$$

gives upon substitution into Eq. (82)

$$
\begin{aligned}
S^{*}_{rr} &= \left(\hat{w} + T^{T}_{wT}\right)^{-1}\hat{w}\hat{w}^{-1}\left[\left(\hat{w} + T^{T}_{wT}\right)^{-1}\hat{w}\right]^{T} \\
&+ \left(\hat{w} + T^{T}_{wT}\right)^{-1}T^{T}_{ww}{}^{-1}\left[\left(\hat{w} + T^{T}_{wT}\right)^{-1}T^{T}_{w}\right]^{T} \\
&= \left(\hat{w} + T^{T}_{wT}\right)^{-1}\left[\left(\hat{w} + T^{T}_{wT}\right)^{-1}\hat{w}\right]^{T} \\
&+ \left(\hat{w} + T^{T}_{wT}\right)^{-1}\left[\left(\hat{w} + T^{T}_{wT}\right)^{-1}T^{T}_{wT}\right]^{T} \\
&= \left(\hat{w} + T^{T}_{wT}\right)^{-1}\left[\left(\hat{w} + T^{T}_{wT}\right)^{-1}\left(\hat{w} + T^{T}_{wT}\right)\right]^{T} \\
&= \left(\hat{w} + T^{T}_{wT}\right)^{-1} = C^{-1}
\end{aligned}
\tag{83}
$$

As in case of weighted least squares Eq. (82) assumes that the true value of r and the calculated value of r are sufficiently close so that the T matrix is the same for both. If this is not true, a considerable error may be introduced.

To summarize the technique of Bayesian estimation, we iteratively solve the sequence

$$T = T\left(r_e\right) \tag{84}$$

$$S = \left(\hat{w} + T^{T}wT\right)^{-1} = S\left(r_e\right) \tag{85}$$

$$G = ST^{T}w = G\left(r_e\right) \tag{86}$$

$$r = r_o + G\left[u_o - u_e - T\left(r_o - r_e\right)\right. \tag{87}$$

and repeat the next sequence with r replacing r_e. We continue to iterate until the difference between r and r_e

becomes sufficiently small and the sequence has therefore converged. The final value of S is S^*_{rr}, the revised parameter covariance matrix. It should be noted that when the response is linear with respect to the parameters, only one iteration is required. This means that since r_e is always set equal to r_o for the first iteration, the term $(r_o - r_e)$ in Eq. (87) is zero for the linear case. Alternatively, as will be noted later, one can choose to set both r_e and u_e equal to zero for the linear case.

When sequential batch processing is used, the Bayesian technique should yield the same solution as that which would be obtained by processing all batches together without a Bayesian prior. To test this, let us confine ourselves to two batches denoted by indices 1 and 2 along with a linear estimator. The processing of the first batch uses no prior estimate and gives a parameter estimate (Eq. (77)):

$$r_1 = \left(T_1^T w_1 T_1\right)^{-1} T_1^T w_1 u_{o_1} \tag{88}$$

and a revised covariance

$$S^*_{rr_1} = \left(T_1^T w_1 T_1\right)^{-1} = \hat{w}_2^{-1} \tag{89}$$

The estimate and the covariance of Eqs. (88) and (89) are input as information about the prior for the second batch. This gives (Eq. (77))

$$\begin{aligned} r_2 &= \left(\hat{w}_2 + T_2^T w_2 T_2\right)^{-1}\left(\hat{w}_2 r_1 + T_2^T w_2 u_{o_2}\right) \\ &= \left(T_1^T w_1 T_1 + T_2^T w_2 T_2\right)^{-1}\left(T_1^T w_1 u_{o_1} + T_2^T w_2 u_{o_2}\right) \end{aligned} \tag{90}$$

Eq. (90) gives the estimate r_2 resulting from a linear accumulation of all the experimental data, hence, proving the affect of the Bayesian prior. For K batches of data this gives

$$r = \left(\sum_{i=1}^{K} T_i^T w_i T_i \right)^{-1} \sum_{i=1}^{K} T_i^T w_i u_{o_i} \tag{91}$$

The proof can readily be extended to the nonlinear case. Here, however, the final value of T_i for each batch will not necessarily be the same thereby yielding a different estimate for the final batch. If the system defining u is highly nonlinear such that large variations in T_i are encountered from batch to batch, the error could be substantial.

The procedure outlined in this section is correct provided that the covariance matrices of the observations and the prior are correct. As noted in the earlier sections, the new parameter estimate has little merit if wrong covariances are employed.

Eqs. (84) through (87) constitute the most general case of parameter estimation, and the reader will find that the equations of the previous sections are special cases of this system. However, the Bayesian aspect which has been added in this section is particularly appealing in the nonlinear case for three reasons:

1. The prior parameter estimate constitutes a good guess of the parameter estimate and hence increase the chances for convergence.

2. The Bayesian formulation drives the solution closer to the prior than does minimum variance (the Bayesian technique with no prior). This also leads to faster convergence.

3. As seen from Eq. (69) the dependency of the Bayesian formulation on the prior is linear. This means that as the dependency on the prior is increased (via S_{rr}) the problem becomes more linear and convergence is enhanced.

In addition to the above observations, the addition of a Bayesian prior to both linear and nonlinear problems renders the C matrix of the resulting set of equations more diagonally dominant and hence more non-singular. This is why experiments have shown that when a prior estimate is used, the number of parameters may be increased substantially without generating a Hilbert-like matrix.

The use of a prior estimate is not restricted to sequential batch processing. Often, for example, in ground shock calculations, the analyst may want to process a single batch of experimental data and incorporate what he believes to be a reasonable estimate of the parameters, along with the error estimates of these parameters. If these incorporated values are reasonable, the Bayesian technique becomes a powerful tool, particularly when the number of observations is relatively small. The analyst should be cautioned however, against using this tool for a small number of observations and then attaching a relatively large error to the prior estimate. This in effect attributes a small level of credence to the prior, and in the limit, will generate a solution for an underdetermined system. Obviously, the confidence level for the evolved parameter estimate will be quite small indicating the solution to be useless.

SUMMARY

The different types of optimization which have been analyzed here can be summarized by catagorizing the estimator type, the structure of the covariance matrix for the observations, and the structure of the covariance matrix for the prior estimates.

The estimator type can be linear or non-linear. When a linear estimator is employed, no iterations are required. For this case, the general nonlinear formulation can be employed with the initial estimate r_e and the initial calculated response u_e, both set equal to zero. From Eq. (79) the revised estimate is

$$r = r_o + G(u_o - Tr_o) \tag{92}$$

where G is defined by Eq. (80). The revised estimate can be obtained alternatively from Eq. (77)

$$r = (\hat{w} + T^T wT)^{-1}(\hat{w}\, r_o + T^T w u_o). \tag{93}$$

In either case, the solution is obtained without iteration by applying either Eq. (92) or (93). The revised covariance matrix is given by Eq. (83).

The structure of the covariance matrix for the observations can be either identity, diagonal, or full. The case where the matrix is identity corresponds to unweighted least squares. When the matrix is non-unit diagonal, the residuals are weighted with no cross-correlation between the observations. When the covariance matrix is non-diagonal, cross-correlation among the observations has been assumed. As has been noted earlier, the covariance matrix for the observations will always be symmetric.

The covariance matrix for the prior estimate can be either infinite, diagonal or full. The case where the elements of the matrix are infinite in value, corresponds to complete lack of confidence in the prior estimate and is equivalent to the absence of a Bayesian prior. The associated weight matrix, $\hat{w}$, will be null, and the estimator will attempt to drive the calculated response toward the data. When the covariance matrix is diagonal, a prior estimate has been specified, but no cross-correlation is postulated among its elements. Lastly, when the covariance matrix is full, cross-correlation has been assumed between the components of the prior estimate. As with the observation covariance matrix, the covariance matrix for the prior estimate will always be symmetric.

The various combinations of the two governing covariance matrices are depicted in Table 2. The four boxes on the lower right-hand side give the possible combinations for a Bayesian prior estimate and are therefore separated from the rest of the table by a bold line. Note the two empty boxes on the left-hand side. This is because the use of a diagonal or full prior covariance matrix along with an identity observation covariance matrix would result in a system of incompatible units for the objective function of Eq. (63), and is therefore meaningless. It should also be noted that the seven cases shown in the table can be applied with either a linear or nonlinear estimator giving a total of fourteen possible combinations.

The revised estimates and covariances for the various methods discussed here are summarized in Table 3. For the linear case, no iterations are required and the solution is immediate. For

COVARIANCE MATRIX FOR PRIOR	COVARIANCE MATRIX FOR OBSERVATIONS: IDENTITY	DIAGONAL	FULL
INFINITE	UNWEIGHTED LEAST SQUARES	WEIGHTED LEAST SQUARES AND NO PRIOR	MINIMUM VARIANCE AND NO PRIOR
DIAGONAL		WEIGHTED LEAST SQUARES AND NO CROSS-CORRELATION ON PRIOR	MINIMUM VARIANCE AND NO CROSS-CORRELATION ON PRIOR
FULL		WEIGHTED LEAST SQUARES AND CROSS-CORRELATION ON PRIOR	MINIMUM VARIANCE AND CROSS-CORRELATION ON PRIOR

Table 2. Optimization Schemes Resulting From Various Combinations of Governing Covariance Matrices. Portion of table with bold-face border uses Bayesian prior estimate.

Table 3. Summary of Estimation Methods

METHOD	REVISED ESTIMATE, r	REVISED COVARIANCE, S^{*}_{rr}
LINEAR LEAST SQUARES	$\left(T^{T}T\right)^{-1}T^{T}u_{o}$	$\left(T^{T}T\right)^{-1}T^{T}S_{\varepsilon\varepsilon}T\left(T^{T}T\right)^{-1}$
LINEAR WEIGHTED LEAST SQUARES AND LINEAR MINIMUM VARIANCE	$\left(T^{T}S^{-1}_{\varepsilon\varepsilon}T\right)^{-1}T^{T}S^{-1}_{\varepsilon\varepsilon}u_{o}$	$\left(T^{T}S^{-1}_{\varepsilon\varepsilon}T\right)^{-1}$
NONLINEAR WEIGHTED LEAST SQUARES AND NONLINEAR MINIMUM VARIANCE	$r_{e} + \left(T^{T}S^{-1}_{\varepsilon\varepsilon}T\right)^{-1}T^{T}S^{-1}_{\varepsilon\varepsilon}\left(u_{o} - u_{e}\right)$	$\left(T^{T}S^{-1}_{\varepsilon\varepsilon}T\right)^{-1}$
LINEAR BAYESIAN ESTIMATION	$r_{o} + \left(S^{-1}_{rr} + T^{T}S^{-1}_{\varepsilon\varepsilon}T\right)^{-1}T^{T}S^{-1}_{\varepsilon\varepsilon}\left(u_{o} - T\,r_{o}\right)$ OR $\left(S^{-1}_{rr} + T^{T}S^{-1}_{\varepsilon\varepsilon}T\right)^{-1}\left(S^{-1}_{rr}r_{o} + T^{T}S^{-1}_{\varepsilon\varepsilon}u_{o}\right)$	$\left(S^{-1}_{rr} + T^{T}S^{-1}_{\varepsilon\varepsilon}T\right)^{-1}$
NONLINEAR BAYESIAN ESTIMATION	$r_{o} + \left(S^{-1}_{rr} + T^{T}S^{-1}_{\varepsilon\varepsilon}T\right)^{-1}T^{T}S^{-1}_{\varepsilon\varepsilon}\left[u_{o} - u_{e} - T\left(r_{o} - r_{e}\right)\right]$ OR $r_{e} + \left(S^{-1}_{rr} + T^{T}S^{-1}_{\varepsilon\varepsilon}T\right)^{-1}\left[S^{-1}_{rr}\left(r_{o} - r_{e}\right) + T^{T}S^{-1}_{\varepsilon\varepsilon}\left(u_{o} - u_{e}\right)\right]$	$\left(S^{-1}_{rr} + T^{T}S^{-1}_{\varepsilon\varepsilon}T\right)^{-1}$

the nonlinear case, the solution is obtained by iteratively replacing r_e by r until the difference between r_e and r is deemed to be sufficiently small. For the linear case, the solution obtained is that for the true extremum of the objective function. For the nonlinear cases, the method may converge to a local minimum or may even diverge. When this occurs, special methods should be employed to increase the so-called radius of convergence.

The analysis shown here does not include possible errors in the measurement of the independent variables since they are usually relatively negligible. However, there are situations in which both the dependent and independent variables contain errors of equal magnitude. For these cases, a new estimator must be evolved.

REFERENCES

1. Wolberg, J.R., "Prediction Analysis", Van Nostrand, New York, 1967.

2. Ralston, A. "A First Course in Numerical Analysis," McGraw-Hill, New York, 1965.

3. Wolberg, J.R. and J. Isenberg, "A Nonlinear Least Squares Search Algorithm", Computer Methods in Applied Mechanics and Engineering, Vol. 5, pp. 1-9, 1975.

NOMENCLATURE

C = matrix for linear set of equations

D = determinant of Hilbert-like matrix

E = expectation operator

F = objective function

g = linear least squares operator

G = linear transformation matrix

m = number of independent variables

n = number of observations

r = parameter vector

R = perturbation vector for nonlinear estimation

S = covariance matrix

T = sensitivity matrix

p = number of parameters

u = response vector

U = residual or difference between observed and calculated response

V = free vector for linear set of equations

w = observation weight matrix

$\hat{w}$ = parameter weight matrix

z = random error

Subscripts

e = latest iterative estimate

o = known prior, either experimentally or analytically

rr = associated with parameter

εε = associated with observation

Superscripts

* = revised

APPENDIX B

VERIFICATION AND CHECK-OUT OF THE COMPUTER PROGRAM, PEBLS*

SUMMARY

When the computer program "fitted" Brown and Black's test data using a near-linear force-deflection characteristic, there occurred the gnawing uncertainty, "Was the computer program coded correctly?" To verify that indeed the program was working properly, it was decided to estimate the parameters of a bi-linear textbook example (for which an analytical solution was available). The estimation procedure was successful for this example, and the results are reported in this appendix.

B.1 Results from Biggs' Text (Reference 2)

There are a few non-linear problems of elasto-plastic systems where exact solutions are available. One such exact solution is given in Biggs' text, Reference 2, Section 2.7 (p. 69 ff). Figure B-1 describes the problem, namely an elasto-plastic beam subjected to a Heaviside step-function loading. Biggs gives a graph of the response (see Figure B-1) and also formulas from which the response u(t) can be computed at any time. (For further details consult Reference 2.)

*Parameter Estimation of Blast-Loaded Structures

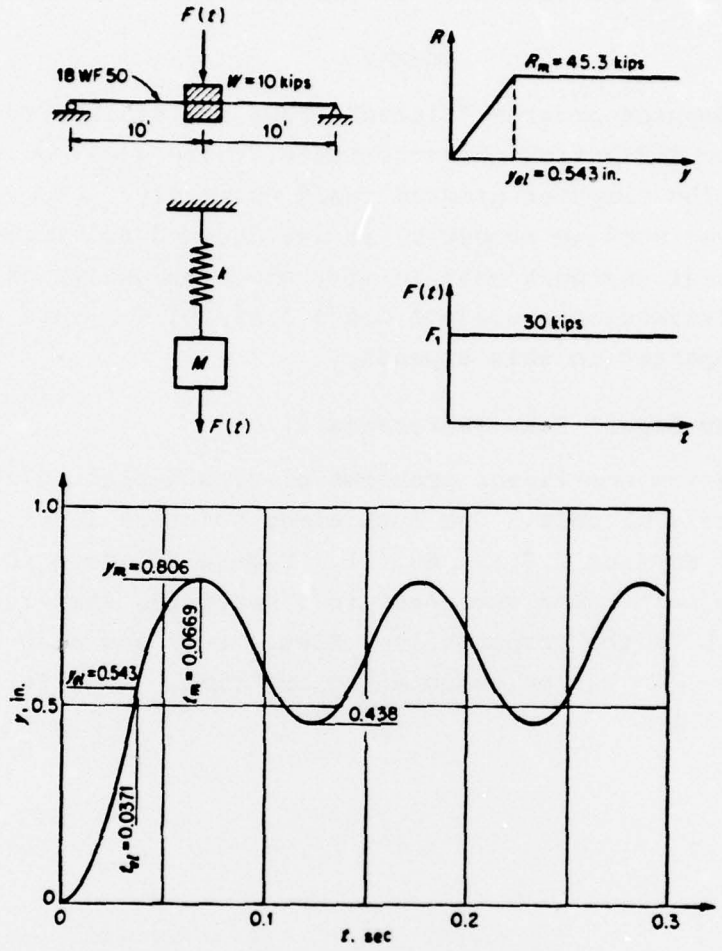

FIGURE 2.22 Example. Response of elasto-plastic one-degree structure to suddenly applied constant force.

Figure B-1. Exapmle From Biggs Text

B.2 Input Data to PEBLS Computer Program

The input data used for this example is shown below. Note that the initial estimate of P_{lin} was 45.3 and the initial estimate of d_{lin} was .543, exactly the values from Biggs text (cf. Figure B-1). These two parameters were input with a confidence of 10% on each, as shown in the input data. The "experimental" data (which in this case was computed, using the equations from Biggs' text) is shown on page B-4. This "experimental" response was taken at seven time points (t_1, t_2, ...t_7) and was assumed to be known with an accuracy of about 2%. There were just two points required to define the pressure-time history, since it was a step-function.

PARAMETER ESTIMATION FOR BLAST-LOADED STRUCTURES

1-DOF ELASTIC-PLASTIC TEST

ITERATION LIMIT = 12

BACKSTEP LIMIT = 4

CONVERGENCE CRITERION ON OBJECTIVE FUNCTION = 0.00500

CONVERGENCE CRITERION ON CHANGE IN PARAMETERS = 0.01000

MOUSE STEP REDUCTION FACTOR = 1.00000

PARAMETER MOVE LIMIT = 0.20000

THE TIME HISTORY USES AT MOST 160 TIME POINTS

THE TIME INCREMENT = 0.50000E-03 SECONDS

THE MAXIMUM TIME THUS = 0.79500E-01 SECONDS

THE SLAB MASS PER UNIT AREA = 0.25907E-01

INITIAL ESTIMATES OF PARAMETERS

PARAMETER	ESTIMATION CODE	INITIAL ESTIMATE	VARIANCE	PERCENT CONFIDENCE
PLIN	1	45.300	20.521	10.000
DLIN	1	0.54300	0.29485E-02	10.000
EPLS	0	0.00000	0.00000	0.00000
EMU0	0	1.0000	0.00000	0.00000
EMU1	0	1.0000	0.00000	0.00000
EMUD	0	9.9000	0.00000	0.00000
ALP0	0	1.0000	0.00000	0.00000
ALP1	0	1.0000	0.00000	0.00000
ALPD	0	9.9000	0.00000	0.00000
BETA	0	0.00000	0.00000	0.00000
PSCL	0	1.0000	0.00000	0.00000

THE TOTAL NUMBER OF PARAMETERS BEING ESTIMATED (NP) = 2

EXPERIMENTAL BLAST AND RESPONSE OBSERVATIONS - DATA SET 1

DISPLACEMENT RESPONSE

THE NUMBER OF PRESSURE DATA POINTS = 2

THE NUMBER OF RESPONSE DATA POINTS = 7

EXPERIMENTAL RESPONSE DATA

POINT	TIME (SEC)	RESPONSE	VARIANCE	CONFIDENCE (()
1	0.10000E-01	0.56530E-01	0.12780E-05	0.19998E-01
2	0.20000E-01	0.20836	0.17370E-04	0.20003E-01
3	0.30000E-01	0.40781	0.66520E-04	0.19999E-01
4	0.37100E-01	0.54300	0.11790E-03	0.19997E-01
5	0.45000E-01	0.66363	0.17620E-03	0.20002E-01
6	0.55000E-01	0.76352	0.23320E-03	0.20001E-01
7	0.66900E-01	0.80551	0.25950E-03	0.19999E-01

BLAST RECORD

POINT	TIME (SEC)	PRESSURE
1	0.00000E+00	0.30000E+02
2	0.10000E+01	0.30000E+02

B.3 Initial PEBLS Results for Biggs Example

The results of the first iteration of the program PEBLS are shown in Table B-1. Note particularly that the analytic response (computed within PEBLS using numerical integration) did not agree exactly with the observed response (computed by hand using Biggs analytical equations 2.57a, and 2.61, p. 75, Reference 2). Also note that the RMS error in observations was computed as $.889 \times 10^{-3}$, i.e., .000889, which gives the reader an idea of the "goodness of fit" between the model (u-analytic) and the data (u-observed).

After three iterations, the results were as shown in Table B-2. Note that now u-analytic (computed by PEBLS) is slightly closer to u-observed (the "experimental" data) and the RMS error in observations has been halved, i.e., it is now $.399 \times 10^{-3}$ (.000399). The final information output by the program is shown in Table B-3). Note that the parameters (P_{lin} and d_{lin}) have been estimated at 45.314 and .54443, respectively, although Biggs exact values are 45.3 and .543. Thus, the estimation procedure will not exactly reproduce the parameters of our mathematical example. This (slight) discrepancy may be due to small errors in numerical integration (which, after all, is not exact) or due to the fact that the "test data" were input with a confidence of 2% (and were thus not known exactly).

Table B-1

COMPUTED AND OBSERVED DISPLACEMENT RESPONSE

POINT	TEST TIME	U-ANALYTIC	U-OBSERVED	Y=U-UTEST
1	0.10000E-01	0.56367E-01	0.56530E-01	-0.16342E-03
2	0.20000E-01	0.20780	0.20836	-0.56424E-03
3	0.30000E-01	0.40682	0.40781	-0.99456E-03
4	0.37100E-01	0.54280	0.54300	-0.19620E-03
5	0.45000E-01	0.66310	0.66363	-0.52977E-03
6	0.55000E-01	0.76250	0.76352	-0.10177E-02
7	0.66900E-01	0.80382	0.80551	-0.16868E-02

OBJECTIVE DUE TO OBSERVATIONS = 0.714206E-01 RMS ERROR IN OBSERVATIONS = 0.889176E-03
OBJECTIVE DUE TO PARAMETERS = 0.000000 TOTAL OBJECTIVE FUNCTION = 0.714206E-01

Table B-2

COMPUTED AND OBSERVED DISPLACEMENT RESPONSE

POINT	TEST TIME	U-ANALYTIC	U-OBSERVED	Y=U-UTEST
1	0.10000E-01	0.56370E-01	0.56530E-01	-0.15988E-03
2	0.20000E-01	0.20785	0.20836	-0.51105E-03
3	0.30000E-01	0.40706	0.40781	-0.75332E-03
4	0.37100E-01	0.54331	0.54300	0.31064E-03
5	0.45000E-01	0.66396	0.66363	0.32806E-03
6	0.55000E-01	0.76376	0.76352	0.23720E-03
7	0.66900E-01	0.80548	0.80551	-0.27962E-04

OBJECTIVE DUE TO OBSERVATIONS = 0.452413E-01 RMS ERROR IN OBSERVATIONS = 0.399177E-03
OBJECTIVE DUE TO PARAMETERS = 0.706864E-03 TOTAL OBJECTIVE FUNCTION = 0.459481E-01

Table B-3

PARAMETER CONFIDENCE LEVELS

PARAMETER	INITIAL ESTIMATE	LATEST ESTIMATE	VARIANCE	PERCENT CONFIDENCE
PLIN	45.300	45.314	1.9332	3.0693
DLIN	0.54300	0.54443	0.74290E-03	5.0196

B.4 PEBLS Results for a Poorer Initial Model

If the initial model had been in error, say one had P_{lin} of 49 and d_{lin} of .45 (versus the exact values of 45.3 and .543 from Biggs text), the question was, "How well will PEBLS perform?" The input data for this case is shown on page B-8. Note that now the confidence in the parameters is given as 20%, whereas formerly it was 10% (cf. page B-3). The "experimental" response data were taken to be the same as previously; (see page B-4). The results of the first iteration with this input data are shown in Table B-4. Note that the maximum value of u-analytic was calculated as .51185, whereas the "data" gave .80551 for the same time point, point number 7. Also note that the RMS error in observations went up to .1401, whereas in the previous example it was .000899, initially.

After the three iterations, PEBLS gave the results shown in Table B-5. Note that the RMS error has been reduced (from .1401) to .0046, and a significant improvement in "fitting" the dynamic data had been achieved. The final estimated values of the parameters P_{lin} and d_{lin} are also shown in Table B-5, where the former (P_{lin}) is given as 43.8 and the latter (d_{lin}) is .51285. For comparison purposes, the "exact" values (used in Biggs example) were 45.3 and .543, respectively. It is noteworthy that a relatively "good" fit to the data (RMS error of .0046) was obtained, although the estimated parameters p_{lin} and d_{lin} are only within about 5% of their "exact" values.

PARAMETER ESTIMATION FOR BLAST-LOADED STRUCTURES

1-DOF ELASTIC-PLASTIC TEST

ITERATION LIMIT = 12

BACKSTEP LIMIT = 4

CONVERGENCE CRITERION ON OBJECTIVE FUNCTION = 0.00500

CONVERGENCE CRITERION ON CHANGE IN PARAMETERS = 0.01000

MOUSE STEP REDUCTION FACTOR = 1.00000

PARAMETER MOVE LIMIT = 0.20000

THE TIME HISTORY USES AT MOST 160 TIME POINTS

THE TIME INCREMENT = 0.50000E-03 SECONDS

THE MAXIMUM TIME THUS = 0.79500E-01 SECONDS

THE SLAB MASS PER UNIT AREA = 0.25906E-01

INITIAL ESTIMATES OF PARAMETERS

PARAMETER	ESTIMATION CODE	INITIAL ESTIMATE	VARIANCE	PERCENT CONFIDENCE
PLIN	1	49.000	96.040	20.000
DLIN	1	0.45000	0.81000E-02	20.000
EPLS	0	0.00000	0.00000	0.00000
EMU0	0	1.0000	0.00000	0.00000
EMU1	0	1.0000	0.00000	0.00000
EMUD	0	9.9000	0.00000	0.00000
ALP0	0	1.0000	0.00000	0.00000
ALP1	0	1.0000	0.00000	0.00000
ALPD	0	9.9000	0.00000	0.00000
BETA	0	0.00000	0.00000	0.00000
PSCL	0	1.0000	0.00000	0.00000

THE TOTAL NUMBER OF PARAMETERS BEING ESTIMATED (NP) = 2

Table B-4

COMPUTED AND OBSERVED DISPLACEMENT RESPONSE

POINT	TEST TIME	U-ANALYTIC	U-OBSERVED	Y=U-UTEST
1	0.10000E-01	0.55906E-01	0.56530E-01	-0.62388E-03
2	0.20000E-01	0.20094	0.20836	-0.74243E-02
3	0.30000E-01	0.37623	0.40781	-0.31580E-01
4	0.37100E-01	0.47976	0.54300	-0.63235E-01
5	0.45000E-01	0.55280	0.66363	-0.11083
6	0.55000E-01	0.57960	0.76352	-0.18392
7	0.66900E-01	0.51185	0.80551	-0.29366

OBJECTIVE DUE TO OBSERVATIONS = 95.9008 RMS ERROR IN OBSERVATIONS = 0.140101
OBJECTIVE DUE TO PARAMETERS = 0.000000 TOTAL OBJECTIVE FUNCTION = 95.9008

Table B-5

COMPUTED AND OBSERVED DISPLACEMENT RESPONSE

POINT	TEST TIME	U-ANALYTIC	U-OBSERVED	Y=U-UTEST
1	0.10000E-01	0.56331E-01	0.56530E-01	-0.19898E-03
2	0.20000E-01	0.20725	0.20836	-0.11113E-02
3	0.30000E-01	0.40433	0.40781	-0.34829E-02
4	0.37100E-01	0.53761	0.54300	-0.53946E-02
5	0.45000E-01	0.65640	0.66363	-0.72328E-02
6	0.55000E-01	0.75901	0.76352	-0.45133E-02
7	0.66900E-01	0.81159	0.80551	0.60765E-02

OBJECTIVE DUE TO OBSERVATIONS = 0.169110 RMS ERROR IN OBSERVATIONS = 0.466160E-02
OBJECTIVE DUE TO PARAMETERS = 0.767073 TOTAL OBJECTIVE FUNCTION = 0.936183

PARAMETER CONFIDENCE LEVELS

PARAMETER	INITIAL ESTIMATE	LATEST ESTIMATE	VARIANCE	PERCENT CONFIDENCE
PLIN	49.000	43.820	8.1278	5.8182
DLIN	0.45000	0.51285	0.31881E-02	12.547

B.5 Conclusions

Additonal work was done to verify that sequential processing of the experimental data gave similar results. Basically, the result of this exercise was to convince the authors that the program PEBLS was functioning correctly and numerically integrating properly. Since exact analytical examples are not available with varying μ, α, etc., all the loops and logic of PEBLS have not been verified by hand calculations. Nevertheless, the authors can state with some confidence that the program is completely functional, and it appears to be properly coded.

DISTRIBUTION LIST

DEPARTMENT OF DEFENSE

Assistant to the Secretary of Defense
Atomic Energy
ATTN: ATSD (AE)

Director
Defense Civil Preparedness Agency
Assistant Director for Research
ATTN: G. Sisson

Director
Defense Communications Agency
ATTN: CCTC/C672, F. Moore

Defense Documentation Center
Cameron Station
12 cy ATTN: TC

Director
Defense Intelligence Agency
ATTN: DB-4C2, T. Ross
ATTN: DT-1C
ATTN: DT-2, Wpns. & Sys. Div.
ATTN: DB-4C1

Director
Defense Nuclear Agency
ATTN: DDST
ATTN: TISI
ATTN: SPAS
ATTN: STSP
2 cy ATTN: SPSS
3 cy ATTN: TITL

Commander, Field Command
Defense Nuclear Agency
ATTN: FCPR
ATTN: FCT

Director
Joint Strat. Tgt. Planning Staff
ATTN: JLTW-2

Chief
Livermore Division, Field Command, DNA
Lawrence Livermore Laboratory
ATTN: FCPRL

Under Secretary of Def. for Rsch. & Engrg.
ATTN: S&SS (OS)

DEPARTMENT OF THE ARMY

Program Manager
BMD Program Office
ATTN: CRDABM-NE

Commander
BMD System Command
ATTN: BMDSC-TEN, N. Hurst

Director
Construction Engineering Rsch. Lab.
ATTN: CERL-SL

DEPARTMENT OF THE ARMY (Continued)

Dep. Chief of Staff for Rsch. Dev. & Acq.
ATTN: DAMA-CSM-N, LTC G. Ogden

Chief of Engineers
ATTN: DAEN-RDM
ATTN: DAEN-MCE-D

Deputy Chief of Staff for Ops. & Plans
ATTN: Dep. Dir. for Nuc. Chem. Matters

Commander
Harry Diamond Laboratories
ATTN: DELHD-NP

U.S. Army Armament Research & Development Command
ATTN: N. Slagg

Director
U.S. Army Ballistic Research Labs.
ATTN: DRDAR-BLE, J. Keefer
ATTN: C. Kingery
ATTN: DRXBR-X, J. Meszaros

Division Engineer
U.S. Army Engineer Div., Huntsville
ATTN: HNDED-SR

Director
U.S. Army Engr. Waterways Exper. Sta.
ATTN: F. Brown
2 cy ATTN: G. Jackson
2 cy ATTN: W. Flathau

Commander
U.S. Army Foreign Science & Tech. Ctr.
ATTN: Rsch. & Data Branch

DEPARTMENT OF THE NAVY

Chief of Naval Material
ATTN: NMAT 044

Chief of Naval Operations
ATTN: Op-981

Chief of Naval Research
ATTN: Code 474, N. Perrone
ATTN: Code 461, J. Warner

Officer-in-Charge
Civil Engineering Laboratory
Naval Construction Battalion Center
ATTN: R. Odello
ATTN: W. Shaw
ATTN: S. Crawford

Commander
David W. Taylor Naval Ship R&D Ctr.
ATTN: Code 1740-5, B. Whang
ATTN: Code 1700, W. Murray

Commander
Naval Facilities Engineering Command
ATTN: Code 03A
ATTN: Code 04B

DEPARTMENT OF THE NAVY (Continued)

Commander
Naval Ocean Systems Center
ATTN: E. Cooper

Superintendent (Code 1424)
Naval Postgraduate School
ATTN: Code 1424

Director
Naval Research Laboratory
ATTN: Code 8440, F. Rosenthal
ATTN: Code 8403, R. Belshem
ATTN: Code 8440, G. O'Hara

Commander
Naval Sea Systems Command
ATTN: Code 03511
ATTN: SEA-9931, R. Lane
ATTN: Code 0351

Commander
Naval Ship Engineering Center
ATTN: NSEC 6105

Officer-in-Charge
Naval Surface Weapons Center
ATTN: Code 243
ATTN: Code 240
ATTN: Code WA501
ATTN: Code 241

Commander
Naval Surface Weapons Center
Dahlgren Laboratory
ATTN: W. Wisherd

Commander
Naval Weapons Center
ATTN: J. Bowen
ATTN: C. Austin

Commanding Officer
Naval Weapons Evaluation Facility
ATTN: R. Hughes

Director
Strategic Systems Project Office
ATTN: NSP-272

DEPARTMENT OF THE AIR FORCE

Commander
ADCOM/DC
ATTN: KRX

Commander
ADCOM/XPD
ATTN: XP
ATTN: XPX
ATTN: XPDQQ

AF Armament Laboratory, AFSC
ATTN: AFATL/DLYV, J. Collins

AF Geophysics Laboratory, AFSC
ATTN: LWW, K. Thompson

AF Institute of Technology, AU
ATTN: Commander

DEPARTMENT OF THE AIR FORCE (Continued)

AF Weapons Laboratory, AFSC
ATTN: DES-S, M. Plamondon
ATTN: DEV, J. Bratton
ATTN: DE, Lt Col J. Leech

Headquarters
Air Force Systems Command
ATTN: DLCAW

Commander
Foreign Technology Division, AFSC
ATTN: PDBF, S. Spring

Hq. USAF/RD
ATTN: RDQRM, Col S. Green
ATTN: RDQSM

Commander
Rome Air Development Center, AFSC
ATTN: Commander

SAMSO/DE
ATTN: DEB, MNNH, MNI
ATTN: MMH

Commander in Chief
Strategic Air Command
ATTN: XPFS
ATTN: OAI

DEPARTMENT OF ENERGY

Department of Energy
Albuquerque Operations Office
ATTN: Director

University of California
Lawrence Livermore Laboratory
ATTN: T. Gold
ATTN: T. Butkovich
ATTN: J. Cortez
ATTN: L. Woodruff

Los Alamos Scientific Laboratory
ATTN: T. Dowler

Sandia Laboratories
ATTN: W. Roherty
ATTN: W. Caudle
ATTN: L. Vortman
ATTN: W. Herrmann

OTHER GOVERNMENT AGENCY

Central Intelligence Agency
ATTN: RD/SI, Rm. 5G48, Hq. Bldg., for
NED/OSI-5G48 Hqs.

DEPARTMENT OF DEFENSE CONTRACTORS

Aerospace Corp.
ATTN: L. Selzer
ATTN: P. Mathur

Agbabian Associates
ATTN: M. Agbabian

Artec Associates, Inc.
ATTN: S. Gill

DEPARTMENT OF DEFENSE CONTRACTORS (Continued)

Battelle Memorial Institute
ATTN: R. Klingsmith

BDM Corporation
ATTN: A. Lavagnino

BDM Corporation
ATTN: R. Hensley

Bell Telephone Laboratories
ATTN: J. White

Boeing Company
ATTN: J. Wooster
ATTN: R. Carlson
ATTN: R. Dyrdahl
ATTN: R. Holmes

Brown Engineering Company, Inc.
ATTN: M. Patel

California Research & Technology, Inc.
ATTN: K. Kreyenhagen
ATTN: S. Shuster

Center for Planning & Rsch., Inc.
ATTN: R. Shnider

Civil/Nuclear Systems, Corp.
ATTN: R. Crawford

University of Denver
Colorado Seminary
Denver Research Institute
ATTN: Sec. Officer for J. Wisotski

Electromechanical Sys. of New Mexico, Inc.
ATTN: R. Shunk

Engineering Decision Analysis Co., Inc.
ATTN: R. Kennedy

Franklin Institute
ATTN: Z. Zudans

Gard, Inc.
ATTN: G. Neidhardt

General Dynamics Corp.
Pomona Division
ATTN: K. Anderson

General Dynamics Corp.
Electric Boat Division
ATTN: M. Pakstys

General Electric Company
Space Division
ATTN: M. Bortner, Space Sci. Lab.

General Electric Co.-TEMPO
Center for Advanced Studies
ATTN: DASIAC

H-Tech Laboratories, Inc.
ATTN: B. Hartenbaum

DEPARTMENT OF DEFENSE CONTRACTORS (Continued)

IIT Research Institute
ATTN: R. Robinson
ATTN: A. Longinow

Institute for Defense Analyses
ATTN: Director

J. H. Wiggins, Co., Inc.
ATTN: J. Collins
ATTN: D. Evensen
ATTN: A. Bronowicki

Kaman AviDyne
Division of Kaman Sciences Corp.
ATTN: N. Hobbs
ATTN: F. Criscione

Kaman Sciencies Corp.
ATTN: D. Sachs

JAYCOR
ATTN: M. McKay

Lockheed Missiles & Space Co., Inc.
ATTN: T. Geers

Lovelace Foundation for Medical
Education and Research
ATTN: R. Jones

Martin Marietta Corp.
Orlando Division
ATTN: A. Cowan
ATTN: G. Fotieo

McDonnell Douglas Corp.
ATTN: R. Halprin
ATTN: J. Logan

Merritt CASES, Inc.
ATTN: J. Merritt

Mitre Corp.
ATTN: Director

University of New Mexico
Dept. of Campus Security & Police
ATTN: G. Triandafalidis

Nathan M. Newmark
Consulting Engineering Services
ATTN: W. Hall
ATTN: N. Newmark

University of Oklahoma
ATTN: J. Thompson

Pacifica Technology
ATTN: R. Allen
ATTN: G. Kent
ATTN: R. Bjork

Physics International Co.
ATTN: F. Sauer
ATTN: F. Moore
ATTN: L. Behrmann
ATTN: D. Orphal
ATTN: R. Swift
ATTN: C. Vincent
ATTN: C. Godfrey

DEPARTMENT OF DEFENSE CONTRACTORS (Continued)

R&D Associates
ATTN: H. Brode
ATTN: A. Latter
ATTN: R. Port
ATTN: C. Knowles
ATTN: J. Carpenter
ATTN: W. Wright, Jr.
ATTN: J. Lewis

R&D Associates
ATTN: H. Cooper

Rand Corporation
ATTN: A. Laupa
ATTN: C. Mow

Science Applications, Inc.
ATTN: H. Wilson

Science Applications, Inc.
ATTN: S. Oston

Science Applications, Inc.
ATTN: D. Maxwell

Science Applications, Inc.
ATTN: B. Chambers
ATTN: W. Layson

Science Applications Inc.
ATTN: J. Cramer

Southwest Research Institute
ATTN: W. Baker
ATTN: A. Wenzel

SRI International
ATTN: G. Abrahamson
ATTN: W. Wilkinson
ATTN: A. Florence

DEPARTMENT OF DEFENSE CONTRACTORS (Continued)

Systems, Science & Software, Inc.
ATTN: D. Grine
ATTN: K. Pyatt

Terra Tek, Inc.
ATTN: S. Green
ATTN: A. Jones

TRW Defense & Space Sys. Group
ATTN: P. Dai
ATTN: D. Jortner
ATTN: A. Narevsky
ATTN: P. Bhutta, R1-1104
ATTN: A. Feldman
ATTN: N. Lipner

TRW Defense & Space Sys. Group
San Bernardino Operations
ATTN: G. Hulcher
ATTN: E. Pieper
ATTN: E. Wong

Universal Analytics, Inc.
ATTN: E. Field

The Eric H. Wang
Civil Engineering Rsch. Fac.
ATTN: N. Baum
ATTN: L. Bickle

Weidlinger Assoc., Consulting Engineers
ATTN: M. Baron

Weidlinger Assoc., Consulting Engineers
ATTN: J. Isenberg

Westinghouse Electric Corp.
Marine Division
ATTN: W. Volz